uOttawa

L'Université canadienne
Canada's university

FACULTÉ DES ÉTUDES SUPÉRIEURES ET POSTOCTORALES

uOttawa

L'Université canadienne
Canada's university

FACULTY OF GRADUATE AND POSDOCTORAL STUDIES

Kristin R. Willemsen
AUTEUR DE LA THÈSE / AUTHOR OF THESIS

M.Sc. (Microbiology and Immunology)
GRADE / DEGREE

Department of Biochemistry, Microbiology and Immunology
FACULTÉ, ÉCOLE, DÉPARTEMENT / FACULTY, SCHOOL, DEPARTMENT

Improving adenoviral vectors for muscle-directed gene therapy

TITRE DE LA THÈSE / TITLE OF THESIS

Dr. Robin Parks
DIRECTEUR (DIRECTRICE) DE LA THÈSE / THESIS SUPERVISOR

CO-DIRECTEUR (CO-DIRECTRICE) DE LA THÈSE / THESIS CO-SUPERVISOR

EXAMINATEURS (EXAMINATRICES) DE LA THÈSE / THESIS EXAMINERS

Dr. Kathryn Wright

Dr. Stephen Gee

Gary W. Slater
Le Doyen de la Faculté des études supérieures et postdoctorales / Dean of the Faculty of Graduate and Postdoctoral Studies

# Improving adenoviral vectors for muscle-directed gene therapy

**Kristin R Willemsen**

THESIS
Submitted to the Faculty of Graduate and Postdoctoral Studies
In partial fulfillment of the requirements
For the Master of Science degree in Microbiology and Immunology

Department of Biochemistry, Microbiology and Immunology
Faculty of Medicine
University of Ottawa

*Your file Votre référence*
*ISBN: 978-0-494-51864-9*
*Our file Notre référence*
*ISBN: 978-0-494-51864-9*

## *Abstract*

Gene therapy is a promising approach for the treatment of Duchenne Muscular Dystrophy (DMD). Adenoviral vectors (Ad) are the most commonly used vectors in gene therapy studies however, the overall large size of the Ad particles (162nm), due in part to the fiber proteins that extrude from the surface of the virion, prevent their efficient distribution in muscle. The objective of this project was to evaluate the transduction performance of Ad5 based vectors genetically modified to encode shorter fiber proteins derived from Ad serotypes 35 and 9. Optimal transduction was dependent on fiber length in some cell lines and in *mdx* muscle. However, fiber-modified viruses have an improved viral dispersion and improved transduction up to 10-fold in normal muscle. In addition, an optimized non-immunogenic reporter gene ideal for monitoring vector function in murine disease models was presented. The results of these experiments will contribute to the understanding of Ad transduction in muscle and aid in the design of efficient vectors for DMD therapy.

## *Acknowledgements*

I would like to thank Dr. Robin J Parks for the opportunity to pursue graduate studies in his lab and for allowing me to attend scientific meetings and conferences.

To Joel Ross, and for all those hours spent talking science and doing science together- you have made graduate work so incredibly fun. Thank you for all of your guidance, I've learned some indispensible lessons from you about technique, critical analysis, and what it means to be a good scientist. I've been so fortunate to have you as my academic role model.

Above all, I would like to thank my loving family: Herman, Mary and Michael Willemsen for support and encouragement. I couldn't have done this without you and all you have given me. I can only aspire to be the next 'trained observer of nature' in our family.

## *Contributions of Collaborators*

Dr. Bernard J. Jasmin, of the University of Ottawa, was our primary collaborator, and committed financial investment in all *in vivo* experiments. He also helped guide this project by serving on my thesis advisory committee. Dr. Jasmin contributed technical expertise through the help of his talented technician, John Lunde who performed intramuscular injections for our first *in vivo* experiment, which is represented as preliminary data in Figure 9A and B. I wish to thank John very much for his guidance and assistance throughout all *in vivo* experimentation.

Dr. Illona Skerjanc, of the University of Ottawa, contributed to the guidance of this project by serving on my thesis advisory committee.

Dr. Dmitry Shayakhmetov of the University of Washington generously provided plasmids containing Ad5s, Ad5/35s, and Ad5/9s modified fiber constructs.

Marisa Rossi, an undergraduate summer student at the University of Ottawa, contributed significantly the side project outlined in Chapter 4. Specifically, she generated mSEAPΔ-H451E and did the preliminary *in vitro* heat inactivation experiment.

# *Table of Contents*

# *List of Abbreviations*

| | |
|---|---|
| AAT | alpha-1 antitrypsin |
| AAV | adeno-associated virus |
| Ad | adenovirus |
| AFP | alpha-feto protein |
| AP | alkaline phosphatase |
| APCs | antigen presenting cells |
| BFU | β-gal forming units |
| BGH | bovine growth hormone |
| BMD | Becker muscular dystrophy |
| BSA | bovine serum albumin |
| CEA | carcinoembryonic antigen |
| CFU | colony forming units |
| CMV | cytomegalo virus |
| CP | classical pathway |
| CTL | cytotoxic T lymphocyte |
| DC | dendritic cell |
| DCM | dilated cardiomyopathy |
| DFZ | deflazacourt |
| DGC | dystrophin glycoprotein complex |
| DMD | Duchenne muscular dystrophy |
| DPBS | Dulbecco's phosphate buffered saline |
| DYS | dystrophin |
| E | glutamic acid |
| E-# | embryonic day # |
| EDTA | ethylene diamine tetraacetic acid |
| EGFP | enhanced green fluorescent protein |
| EM | electron microscopy |
| e-MHC | embryonic myosin heavy chain |
| F(X) | human blood coagulation factor 10 |
| FGAd | first-generation adenoviral vector |
| FIX | factor IX |
| GFP | green fluorescent protein |
| Glu | glutamic acid |
| H | histidine |
| HDAd | helper-dependent adenoviral vector |
| hFIX | human blood coagulation factor IX |
| HIV | human immunodeficiency virus |
| hSEAP | human secreted embryonic alkaline phosphatase |
| HSV | herpes-simplex virus |
| IFN | interferon |
| Il-12 | interleuken 12 |
| Il-6 | interleuken 6 |

| | |
|---|---|
| IM | intramuscular |
| ITR | inverted terminal repeats |
| IV | intravenous |
| JNK1 | c-Jun N-terminal kinase 1 |
| K | lysine |
| KDa | kiloDalton |
| *lacZ* | Beta galactosidase expression cassette |
| LTR | long terminal repeat |
| MAPK | mitogen-activated protein kinases |
| MCK | muscle creatine kinase |
| MD | muscular dystrophy |
| *mdx* | murine model of X-chromosome linked muscular dystrophy |
| MHC I | major histocompatability complex I |
| MHC II | major histocompatability complex II |
| MHC | myosin heavy chain |
| micro-DYS | micro dystrophin |
| mini-DYS | mini dystrophin |
| MOI | multiplicity of infection |
| mSEAP | murine secreted embryonic alkaline phosphatase |
| MTT | myoblast transfer therapy |
| NAb | neutralizing antibodies |
| NF-ATc1 | nuclear factor of activated T cells 1 |
| NF-κB | nuclear factor kappa B |
| NK | natural killer |
| nm | nanometers |
| ORI | origin of replication |
| PEG | polyethyleneglycol |
| pfu | plaque forming units |
| PI-G | phoshatidylinositol-glycan |
| qPCR | quantitative polymerase chain reaction |
| R | arginine |
| RLU | relative light units |
| RPA | replication protein A |
| SC | satellite cell |
| SCID | severe combined immunodeficiency |
| SEAP | secreted embryonic alkaline phosphatase |
| SGAd | second-generation adenoviral vector |
| SP | side population |
| T | threonine |
| TA | tibialis anterior |
| TCR | T cell receptors |
| Th1 | T helper cell 1 |
| Th2 | T helper cell 2 |
| TLR | toll-like receptors |

| | |
|---|---|
| TNF | tumor necrosis factor |
| Ubc | ubiquitin C |
| VEGF | vascular endothelial growth factor |
| VSV | vesicular stomatitis virus |
| xg | g force |
| X-gal | Beta-galatosidase substrate |
| β-gal | Beta-galatosidase |

## *List of Figures*

# *List of Tables*

# *Chapter 1: Introduction*

## *1.1 Duchenne Muscular Dystrophy*

Duchenne muscular dystrophy (DMD) is the most common form of muscular dystrophy (MD), affecting 1 in 3500 boys worldwide (1, 2). DMD is a debilitating muscle wasting disease caused by mutations in the dystrophin (DYS) gene. At 2.4 million base pairs, DYS is the largest gene associated with a disease, which frequently accrues multiple types of *de novo* mutations such as nonsense mutations, deletions, and frameshift mutations (3 , 4). In 72% of cases, mutations that cause DMD are the result of large deletions in the DYS gene that do not produce a functional protein (5).

### *1.1.1 Dystrophin glycoprotein complex*

DYS is a large, rod-like sarcolemmal cytoskeletal protein located under the plasma membrane, at the periphery of muscle fibers (Figure 1). By joining the extra cellular dystroglycan and the transmembrane sarcoglycan sub-complexes to the intracellular syntrophin and dystrobrevin complex (6), DYS forms the dystrophin glycoprotein complex (DGC) (Figure 1) (reviewed in (7)) and is the link tethering the extracellular matrix to the intracellular F-actin network (3). Although the function of DYS in its entirety has yet to be elucidated (reviewed in (8)), its primary role is to mechanically stabilize the muscle plasma membrane such that the loss of DYS results in extensive, irreversible muscle damage during mechanical contraction (9, 10). This muscle instability causes multiple rounds of progressive muscle degeneration followed by regeneration, until the regenerative capacity of the muscle is exhausted (11). Degenerated muscle fibers become infiltrated by fibrotic,

**Figure 1: The dystrophin glycoprotein complex**.

The DGC consists of an extracellular dystroglycan complex, a transmembrane sarcoglycan complex and an intra-cellular syntrophin and dystrobrevin complex. The dystroglycan complex connects laminin-2, a component of the basal lamina, in the extracellular matrix through α-dystroglycan and β-dystroglycan to intracellular DYS (12). In smooth muscle the sarcoglycan complex consists of a group of transmembrane proteins termed α, δ, and β sarcoglycans and scarcospan. The sarcoglycan complex connects the plasma membrane to DYS through β-dystroglycan and serves to enhance the stability of the α-β-dystroglycan interaction (13). The syntrophins (α, β1 and β2) directly bind dystrobrevin in the cytosol of muscle fibers and are thought to be scaffolds for signaling proteins (14). Syntrophins and dystrobrevin bind the C-terminus of DYS where the N-terminus is bound to cytoskeletal F-actin. Figure adapted from (15).

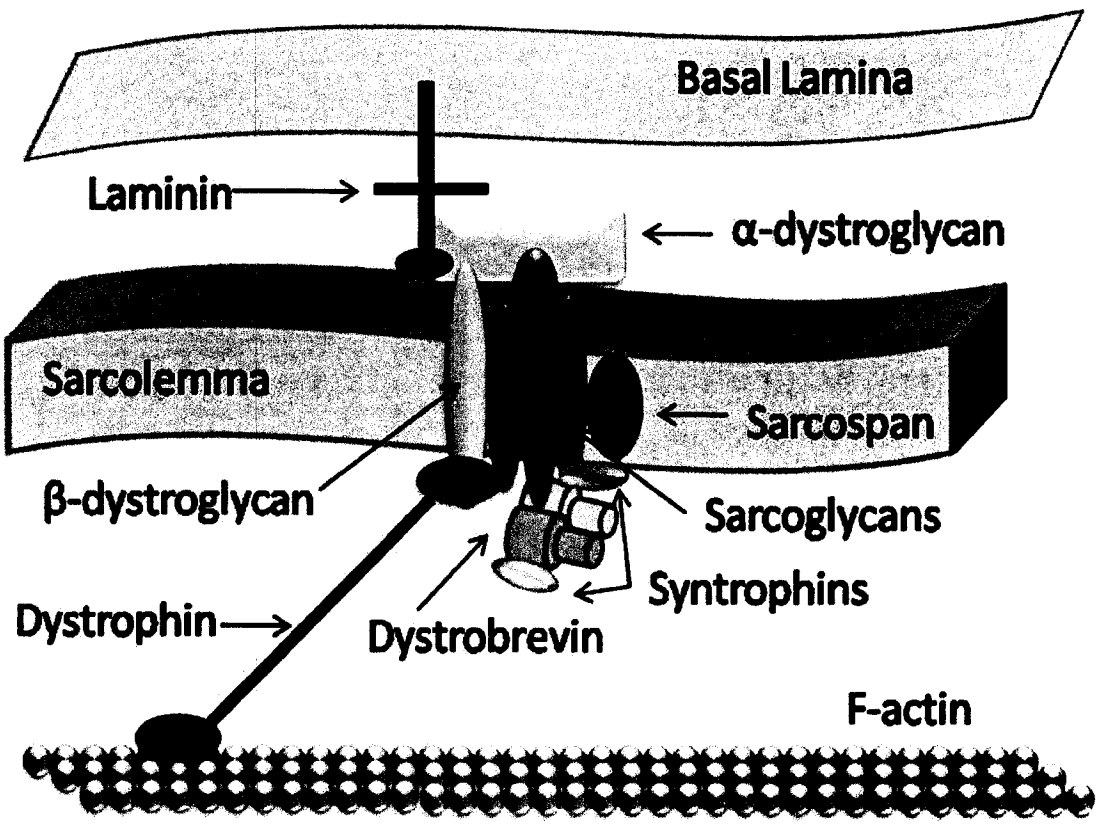
Basal Lamina
Laminin
α-dystroglycan
Sarcolemma
Sarcospan
β-dystroglycan
Sarcoglycans
Syntrophins
Dystrophin
Dystrobrevin
F-actin

fatty connective tissue, ultimately resulting in the loss of muscle function and death of the patient. In affected individuals, muscle weakness and reduced motor function becomes apparent within their first few years of life (16). Diagnosis typically occurs at 3-5 years of age when difficulty walking or balancing due to contractures, or permanent muscle tightening, is first observed. This progressive disease advances quickly thereafter; patients usually require the use of a wheelchair by 10-12 years of age and typically succumb to the disease in their early twenties due to respiratory or cardiac failure (16).

### *1.1.2 Accepted Therapies for DMD*

Accepted DMD therapies that are now in practice focus on the daily management of the symptoms. DMD patients must eat a well balanced diet and engage in non-strenuous physical activity, as inactivity can accelerate muscle weakness and cause constipation (3). The health care team includes physical and occupational therapists, who play an important role in coordinating passive stretches and exercises that help prolong mobility and improve patient comfort (17). When patients experience difficulty walking, weakened leg and ankle muscles are supported with lightweight splints, which extend ambulation by up to 2 years (18). Alternatively, muscle contractures can be surgically corrected to prolong ambulation (3, 17). Physicians closely monitor pulmonary and cardiac function throughout the disease progression, especially in the final stages of DMD (17). Dilated cardiomyopathy (DCM) occurs in 90% of DMD patients over 18 years of age and is responsible for 20% of patient deaths (19). Early DCM is treated with angiotensin converting enzyme inhibitors, beta blockers, and diuretics (16). The development of scoliosis, concurrent with the loss of

ambulation, may make breathing more difficult; surgical correction of spinal curvature may help to improve respiration (17). Ailments that are considered benign to the general population, like minor respiratory infections, must be swiftly treated in DMD patients such that built up mucus, that could normally be cleared by coughing in a healthy individual, is eliminated to prevent re-occurring infection (3). DMD patients experience difficulty coughing and assisted coughing or suctioning devices are often used to clear excess secretions. As the function of the diaphragm and intercostals muscles diminish, assisted respiration is eventually required. First, a non-invasive nasal ventilation intervention is pursued and, as the disease worsens, patients often resort to an invasive tracheotomy to prolong survival (3, 20). The gradual decline of patient health must be closely monitored in order to tailor the treatment of symptomatic relief.

Without a cure for DMD, patients are treated with interventions designed to alleviate cardiac and respiratory symptoms, often concurrent with the use of corticosteroids to improve muscle function (21). Steroids (primarily Prednisone and Deflazacort) have been routinely used to treat DMD after the long-term benefits of their use were initially described to prolong ambulation by up to 2 years (22). Originally, it was hypothesized that steroids slowed the progression of the disease by preserving existing muscle fibers, primarily through an anti-inflammatory and immunosuppressive effect (23, 24). However, it was later shown that Deflazacort (DFZ) improves the dystrophic phenotype by targeting muscle-specific gene expression by counteracting inappropriate c-Jun N-terminal kinase 1 (JNK1) activation (25). DFZ mitigates the DMD phenotype in muscle by activating calcineurin, which dephosphorylates nuclear factor of activated T cells 1 (NF-ATc1) and is a

downstream target of JNK1 signaling (26). Of the many conflicting clinical trials performed to date (reviewed in (27)), there is evidence that steroid use does improve muscle strength and function in DMD. However, stringent nutritional intervention is required while on this treatment due to the unfavorable side effects of weight gain, hyperglycemia, retarded growth and reduced bone density, among others (21). Even though corticosteroid treatment is the best available treatment for DMD (16), a cure for DMD must be sought.

### *1.1.3 Experimental Therapies for DMD*

Much progress has been made in generating new experimental treatments for DMD. For example, anti-sense oligonucleotides have been used to induce exon-skipping in an attempt to by-pass the transcription of deleterious point mutations that generate defective DYS protein (28). This approach is applicable to approximately 20% of DMD patients and clinical trials are currently underway, with much success (29). Continuous administration of the oligonucleotides restored DYS expression in up to 97% of dystrophic muscle fibers near the site of administration in humans (29), but these oligonucleotides must be individually designed to suit specific types of mutations for the treatment to be successful.

Recently, PTC124 was published as an oral drug capable of inducing a dose–dependent ribosomal read-through of premature stop codons that cause missense mutations in DYS (30). PTC124 was shown to promote functional DYS production in *in vitro* and *in vivo* models of DMD (30). Phase I clinical trials confirmed that PTC124 was safe, well tolerated, and acted selectively on premature stop codons (31). Preliminary Phase II data from PTC Therapeutics suggest that PTC124 was able to increase DYS expression in a dose-dependent

manner and patients experienced some improvements in strength and ambulation (31). Unfortunately, PTC124 is only applicable for 10-15% of DMD patients with stop codon mutations and regular administration of the drug is required because this strategy modifies mRNA translation (27).

Both exon-skipping and premature stop codon read-through approaches offer great promise to lessen the disease phenotype for a proportion of seriously affected DMD patients. However, expensive genetic testing would be required to validate these options for a particular individual.

Cell-based therapies aim to replace the dystrophic muscle with normal tissue (reviewed in (32)). Myoblast transfer therapy (MTT) has long been studied as a treatment for DMD (33). MTT works by isolating healthy donor myoblasts that are then expanded *ex vivo* and intra-muscularly delivered to fuse with existing dystrophic fibers (34). Unfortunately, human clinical trials were unsuccessful since few myoblasts survived transplantation (35). After these early trials, extensive research has focused on attempting to understand the massive myoblast apoptosis, minimal cell migration post-transplantation, and host-graft rejection in order to improve the efficacy of MTT treatment. Recent clinical trials are employing simultaneous high-density, intra-muscular injections of myoblasts (approximately 100 injections per square cm of muscle surface) to compensate for massive cell loss and minimal cell migration *in vivo* (36). High-density cellular injections restored DYS expression to 26-30% of muscle fibers near the site of administration (36-38); however this route of delivery is not clinically feasible, even for the treatment of an entire muscle group.

Unfortunately, graft rejection cannot be circumvented by using the patient's own cells, that are expanded and genetically modified ex-vivo, because DMD myoblasts do not survive long after collection (39). Recently, a side population (SP) of skeletal muscle stem cells was discovered to be somewhat resistant to apoptosis following transplantation and these cells were able to repopulate the endogenous muscle stem cell pool following intravenous (IV) delivery (40-43). SP cells express some hematopoietic stem cell markers like Sca-1, CD34, and CD46, but not satellite cell (SC) markers like MyoD, although they do differentiate into SCs post-transplantation (44, 45). Strict techniques must be used to isolate pure populations of SP cells, consequently limiting the yield of therapeutic cells recovered. Thus, levels of SP cell engraftment have not reached therapeutic significance (32). Therefore, the high susceptibility of therapeutic cells to apoptosis and their inefficient isolation procedures greatly limit the application of cell-based transplantation therapy (46).

In summary, all existing experimental and clinical treatments for DMD use the approach of either (i) slowing the progression of the disease, (ii) reducing the severity of the phenotype, or (iii) the replacement of affected muscle. Currently, there is no genetic 'cure' for DMD.

## *1.2 Gene Therapy*

Gene therapy is an experimental approach with the potential to cure many genetic diseases and disorders. The success of this strategy is contingent upon (i) safe and efficient delivery of the therapeutic gene to specific target cells or organs and (ii) insuring stable, long term expression of the therapeutic gene.

Gene therapy approaches commonly exploit the evolved ability of a virus to enter host cells and deliver their genetic material to a target tissue. The field of gene therapy was founded upon early studies that identified the pathogenic components of the viral genomes and separated them from the remainder of genetic elements, thus producing vectors that could not replicate and cause disease. Of the many viruses that could be used as vectors, ideal gene therapy vectors are easily manipulated and produced to high titer. Viral vectors should also be capable of targeting the tissue of interest (either dividing or non-dividing cells) and appropriately expressing the therapeutic gene (either by integration or by persisting episomally) without causing any adverse effects. Commonly used gene therapy vectors include retroviruses, lentiviruses, herpes simplex viruses, adenoviruses (Ad) and adeno-associated viruses (AAV) (47), summarized in Table 1. However, the most frequently used vector for gene therapy is Ad (48).

### *1.2.1 Adenoviral Vectors*

For many reasons, Ad is the most prevalent vector used in clinical gene therapy studies (48). The relatively large Ad genome is readily manipulated; they are easily grown to high titer ($10^{12}$-$10^{13}$ viral particles/ml) (47); Ad also infects a wide variety of dividing and non-dividing cell types with high efficiency (49). There are 50 immunologically distinct serotypes of human Ad, which is divided into 6 subgroups (A through F). Ad5, of sub group C, is the most commonly used for gene therapy. Herein, Ad5 will be referred to as "Ad" unless otherwise specified. Ad infection in humans is benign and usually restricted to the respiratory tract (50). Even though Ad was the first virus described to cause tumorigenesis in animals (51), no evidence has since been reported linking Ad to malignant disease in

## Table 1: Viral Vectors used in gene therapy applications

| | Viral genome | Cloning capacity | Tropism | Inflammation | Vector genome forms | Main limitations | Main advantages |
|---|---|---|---|---|---|---|---|
| **Enveloped** | | | | | | | |
| Retrovirus | RNA | 8 kb | Dividing cells only | Low | Integrated | Integration might induce oncogenesis in some applications | Transduces dividing cells; integration might induce insertional mutagenesis and oncogenesis |
| Lentivirus | RNA | 8 kb | Broad | Low | Integrated | Toxic and inflammatory; transient transgene expression in target tissues except neurons | Stable gene expression in replicating cells |
| HSV-1 | dsDNA | 40 kb[a]<br>150 kb[b] | Neurons/ broad | High | Episomal | | Stable gene expression in most tissues<br>Large cloning packaging capacity; broad cell tropism and strong tropism for neurons |
| **Unenveloped** | | | | | | | |
| AAV | ssDNA | <5 kb | Broad | Low | Episomal (>90%), Integrated (<10%) | Small cloning capacity | Broad cell tropism; noninflammatory and nonpathogenic |
| Adenovirus | dsDNA | 7.9 kb[a]<br>30 kb[c] | Broad | High | Episomal | Capsid mediates an inflammatory response; preexisting anti-Ad antibodies in most humans | Highly efficient transduction of most tissues; large cloning capacity; high titer and long-term expression[c] |

HSV-1, herpes simplex type 1 recombinant vector; AAV, adeno-associated viral vector; ssDNA, single-stranded DNA; dsDNA, double-stranded DNA.
[a] Replication defective
[b] Amplicon
[c] Helper-dependent high capacity adenoviral vectors

humans (53). Therefore, Ad is generally accepted as a safe vector for gene therapy studies. Further, Ads can be adapted into improved vector systems that are replication-defective and less immunogenic by omitting key genes from their genome (54, 55).

### *1.2.2 Adenovirus biology*

Ad is a linear, double-stranded DNA virus with a 36 kb genome. The Ad genome is flanked by two inverted terminal repeats (ITRs) with a 5` *cis*-acting packaging sequence (53). Ad genes are classified into 3 groups: the early (E1A, E1B, E2, E3, E4), delayed (IX, IVa2, VA RNAI,II), and the major late transcriptional units (L1-5) which are transcribed by cellular RNA polymerase II and, after multiple splicing events, produce more than 50 proteins (53). For a thorough review of Ad biology, refer to (53). E1A is a widely studied oncogene that hijacks key cell cycle regulators by binding the Rb tumor suppressor and indirectly activates the Myc proto-oncogene to induce apoptotic signaling in the host cell (56). E1B encodes two proteins that functionally interact with E1A, inducing cell growth, thus keeping the host cells alive. Proteins from the E2 region are involved in replication. The E3 region encodes proteins which antagonize the host's immune response to viral antigen. The E4 region mediates transcriptional regulation. The delayed transcriptional unit (with the exception of VA RNAs, which block host transcription) and the major late genes produce the structural components of the viral capsid. The structural protein hexon (pII) and its associated proteins (pVI, pVII, pIX, pIIa) spontaneously assemble with an icosahedral symmetry (53). The capsomere is completed with the independent assembly of the penton base (pIII) (that is composed of 5 proteins) with a trimer of fiber proteins (pIV) (that end in terminal knob domains), which protrude out from the surface of the virion at the 12 vertices of the

icosohedron (53). Virus assembly is complete with association of viral DNA with the capsid, mediated by the packaging sequence. The linear Ad genome is organized in the core through interactions with four viral proteins ((pVII, pX, pV, and the Terminal Protein) (53).

Adsorption of Ad onto the cell is facilitated by a high affinity interaction with the knob protein and its primary receptor, coxsackievirus adenovirus receptor (CAR), which is located on the cell surface (57). It was recently discovered that the majority of subgroup B adenoviruses (ie. Ad3, 7, 11, 35) bind CD46 (an inhibitory complement receptor) as their cellular receptor (58, 59) and Ad3 can also utilize CD80 and CD86 as primary receptors, which are present on B cells and Antigen Presenting Cells (APCs), respectively (60). This initial interaction with the primary cellular receptor is necessary for internalization because it brings the virus in close enough proximity to the plasma membrane to facilitate the secondary interaction of cellular $\alpha_v\beta_3$ and $\alpha_v\beta_5$ integrins with the penton base (Figure 2). The secondary interaction stimulates viral entry by receptor mediated endocytosis. The Ad particle is rapidly and efficiently internalized into an endosome where sequential disassembly of the virion separates the DNA containing core from the penton-fiber structures (Figure 2)(53). Acidification of the early endosome allows the Ad virion to escape into the cytosol where it translocates to the nucleus, releasing viral DNA at the nuclear membrane where viral transcription begins (53). Early transcription initiates concurrent with a low level of late viral gene expression and early genes are continuously expressed at a low level into the late transcription period. Productive Ad infection concludes with host cell lysis at 20-24 hours post-infection *in vitro,* producing up to $10^4$ Ad particles (53).

**Figure 2: Mechanism of Ad5 transduction of a cell.**

The Ad particle consists of an icosahedral virion with fibers that protrude out from each of the 12 vertices. Adsorption is initiated with a high affinity attachment of viral knob domain to the coxsackievirus adenovirus receptor (CAR) followed by a secondary interaction between cellular integrins and the penton base. The Ad virion is internalized into an endosome by receptor-mediated endocytosis. Acidification of the early endosome triggers Ad particle disassembly and release into the cytosol. The Ad virion translocates to the nucleus where viral DNA is released at the nuclear membrane so that viral transcription and translation can then begin (53). Figure adapted from (61).

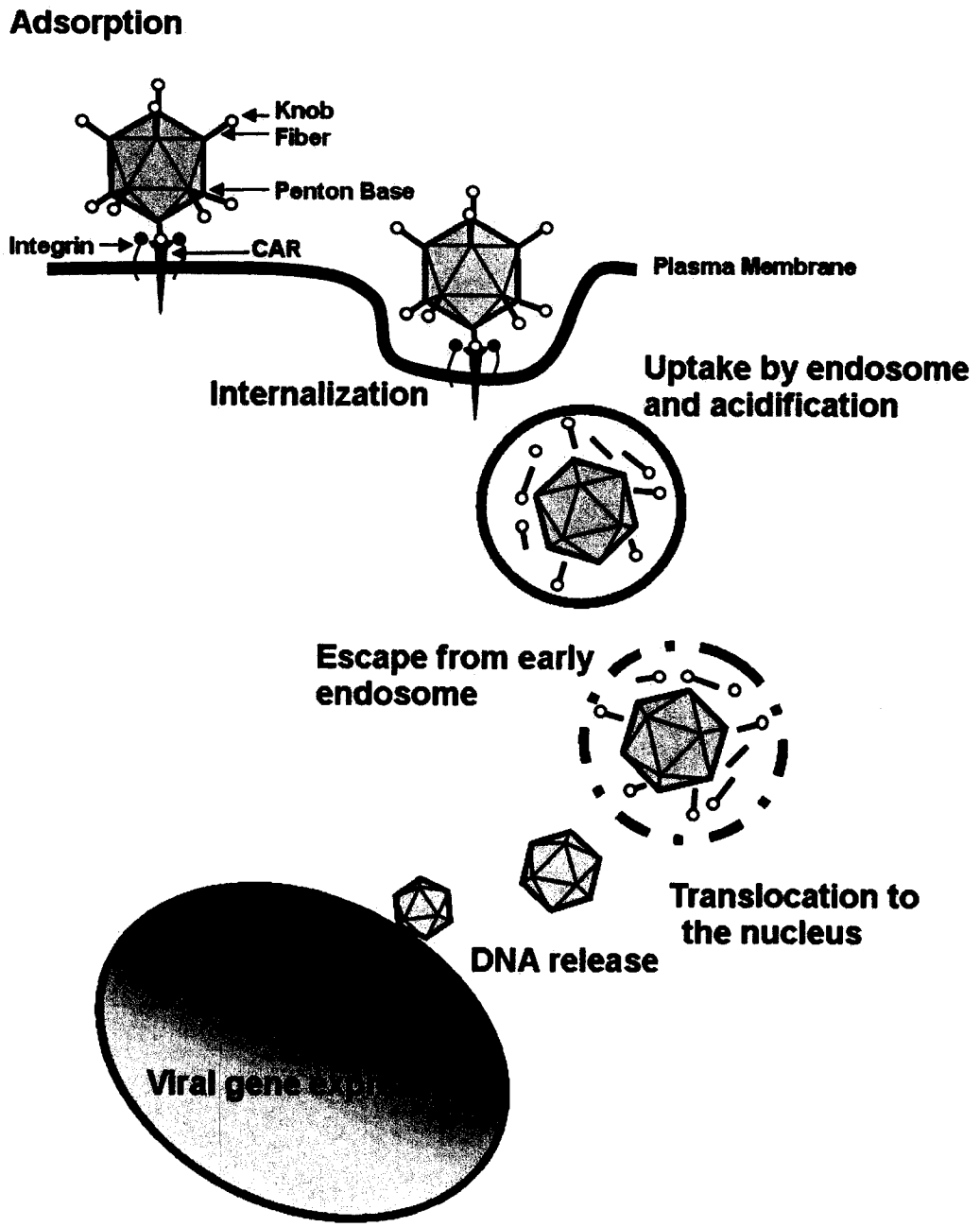
Adsorption
Knob
Fiber
Penton Base
Integrin
CAR
Plasma Membrane
Internalization
Uptake by endosome
and acidification
Escape from early
endosome
Translocation to
the nucleus
DNA release
Viral gene

### *1.2.3 First and second generation adenoviral vectors for gene therapy*

Early gene therapy studies used first generation Ads (FGAds) which were rendered replication defective by deleting the E1 early genes (that are essential for replication) and the non-essential E3 genes, permitting a cloning capacity of 8kb. Therefore, propagation of FGAds requires the E1 genes supplied in *trans* from host cells, like the 293 cell line (62). Despite being replication-defective, the remaining viral genes in FGAd vectors are still transcribed at a low level. Moreover, the amount of viral antigen produced is sufficient to stimulate a cellular immune response *in vivo* resulting in elimination of transduced cells (63-65). Second generation Ads (SGAd) were developed to eliminate this low level of viral late gene expression characteristic of FGAds (66). In addition to E1, SGAds are deleted of portions of E2, with or without additional deletion of E4. The lack of these additional viral genes results in an attenuated immune response compared to FGAds, permitting extended transgene expression (67).

### *1.2.4 The tragic death of Jesse Gelsinger*

Perhaps the most important lesson gained from work with these first and second generation Ad vectors was also the most unfortunate. In 1999, an 18 year-old named Jesse Gelsinger died shortly after receiving an Ad vector in a Phase I clinical trial. Sadly, it was later determined that his death was caused by the Ad vector itself. Jesse suffered from ornithine transcarbamylase (OTC) deficiency, which is a metabolic enzyme required to break down ammonia (68). Jesse volunteered for the study and participated in the third cohort of patients that received a $6x10^{13}$ particle dose of a SGAd containing the OTC gene. Other patients that received the same dose and who had higher levels of circulating

antibodies against Ad, did not experience any severe complications (69). The dose his cohort received was over 10-fold higher than other well tolerated doses from previous clinical trials that employed other routes of vector administration (ie. $1x10^8 - 1x10^{12}$) (70, 71). One factor that may have affected the safety of the Ad vector in this gene therapy trial could have been the fibrotic liver tissue, typical of patients with OTC deficiency that enhances sensitivity to viral and bacterial infections (68). Jesse's unfortunate death alerted the public and the scientific community to the risks of gene therapy. Since, the gene therapy community has been focused on gaining a better understanding about how Ad vectors interact with the immune system, so to avoid a similar situation from happening again.

### *1.2.5 Immune response to Ad vectors*

The immune response to Ad vectors is twofold: the early innate response and the antigen-specific adaptive immune response responsible for long lasting immunity (Figure 3).

#### *1.2.5.1 Innate Immunity*

The innate immune system is the first line of defense against an invading pathogen (72). When Ad is delivered to selectively infect a target tissue, resident tissue macrophages and dendritic cells (DCs) (also called antigen presenting cells, APCs) may recognize the invading pathogen. APCs engulf Ad by phagocytosis and subsequently become activated along with intracellular signal transduction pathways, for example, Mitogen-activated protein kinase (MAPK) activation of the NF-κB pathway. Activation of these signaling pathways initiates transcription of chemokine and cytokine genes which, once secreted, serve to limit viral infection (Figure 3) (73, 74). Transcription of inflammatory response

**Figure 3: Innate and adaptive immune response to adenoviral Infection**

Upon administration of an Ad vector to a target tissue, resident tissue macrophages or dendritic cells (DC) engulf Ad by phagocytosis. Intracellular signal transduction pathways become activated resulting in the transcription of inflammatory genes and the secretion of chemokine and cytokines (74). This inflammation response controls the infection locally and recruits monocytes to present antigen and further amplifies the immune response. The recruited natural killer cells (NK) are the link between the innate and adaptive immune response. NKs perform cytolytic functions and secrete IFN-γ which is essential for the development of the Th1 adaptive immune response (75). The adaptive immune response is initiated by the presentation of viral antigens by major histocompatability complex molecules (MHC) class I and II to naïve T cells. Leukocyte differentiation is stimulated resulting in CD8 T cells and CD4 T helper cells. CD8 T cells mature into cytotoxic T lymphocytes which specifically eliminate virally infected cells. Th1 helper cells amplify the immune response by releasing cytokines to recruit monocytes and Th2 helper cells differentiate into B-cells which produce neutralizing antibodies against the viral antigen. Figure adapted from (72).

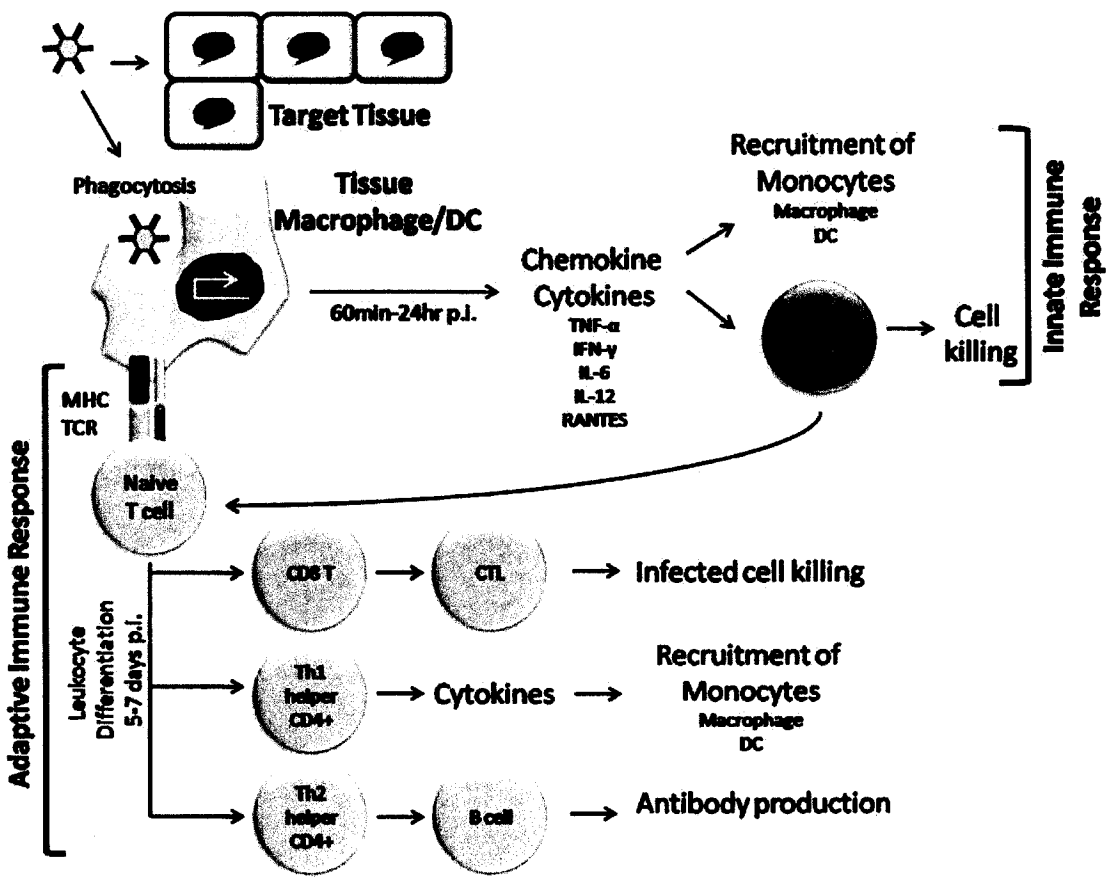
Target Tissue
Phagocytosis
Tissue Macrophage/DC
60min-24hr p.i.
Chemokine Cytokines
TNF-α
IFN-γ
IL-6
IL-12
RANTES
Recruitment of Monocytes
Macrophage
DC
Cell killing
Innate Immune Response
MHC
TCR
Naive T cell
Adaptive Immune Response
Leukocyte Differentiation 5-7 days p.i.
CD8 T
CTL
Infected cell killing
Th1 helper CD4+
Cytokines
Recruitment of Monocytes
Macrophage
DC
Th2 helper CD4+
B cell
Antibody production

genes like TNF-α, IFN-γ, Il-6, IL-12, and RANTES begins as early as 1 hour post-Ad administration and persists up to 6 hours (76, 77). Guided by the induction of cytokines and their receptors, the 'activated' or matured APCs then migrate to the draining lymph nodes where they can interact with naïve T cells, commencing the adaptive immune response (78). The initial local release of cytokines serves to attract natural killer cells (NK) and additional monocytes to the site of infection thus amplifying the innate immune response which persists up to 24 hours post-Ad administration (55, 79). The recruited NK cells are the important link between the innate and adaptive immune response (Figure 3) as they perform cytolytic functions as well as secrete IFN-γ, which is essential for the development of the Th1 adaptive immune response against the viral genes (75).

In general, the innate immune response is invoked in a dose-dependent manner by the Ad capsid (76, 80). Studies utilizing replication-defective vectors and empty Ad capsids elucidated that viral internalization and not transcription is required for the induction of cytokine and chemokine expression (72, 81-83). The inflammation at the site of infection rapidly eliminates a significant amount of vector transduction and recruits leukocytes in order to mount a continuing adaptive immune response (84).

### *1.2.5.2 Adaptive Immunity*

The adaptive immune response is initiated by activated resident tissue APC migration and presentation to naïve T cells of the circulatory system, lymph nodes, or spleen. Naïve T cells recognize viral antigen by an interaction with its T cell receptor (TCR) and major histocompatibility complex (MHC) molecules which determine leukocyte differentiation

necessary for a specific function (reviewed in (85)). CD8 T cells mature into cytotoxic T lymphocytes which specifically kill virally infected cells. CD4+ T lymphocytes, or 'helper T cells,' amplify the immune response by releasing cytokines that recruit monocytes and Th2 helper cells differentiate into B-cells, which produce neutralizing antibodies against the viral antigen (Figure 3). Recent studies suggest that Ad can also activate the humoral response directly via the complement system (86). Complement activation is an essential immune response responsible for opsonization of the antigen and lysis of infected cells (87). Ad4 or Ad5 serotypes have been shown to bind the critical C3 protein which plays a significant role in the induction of acute inflammatory responses through the complement system (86, 88).

In general, the activation of the adaptive immune response occurs at 4 or 5 days post-Ad administration and is responsible for the majority of vector loss over time, observed as transient gene expression (55, 79).

Leaky viral gene expression from FGAds activate the adaptive arm of the immune system causing a CTL response, resulting in transient gene expression (77). The Helper-Dependent Ad system was designed to attenuate this potentially fatal immune response to first and second generation Ad vectors.

### *1.2.6 Helper-Dependent Adenoviral vectors*

Helper-dependent Ads (HDAds) lack all viral protein coding sequences and contain only *cis*-acting elements that are required to replicate and package the vector DNA (Figure 4) (54). Therefore, these vectors have a large cloning capacity of up to 36kb and exhibit a reduced toxicity and inflammation response (54). The production of these vectors requires

**Figure 4: Helper-Dependent Adenoviral Vector System**

HDAds are devoid of all viral genes except the flanking ITRs and *cis*-acting packaging signal. Co-infection with an E1 deleted helper virus is required to make the HDAds *in vitro*. The helper virus contains all the necessary viral genes to make the Ad particles. To ensure only the HDAd genome is packaged and not the helper viruses, HDAds are propagated in a stable 293 Cre cell line. In the presence of Cre, the packaging signal is excised from the helper virus and therefore, the helper virus genome cannot be packaged. Reprinted by permission (54).

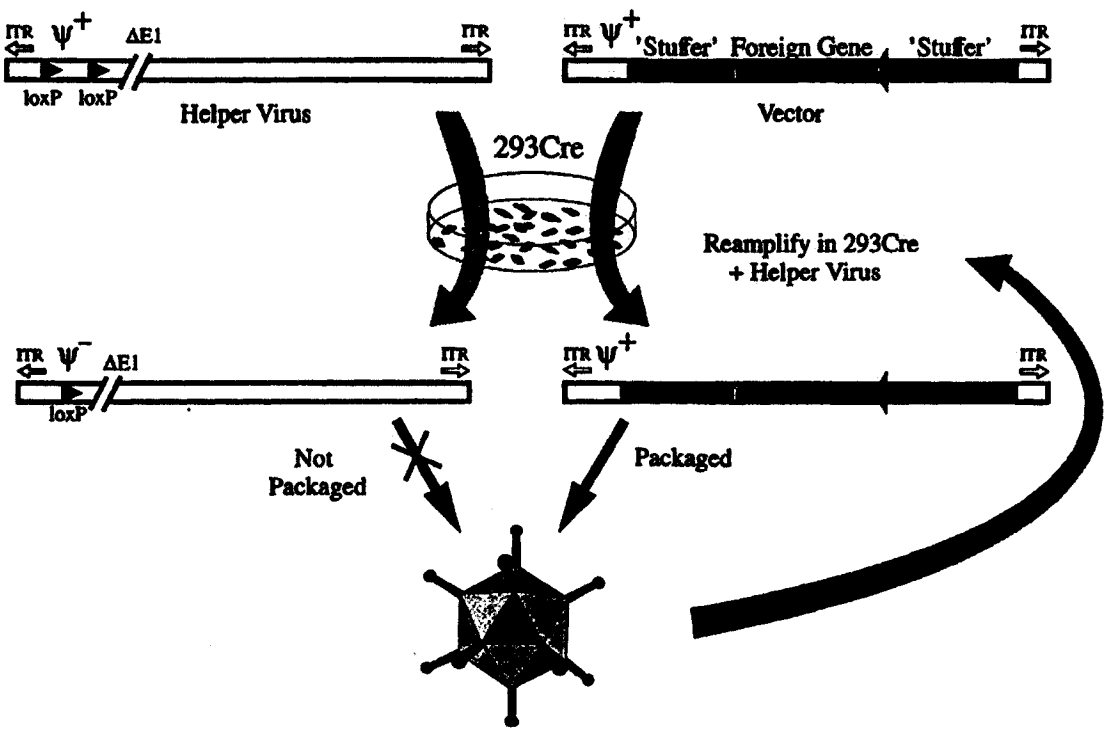
ITR
Ψ+
ΔE1
loxP
loxP
Helper Virus
ITR
ITR
Ψ+
'Stuffer'
Foreign Gene
'Stuffer'
ITR
Vector
293Cre
Reamplify in 293Cre
+ Helper Virus
ITR
Ψ−
ΔE1
loxP
ITR
ITR
Ψ+
ITR
Not
Packaged
Packaged

the co-infection of a helper virus vector into a packaging cell line that express Cre recombinase (293Cre cells) (54). The helper virus encodes all the necessary viral genes to package a vector, but its packaging signal is flanked by two loxP sites, which is excised in the presence of Cre recombinase; thus, only the HDAd shuttle vector containing the transgene is packaged (Figure 4).

The HDAd system has shown great potential as a gene therapy vector. A single IV injection of a modest dose of HDAd expressing the relevant therapeutic transgene has shown lifelong correction of hypercholesterolemia in mice and hyperbilirubinemia in rat models of disease (89, 90). Further, HDAd delivery of a therapeutic gene resulted in sustained functional correction of canine hemophilia for up to 418 days post-injection (PI) (91). Exploring alternative and more targeted routes of delivery has improved HDAd transduction and extended transgene expression. For example, direct HDAd delivery to the surgically isolated liver in nonhuman primates resulted in a high efficiency liver transduction that was sustained at a high level for almost 2 years in the absence of chronic toxicity (92). With the promising clinical potential of HDAds, a great body of work has been done testing the efficacy of HDAds for the treatment of DMD.

## *1.3 Gene Therapy for Muscular Dystrophy*

Currently, gene therapy is an experimental treatment for DMD. At this experimental stage, the efficacy of therapeutic vectors must be demonstrated in animal models of DMD that will be introduced herein. Attaining functional efficacy in these animal models, and ultimately humans, requires achieving certain parameters that will be discussed, followed

by an overview of DMD gene therapy using naked DNA, retroviruses, herpes, AAV and Ad vectors.

### *1.3.1 Disease models for DMD*

The murine *DMD*$^{mdx/mdx}$ strain, referred to as *mdx* mice, is the best characterized genetic and biochemical model of DMD pathology. This model of X-linked muscular dystrophy arose as the result of a point mutation in the DYS gene in the murine C57Bl/10 background causing the complete loss of DYS protein in skeletal and cardiac muscle (93, 94). Generally, attributes of the *mdx* strain can be physically characterized by a greater muscle weight gain and muscle hypertrophy compared to normal mice (95). The disease phenotype is physically indistinguishable from wild type prior to the onset of muscle degeneration at 3 weeks of age (96). However, at 4 weeks of age massive muscle degeneration and mononuclear cell infiltration are observed (95-97). Necrosis peaks at 5-6 weeks of age, followed by regeneration which is marked by the presence of centrally nucleated myofibers (95, 97, 98). At 8-12 weeks of age, degeneration slows such that at 10 weeks, most of the muscle has recovered (97). Eventually, *mdx* mice display physical disabilities beyond a year of age (99). Unlike human DMD pathology, *mdx* muscle contains a greater proportion of muscle fibers with less fibrotic and adipose connective tissue (95). In addition, human DMD muscle gradually becomes deficient in regeneration, where as *mdx* muscle retains its regenerative capacity throughout the lifespan of the animal (11, 100, 101). This persistence of regenerative capacity along with a decrease in muscle degeneration at 8 weeks of age contributes to the lack of physical handicap with only minor muscle weakness observed in the *mdx* strain (95, 102). Overall, *mdx* mouse pathology is more benign than human DMD

because utrophin, a DYS homolog, may be able to compensate in part for the lack of DYS in *mdx* mice (103). Still, *mdx* mice at 3-5 weeks of age are an adequate model of early DMD because muscle necrosis and regeneration are actively occurring resulting in severe muscle pathology (95, 98). *Mdx* mice can also model late stage human DMD pathology because, at greater than 1 year of age, a decline in muscle regenerative capacity begins to affect motor activity, especially when damage is induced by exercise (104-106).

Other animal models for DMD have been crucial in elucidating DMD disease pathology. The murine *mdx*/utrophin double knockout (dko) and the *mdx*/utrophin/α-dystrobrevin triple knockouts are more severe murine models than *mdx* mice, with disease progression more similar to human DMD (103). Models in other species offer slightly different phenotypes than *mdx* mice; for example, the dystrophic hamster has a more pronounced cardiomyopathy phenotype and the dystrophic chicken strain greatly differs in terms of onset of muscle morphology (107). Furthermore, larger animal models like the golden retriever (GRMD) and beagle canine model of DMD ($CXMD_J$) serve as essential links between human and murine physiology. These different disease models are invaluable tools to gain further knowledge about myopathies in general such that treatments for DMD can be tested and developed.

### *1.3.2 Functional Correction of DMD*

To cure DMD, the overall objective requires restoring uniform expression of DYS to 40-50% of body mass, specifically in skeletal muscle of limbs, diaphragm, and cardiac tissue (108). The long functional half life of DYS favors a single gene therapy approach stably

expressing DYS could sustain correction, especially if treatment begins prior to the onset of DMD pathology (109). For example, *in utero* intervention that restored DYS expression to as few as 25 out of 500-600 hind limb muscle fibers (a transduction efficiency of less than 5%) was able to significantly rescue the juvenile muscle mass phenotype and moderately improve the force production compared to untreated *mdx* muscle (110). However, prevention of muscle weakness depends on the achievement of an absolute level of DYS gene expression uniformly distributed throughout the muscle (111, 112). In humans with mild symptoms, 30-40% of normal DYS levels expressed in every myofiber, or normal levels of DYS expression in 50% of evenly distributed or mosaically distributed muscle fibers, could prevent muscle damage (113, 114). Therefore, the ideal gene therapy vector for the treatment of DMD should efficiently and evenly transduce muscle.

To functionally evaluate a particular gene therapy approach for DMD, muscle weakness is assessed primarily by 4 types of measurements: (i) the maximal force, (ii) twitch force, (iii) specific tetanic force, and (iv) force deficit. The twitch force and tetanic force are indirect and direct measures of muscle fatigue, respectively; they are measures of the maximal force generating capacity produced by voluntary contractions in response to muscle stimulation relative to the size of the muscle (115). The force deficit is a measure of force lost during a series of mechanical stretches. Unfortunately, the majority of functional gene therapy studies preformed to date in *mdx* mice do not include a wild type control, thus results are presented herein compare the treated *mdx* mice to untreated *mdx* mice unless otherwise stated.

### *1.3.3 Naked DNA transfer of dystrophin*

Naked DNA transfer was the first gene therapy approach used to restore DYS expression in *mdx* mice and in humans (116, 117). Although direct intramuscular (IM) injection of plasmid DNA was both safe and successful, the DNA transduction efficiency and DYS expression was very low (116, 117). Attempts to improve this efficiency by complexing plasmid DNA with cationic lipids or polymers did improve transduction (118), but these modifications may be highly immunostimulatory (119, 120). Electroporation of the target tissue concurrent with DNA administration enhances transduction, but this procedure damages muscle fibers (121). New routes of delivery are being studied, like hydrodynamic injection, which is capable of achieving transfection efficiencies similar to viral delivery (122). Nevertheless, the efficiency of gene transfer of plasmid DNA into skeletal muscle is relatively low and variable, especially in larger animals and nonhuman primates (123). Therefore, much focus has been on the use of viral vectors for muscle directed gene therapy since they transduce muscle with a much higher efficiency *in vivo* than naked DNA applications (124).

### *1.3.4 Retroviral and lentiviral vectors for DMD gene therapy*

Retroviruses are among the first viral vectors developed for gene therapy and are still the most commonly used RNA vectors (47). Retroviruses have a small cloning capacity of approximately 8kb (Table 1) and cannot accommodate the full length DYS gene of 14kb. Therefore, a truncated mini-DYS construct (Figure 5) derived from a mildly affected Becker muscular dystrophy patient has been used as an alternative to DYS in retroviral vectors for

**Figure 5: Schematic representation of dystrophin, utrophin, and recombinant dystrophin constructs**

The (A) Dystrophin (427 KDa), (B) utrophin (395 KDa), (C) mini-dystrophin (227 KDa), (D) micro-dystrophin (132 KDa) consist of combinations of the following components: N-terminal actin binding domains (ABD), c-terminal domains (CT), cystine rich (CR) domains, hinge regions (H1,3,4), and spectrin like repeats (designated numerically). Reprinted from Biochimica et Biophysica Acta, 17722, Odom GL, Gregorevic, P, Chamberlain JS, Viral-mediated gene therapy for the muscular dystrophies: Successes, limitations and recent advances, 243-262, Copyright (2007), with permission from Elsevier.

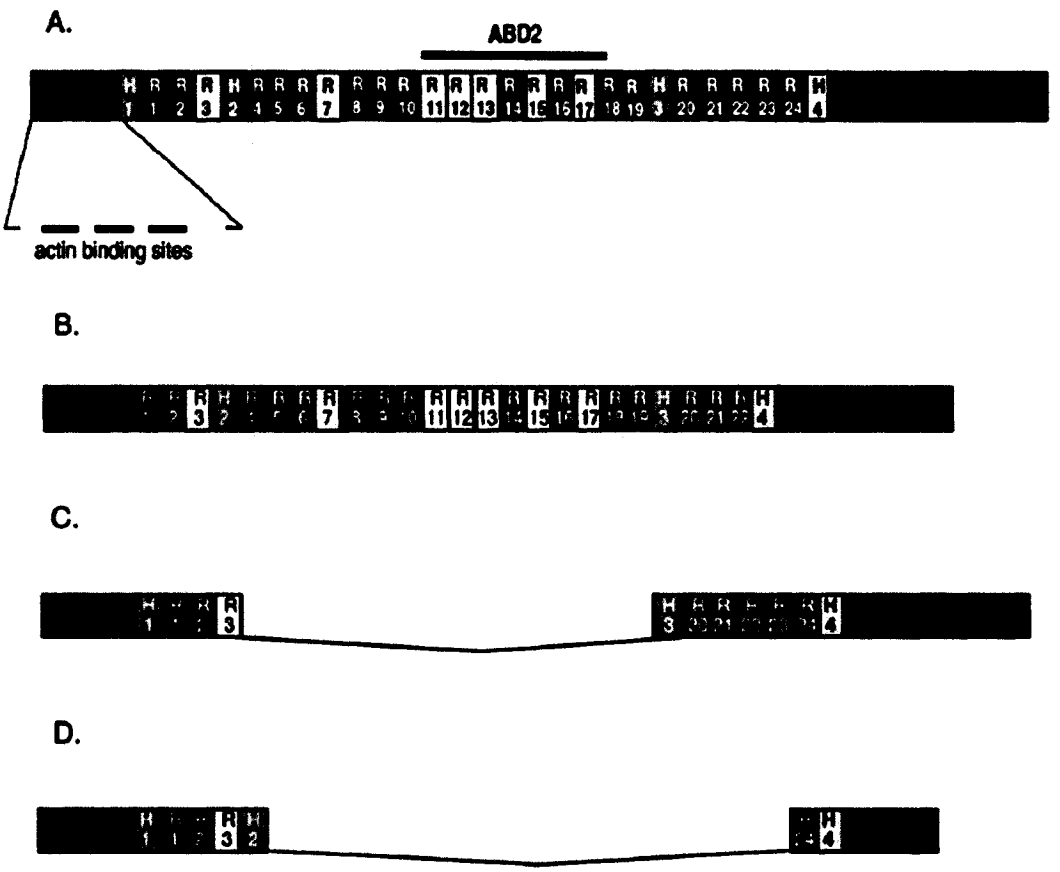
A.
ABD2
actin binding sites
B.
C.
D.

DMD gene therapy (1, 125). The low retroviral muscle transduction observed in the hind limb *mdx* muscle (in approximately 6% of muscle fibers) was attributed to the vectors'dependence on cell division for transduction, as the vectors transduced a small population of proliferating SCs (126).

Lentivirus, a type of retrovirus, can transduce both terminally differentiated and actively regenerating muscles, but are still limited by their very low transduction efficiency and their limited cloning capacity of 8kb (127). Human immunodeficiency virus (HIV) is the most extensively studied lentivirus. However, HIV is a human pathogen and thus raises biosafety concerns for their use and acceptance as gene therapy vectors even though they are made replication-defective and self-inactivating. Only a few studies have explored the use of lentiviral vectors for DMD gene therapy. Vesicular Stomatitus virus G (VSV-G) pseudotyped lentiviral vectors transduce adult murine muscle with a low efficiency (127). Evidence suggests the lentiviral system may be better suited for *ex-vivo* genetic modification of primary cells, as persistent mini-dystrophin transgene expression in primary cells post-proliferation was observed, which did not result in toxicity post-engraftment in the host (127). Further, lentiviral vectors have been successfully applied as an *ex-vivo* gene therapy vector delivering micro-DYS and exon-skipping oligonucleotides in allogenically transplanted monkey and DMD myoblasts respectively (128).

The appeal of retroviral and lentiviral vectors is the ability to integrate and stably express a therapeutic protein, especially in muscle SCs that can differentiate into multiple muscle fibers (126, 129). However, random viral integration risks insertional mutagenesis

and is the main concern surrounding the use of retroviral and lentiviral vectors (47). *In vitro* and *in vivo* studies have shown that retroviral integration preferentially occurs around transcriptional start sites, clustered in gene coding areas (130, 131). Nevertheless, the precise integration site is generally unpredictable as retroviral vectors have been shown to cause leukemia in mice and humans (132, 133). Be it a rare event, insertional mutagenesis and possible viral integration disrupting an oncogene or a tumor suppressor are a significant concern for human gene therapy. Furthermore, retroviral and lentiviral vectors are difficult to produce to a high titer that would be necessary for clinical trials; despite efforts to improve vector concentration and filtration, the titers for these vectors remain low ($10^6$-$10^7$ CFU/ml) in comparison to other vector systems (134). As a result, both retroviral and lentiviral vectors are primarily used to deliver therapeutic genes to cells *in vitro* for MTT studies (128).

### *1.3.5 Herpes amplicon vectors for DMD gene therapy*

Replication defective Herpes simplex virus-1 (HSV-1) vectors are deleted of their lytic viral genes and thus have a very large cloning capacity (Table 1) that can accommodate the full length DYS (135). The major limitation to recombinant HSV-1 vectors is that their remaining viral genes are highly toxic and their expression induces cytoxicity and immune responses (47). Despite this major limitation, HSV-1 vectors are primarily used for neuronal gene therapy applications as the genomes of HSV-1 derived vectors can persist actively or quiescently in neurons (47), as a result they are rarely used for muscle-directed gene therapy. Although HSV-1 can transduce muscle (135), the resulting gene expression is eliminated within days post-infection due to cytotoxicity and an adaptive immune response

attributed to the viral vector (136, 137). Thus, the majority of DMD gene therapy studies utilize AAV and Ad vectors.

### *1.3.6 Adeno-associated viral vectors for DMD gene therapy*

#### *1.3.6.1 AAV biology*

AAV is a non pathogenic human parvovirus with a small, linear, single-stranded DNA 4.7 kb genome that is encapsidated in non-enveloped virion of 20-25nm in diameter (138). The AAV genome encodes two genes, *rep* (required for replication) and *cap* (structural capsid proteins) which are deleted in recombinant AAV vectors (rAAV) leaving behind only two flanking ITRs (47).

Of the many AAV serotypes, AAV2 is the most widely used. AAV2 attachment is mediated by interactions the ubiquitous heparin sulphate residues present on the cell surface (139). Like Ad, AAV internalization is stimulated by a secondary interaction with $\alpha_v\beta_5$ integrins or fibroblast growth factor receptor (140, 141). AAV is taken up into the host cell by receptor-mediated endocytosis where it is subsequently transported to the nucleus (140). Inside the nucleus, viral uncoating proceeds permitting viral replication and transcription (47).

#### *1.3.6.2 AAV vectors for DMD gene therapy*

The development of micro-DYS constructs were essential for the application of AAV vectors to the treatment of DMD because of the limited cloning capacity of these viruses (142). Many groups generated and tested micro-DYS constructs composed of various combinations of rod domain components (Figure 5D). Some were unable to improve muscle

function while others were more effective, abolishing central nucleation in *mdx* muscle and improving specific force (112, 142-146). However, transgenic mouse data suggest micro-DYS constructs cannot fully restore *mdx* pathology while the larger mini-DYS construct can completely correct force deficits (112). As AAV vectors cannot accommodate the mini-DYS construct required to achieve functional correction of DMD, the main limitation to AAV vectors has always been its small cloning capacity.

*Trans*-splicing vectors have been developed in an attempt to double the cloning capacity of AAV, however the efficiency of this process is very low (147, 148). This approach splits a large gene in two portions such that the 5' gene fragment (with a splicing donor sequence) and a 3' gene fragment (with a splicing acceptor sequence) are encoded in two separate vectors; the protein of interest is produced when both complimentary vector sequences are recombined and spliced in the host cell (149). Counter intuitively, the success of this strategy was not limited by the consistent co-infection of two rAAV vectors stably expressing a transgene counterpart in a tissue of interest (150). Instead, the accumulation of spliced mRNA limits the efficiency of this process as the pre-mRNA transcripts are highly unstable (150). Modifications to the gene splitting site have been made to the *trans*-splicing system, allowing for the delivery of a 6kb mini-DYS gene in adult *mdx* mice which was able to improve tetanic and force deficit by 1.4-fold relative to untreated *mdx* muscle (149, 151). However, it is yet to be determined if the trans-splicing rAAV vectors can achieve high enough mini-DYS expression to completely correct the *mdx* phenotype.

The appeal of AAV vectors are their outstanding transduction in muscle. One systemic injection of AAV co-delivered with vascular endothelial growth factor (VEGF) (152) can achieve full body transduction of micro-DYS expression in cardiac and skeletal muscles of *mdx* mice (153, 154). Due to the nature of the truncated DYS construct, complete amelioration of the *mdx* phenotype was not possible. Nevertheless, body wide transduction by AAV vectors is impressive not only because it is achieved through a clinically preferable route of delivery, but because this high level of transduction is required in order to achieve complete correction of a genetic deficiency.

Recently, pre-clinical trials compared regional vascular delivery of different AAV serotypes in *mdx* mice and in non-human primates (155). AAV6 and AAV8 were equally as effective post-IV delivery, transducing approximately 80-90% of muscle fibers and improving force generation in *mdx* mice by 1.3-fold (155). In non-human primates, isolated vascular delivery of an analogous clinically appropriate dose ($2x10^{12}$ vp/kg) of AAV8 expressing enhanced green fluorescent protein (EGFP) transduced between 60-80% of muscle fibers in the hind limb (155). The same group, lead by Dr. JR Mendell at the Columbus Children's Research Institute, has since proceeded with phase I clinical trials assessing the safety of AAV-micro-DYS gene transfer. In January 2008, investigators announced on the Muscular Dystrophy Association website that IM injection of AAV vectors expressing micro-DYS were well tolerated in all six patients at two dosage levels. However, other recent AAV clinical trials raised the question about the utility of these vectors because of their immunogenicity.

### *1.3.6.3 AAV Immunogenicity*

In most inbred murine models of DMD, AAV can evade the immune system; however, this is not the case in severe murine and canine models of DMD, as well as in humans. AAV IM administration in the murine gamma sarcoglycan-null model of DMD and the beagle-based canine model of DMD ($CXMD_J$) elicited a strong cellular and humoral immune response to the transgene, resulting in transient gene expression (156, 157). The same observations hold true for AAV2 and AAV6 IM administration in out bred wild-type dogs, independent of the transgene expressed or muscle injected (158), thus eluding to the likely immunogenicity in humans. AAV immunogenicity in humans was later described as a result of a study involving IV, hepatic administration in clinical trial for hemophilia, which caused an inflammatory response and production of capsid-specific $CD8^+$ T cells (159). These results and others caused researchers to reexamine AAV as an immunogen. It was hypothesized that this response was caused by capsid-specific neutralizing antibodies and memory CD8 T cells from previous exposures to wild type AAV-2 (160). In the general population, there is a wide spread exposure to AAV-2 early in life (160); 10-20% of humans have neutralizing antibodies against AAV-2 in childhood, and 30% as adults (161, 162). Overall, the degree of the AAV specific immune response is affected by the vector serotype, nature of the transgene, and the dose and route of administration (163). Taken together, AAV is a highly effective gene transfer vehicle to muscle, however its limited cloning capacity and the lack of knowledge about its immunogenicity in humans make it less attractive as a candidate vector for DMD.

### *1.3.7 Ad vectors DMD gene therapy*

### *1.3.7.1 First generation Ad vectors for DMD gene therapy*

Initial gene therapy studies with FGAds in *mdx* mice utilized the 6.3kb mini-DYS construct, as the full length DYS was too large to fit within the FGAd backbone (Figure 5). As previously mentioned, evidence from transgenic mouse studies indicates that mini-DYS was functionally corrective (111). Initially, mini-DYS expression from FGAds was shown to be localized to the sarcolemma of 5-50% of neonatal *mdx* muscle fibers persisting up to 6 months PI (164-166). Although encouraging, the correct localization of DYS does not necessary translate to functional improvement (167).

Functional studies show that even variable mini-DYS expression from FGAds improved the force drop of young *mdx* hind limb muscle by 1.4-fold (168). In adult *mdx* mice, mini-DYS expression only modestly improved the twitch (33% increase) and maximal force (14% increase) in the hind limb muscle, but not in the diaphragm (169). It was speculated that the dose required to achieve functional correction by expression of mini-DYS in adult *mdx* muscle approaches the threshold for FGAd induced toxicity. Beyond a FGAd-mini-DYS dose of $5x10^{11}$ viral particles/ml, the maximal force generated by the diaphragm actually worsened (169). These and other studies using transgenic mice (170), severe combined immunodeficiency (SCID) mice (171), and immunosuppressive treatment were critical in elucidating the role of the immune system in FGAd toxicity in muscle (172-174).

Delivery of utrophin is an attractive gene therapy method since utrophin is endogenously expressed in human DMD and therefore no immune response would be mounted against it. Utrophin is a homolog of DYS (Figure 5) and it is thought to bind actin and DYS-associated proteins but its expression is limited to the neuromuscular junctions

(108). Similar to DYS, full length utrophin was too large to fit within the cloning limits of FGAds; therefore, truncated utrophin (approximately 6kb) was used for FGAd studies. In direct comparison, mini-DYS and mini-utrophin expressed from FGAds have the same capability for force restoration in immunologically immature neonatal *mdx* mice (175). It has been shown that truncated utrophin expressed from FGAds was correctly localized at the sarcolemma in young *mdx* muscle at levels several fold higher than endogenous utrophin (176). Stable utrophin expression in 32% of neonatal *mdx* hind limb muscle fibers did not affect maximal force generation but did improve the force deficit by 1.6-fold compared to untreated muscle (177). However, a specific humoral response was elicited in response to the truncated utrophin transgene despite a 92% sequence identity to the endogenous murine utrophin (177). Thus, it is imperative to deliver the full length endogenous therapeutic construct or risk mounting immune response triggered by the FGAd vector.

### *1.3.7.2 HDAds vectors for DMD*

Initial HDAds encoded the full length DYS and restored DYS and DYS-associated proteins to the sarcolemma, while significantly decreasing the proportion of centrally nucleated fibers in *mdx* muscle (178-181). *In utero* HDAd delivery of DYS demonstrated that even very low transduction efficiency (5% of muscle fibers) can improve tetanic force in *mdx* muscle by 21%, achieving 78% of wild type tetanic force production at 9 weeks PI (110). In contrast to prenatal muscle, neonatal muscle was transduced at a much higher efficiency by HDAds (182, 183). In neonatal muscle, 42% of muscle fibers stably express DYS beyond a year PI, despite the induction of a humoral response against DYS (182, 183). This high level of long-

term DYS expression improved the twitch force and tetanic force (achieving up to 88% and 80% of wild type force production, respectively) and reduced the force deficit in *mdx* muscle (7 to 8-fold higher than wild type force levels) (182, 183). These effects were also maintained for at least 1 year after administration (182, 183). Furthermore, HDAd delivery of DYS to neonatal utrophin/dystrophin dko mice increased their weight, lifespan and improved gait length and locomotor activity (184). However, HDAd delivery to juvenile *mdx* hind limb muscle was less efficient, transducing 2.7-fold fewer muscle fibers than in neonatal *mdx* mice (182). Thus, no improvement of twitch and tetanic force was observed in the hind limb of juvenile mice, but the force deficit was reduced by 1.1-fold, making the force deficit of treated mice 2.2-fold higher than wild type force levels (182). HDAd transduction of the juvenile *mdx* diaphragm was comparable to that in the hind limb; restoring DYS expression to 23% of muscle fibers reduced force deficit by 0.7-fold, achieving force production 1.3-fold higher than wild type levels (185). In adult *mdx* muscle, restoring DYS expression to 25-30% of the cross sectional area of hind limb muscle did not improve maximal and specific force, but improved lengthening contraction force by 25%, attaining 62% of wild type force levels (186). In summary, HDAd delivery of full length DYS has been shown to significantly improve at least one measure of force production at all stages of *mdx* mouse development.

A humoral immune response can be triggered by the full length DYS, thus negating any functional corrective effects of the gene therapy treatment (170, 186, 187). In *mdx* mice, DYS is recognized as 'foreign' and thus immunosuppressive treatment improves persistence of DYS expression (173). Another approach used to attenuate the immune response to the

therapeutic gene is to utilize the endogenous DYS homolog, utrophin (Figure 5). Like DYS, full length utrophin is functionally more effective than its truncated forms (188). HDAd delivery of full length utrophin decreased the force deficit in neonatal mice by 2.1-fold (189), while a comparable study using FGAd delivery of mini-utrophin only decreased the force deficit by 1.6-fold (177). In neonatal muscle, HDAd delivery of full length utrophin transduced 58% of muscle fibers, improving the twitch force and tetanic force (0.8 and 1.2-fold, respectively) measured at 2 months PI (189). However, utrophin expression rapidly decreased thereafter as a mild immune response was elicited, likely in response to the HDAd virion. Thus, by 8 months PI, an improvement of force was no longer observed (189). It is also important to note that HDAd delivery of full length utrophin to adult *mdx* muscle was 2.7-fold less efficient than in neonatal muscle and did not improve force generation in adults (189). Therefore, utrophin delivery from an Ad vector has been shown to restore force production in some stages of *mdx* development. Taken together, the HDAd mediated functional correction of the *mdx* phenotype by DYS or utrophin delivery is dependent on the age of intervention and achieving maximal transduction efficiency in muscle.

## *1.4 Research Objectives*

The goal of this work was to improve the Ad gene therapy vector system using two complimentary approaches:

1. Improve Ad vectors for muscle directed-gene therapy.

2. Optimize the murine secreted embryonic alkaline phosphatase (mSEAP) reporter gene.

The first approach was the primary focus and the priority of this thesis as Ad transduction in muscle must be improved to maximize the utility of the vector system for DMD gene therapy applications. Recognizing that initial vector characterization involves testing the efficacy of vector function in murine models of disease, the second approach was undertaken to improve a non-immunogenic reporter gene, ideal for assessing long-term vector function. Together, both approaches address the vector requirements for DMD gene therapy, namely the research goals were to achieve efficient Ad vector transduction in a high number of muscle fibers and develop a tool that would be necessary to describe long-term transgene expression from this improved vector system.

### *1.4.1 Improvement of Ad vectors for muscle-directed gene therapy*

In order to exploit the utility of HDAd vector system as effective gene therapy vectors for DMD, Ad transduction in muscle must be improved. Herein, the barriers to Ad transduction in muscle are identified in an attempt to design a strategy to circumvent their effect.

#### *1.4.1.1 Strong liver tropism*

Following IV delivery of Ad, 90% of the vector genomes are eliminated within 24 hours post-administration, independent of vector dose, viral expression cassette, or immunocompetency of the host (84). Fenestrations of the liver easily trap Ad circulating in the blood, facilitating transduction of resident Kupffer cells (190). Ad transduction of liver cells can occur in a CAR independent manner via an interaction with Ad hexon and coagulation factor (F)X (191, 192). The FX-hexon complex is taken up by hepatocytes through heparin sulfate binding with FX (192). To overcome this rapid vector clearance,

higher doses of Ad vectors are required to achieve therapeutic levels of gene delivery in the tissue of interest. However, administering higher doses of Ad vectors increases the risk of lethal liver toxicity (193). Therefore, efforts to ablate the Ad liver tropism, retarget Ad, and enhance localized delivery are necessary to improve the function and safety of Ad vectors (193).

Various strategies have been employed in attempt to reduce the Ad liver tropism by exploiting specific ligand-receptor interactions (reviewed in (194)). The Ad capsid can be chemically modified by the covalent attachment of inert polyethylene glycol (PEG) polymers that shield Ad from neutralizing antibodies and enzymatic degradation, which improves Ad circulation kinetics *in vivo* by reducing Ad uptake in the liver. Further, the attachment of ligands to the PEG polymers, like an RGD binding motif that mediates Ad internalization through integrin binding, can facilitate Ad infection of malignant tumors (reviewed in (195). Molecular adaptors can also bridge an interaction between the Ad capsid and targeting ligand; these bi-functional fusion proteins commonly use anti-capsid antibodies or CAR fragments fused to a ligand of interest (194). Genetic incorporation of foreign peptides to exposed regions of the Ad capsid is the most direct approach to modifying vector tissue tropism (194). Of the many possible regions that can be modified in the Ad capsid, the H-I loop in the knob domain of fiber is the most efficient location for successfully retargeting Ad using small 83 amino acid polypeptides (196). Polylysine modifications in this region of the Ad5 knob causes the vector to elicit less liver toxicity, producing less IL-6 serum production (197). Ad protein IX can display larger polypeptides like enhanced green fluorescent protein (EGFP) (198, 199) and single chain antibodies (200). Finally, the CAR

binding requirement of Ad5 vectors can be expanded by swapping the fibers with serotype B Ads such that the new chimeric vectors bind CD46, which is present on many cell types (201).

### *1.4.1.2 Maturation dependent infectivity of muscle*

The CAR dependency of Ad5 based vectors substantially limits their efficacy in muscle. It is well characterized that Ad does not efficiently transduce muscle because its primary receptor is not prevalent on mature muscle (202, 203). Ad transduction is more efficient in young muscle compared to adult muscle because CAR is differentially expressed (202-204). CAR is up-regulated in regenerating muscle fibers and FGAds preferentially transduce myofibers that express CAR such that forced muscle fiber regeneration by crush injury or neurotoxin improve Ad transduction in adult muscle (205-207).

It was previously shown that genetically modifying the H-I loop of the knob domain by the addition of a polylysine motif retargets Ad5 to the highly prevalent heparin sulfate and improves transduction in muscle *in vitro*, but this effect is greatly attenuated *in vivo* (208). It is hypothesized that the extended tropism of the vector is still limited by the protective basal lamina surrounding mature muscle (209).

### *1.4.1.3 Basal lamina*

The basal lamina may act as a physical barrier preventing efficient Ad transduction in muscle (209-211). The basal lamina is a component of the extracellular matrix; this molecular mesh, mostly composed of collagen and laminin, surrounds muscle fibers and provides mechanical support as well as orients muscle regeneration (212, 213). Immature

myoblasts have a poorly developed basal lamina, the maturation of which proceeds along with differentiation (214). The basal lamina was first implicated as a barrier to HSV-1 vector transduction in adult muscle (215). The HSV-1 vectors were unable to penetrate the mature basal lamina surrounding adult muscle but were able to transduce mature dy/dy merosin deficient muscle that have impaired extracellular matrices (215). This phenomenon was also observed with Ad vectors. Studies that deliver Ad vectors intramuscularly have reported high transduction efficiency, up to 70-90% of muscle fibers, restricted within a distinct compartment or group of muscle fibers, and not throughout the entire muscle (206). Meulenbroek et al. (198) described that at 30 minutes post-IM injection, Ad particles remain primarily at the site of injection. This lack of viral dispersion *in vivo* contributes to the inefficient nature of Ad transduction in muscle. *In utero* delivery of therapeutic viral vectors is reported to achieve higher transduction and greater viral spread because the muscle mass is small and the basal lamina and connective structures are not yet formed (110, 215). Efficient Ad gene transfer has also been observed in neonatal mice, explained in part because of their underdeveloped basal lamina (203, 216). Furthermore, Ad vectors transduce merosin-deficient muscle fibers greater than 80-fold more efficiently *in vitro* and *in vivo* compared to normal muscle (209).

#### *1.4.1.4 Rationale*

The basal lamina acts as a fine passive molecular sieve; the average size of the mesh that a vector must cross to achieve transduction through the plasma membrane is approximately 40nm in diameter (212). Due to its small size of 20nm in diameter, AAV is not blocked by the mature basal lamina *in vivo* and is able to transduce muscle with a high

efficiency (217). Since Ad5 is 162nm in diameter, the basal lamina is likely a significant barrier to Ad transduction *in vivo* (218). Therefore, decreasing the overall size of the adenovirus particle may overcome the barrier of the basal lamina and enhance transduction in muscle.

### *1.4.1.5 Hypothesis*

*Decreasing the overall diameter of the Ad virion will improve transduction in muscle.*

Restrictions imposed on Ad capsid symmetry limit the manipulation and reduction of its overall size (219). Further, the elimination of the fiber, which protrudes out from the viral capsid, reduces the viral stability and abolishes transduction (220). Therefore, the diameter of the Ad virion was reduced by decreasing the fiber length.

### *1.4.1.6 Specific Objectives*

1. Generate first generation Ad5 based viruses with modified fibers .
2. Compare transduction efficiency of the fiber-modified viruses *in vitro.*
3. Compare the transduction efficiency of fiber-modified viruses in normal muscle.
4. Compare the transduction efficiency of the fiber-modified viruses in *mdx* muscle.

First-generation Ad vectors were designed to investigate the effect of fiber-modified viruses on transduction *in vitro* and *in vivo*. FG-Ads were used in this study instead of HDAds to perform the basic science needed to improve Ad transduction in muscle because they were easier to generate, rescue, and amplify by standard protocols compared to HDAds. The goal of this work was to test a hypothesis that evaluates a particular strategy for vector

design, the implications of which may improve HDAd delivery system towards the achievement of long-term functional correction in *mdx* muscle.

In accordance with improving vectors for gene therapy, a second approach is presented in chapter 3. The reporter gene mSEAPΔ-H451E is described, which is designed to be non-immunogenic and ideal for efficiently tracking long-term vector function in murine experimental models.

### *1.4.2 Optimization of the murine secreted embryonic alkaline phosphatase (mSEAP) reporter gene*

Gene therapy has immense potential for the treatment of human disease. Current challenges in gene transfer vector design include reducing their inherent toxicity and improving transgene expression in target tissues (47). The success of gene therapy is contingent upon (i) the safe and efficient delivery of the therapeutic gene to specific target cells and (ii) ensuring the appropriate level and duration of therapeutic gene expression (221). Vectors designed for gene therapy must be optimized, demonstrating efficiency *in vitro* and *in vivo*. Much work in the field of gene therapy is focused upon physically or genetically modifying the best vector system applicable to the therapeutic strategy to improve vector targeting and gene expression. Optimization of these modifications requires a means of sensitively detecting viral gene expression so that vector targeting, transduction efficiency, and the duration of the gene expression can be determined.

Studies on vector function commonly use reporter genes in place of the therapeutic transgene due to their ease of detection. Among the many reporter genes available, the

most commonly used are: green fluorescent protein (GFP), β-galactosidase, luciferase and human secreted placental alkaline phosphatase (hSEAP). Each reporter gene differs in terms of sensitivity, endogenous background activity, and ease of histochemical detection; however, all of these reporter genes are immunogenic in mice. The human alpha-feto protein (AFP) (222), alpha-1 antitrypsin (AAT) (223), and carcinoembryonic antigen (CEA) (224) reporter genes are also used in gene therapy studies. Although these reporter genes are appropriate for monitoring vector function in some models, they are not ideal for immune-competent murine studies because of the difficulty of their detection and their likely immunogenicity due to their human origin.

Previously, the Parks lab described the development of murine placental-derived secreted embryonic alkaline phosphatase (mSEAP) as a sensitive, non-immunogenic reporter gene in mice (225). mSEAP was expressed from an Ad vector at high levels *in vivo* up to a month post-IV injection. In contrast, hSEAP expression levels declined gradually to background, due to the production of antibodies against the human protein. The mSEAP reporter gene also proved crucial in characterizing the immune response to HDAds (55), whereupon it was observed that in the absence of anti-transgene immunity, HDAd vectors induce attenuated immune responses. HDAd vectors expressing β-galactosidase and not mSEAP, elicited a significant immune response characterized by enhanced cytokine and chemokine expression in the liver as well as CD3 infiltration and cytotoxic T lymphocyte (CTL) response (225). Thus, in the context of HDAd, immune responses to the transgene protein ultimately compromise vector function.

Although mice encode several different alkaline phosphatase (AP) genes, mSEAP has the closest homology to hSEAP (226). Much like mSEAP, native hSEAP remains mostly cell associated due to a hydrophobic tail and phosphatidylinositol glycan (GPI) linkage (227). However, the commercially available hSEAP has been engineered for higher levels of secretion through the removal of the hydrophobic tail (228), and is naturally heat stable, whereas mSEAP is not (229). Since all cells have some level of endogenous AP activity, the inability to reduce background AP activity through heat treatment of samples reduces the sensitivity of mSEAP.

### *1.4.2.1 Rationale*

In this project, the remaining drawbacks of the mSEAP construct are addressed, namely poor secretion and heat stability. The strategy was to modify mSEAP to mimic the secretion and heat stability of hSEAP. mSEAP contains a C-terminal transmembrane domain that allows it to remain cell associated. The identical approach used to make hSEAP secretable could be employed to improve the secretion of mSEAP, specifically by removing the C-terminal transmembrane domain (230). In addition, the residue responsible for the heat stability of hSEAP has been identified as glutamic acid-429, which is located in the crown domain of the protein (231). However, a histidine is in place of the glutamic acid at this key site in the mSEAP construct. Therefore, the analogous residue to Glu-429 in mSEAP , or His-451, could be mutated to improve its heat stability.

### *1.4.2.2 Hypothesis*

*The heat stability of mSEAP and its release from the cell will be improved by mutating the histidine to a glutamic acid at position 451 on the mSEAP construct and by truncating the C-terminal transmembrane domain, respectively.*

### *1.4.2.3 Specific Objectives*

1. Generate a C-terminal truncated mSEAP construct and test the efficacy of AP release from the cell as expressed from DNA plasmids *in vitro*.

2. Generate the histidine to glutamic acid mutation at position 451 of the mSEAP construct and test its heat stability as expressed from DNA plasmids *in vitro*.

3. Demonstrate the efficacy of the modified mSEAP reporter constructs *in vitro* as expressed from FGAd vectors.

# *Chapter 2: Methods and Materials*

## *2.1 Cloning*

### *2.1.1 Cloning of Ad5s, Ad5/9s, Ad5/35s*

Small scale preparations of DNA plasmids were prepared according to the alkaline lysis method as described in Birnboim and Doly (232) and large scale preparations of DNA plasmids were prepared using the cesium chloride purification method as described in Sambrook et al. (233). Standard reagents for these methods are described in Appendix I.

Fiber-modified viruses were generated using Ad5s, Ad5/9s, and Ad5/35s chimeric fiber constructs generously provided by Dmitry Shayakhmetov (University of Washington, Seattle, USA). These plasmids encoded E1/E3-deleted Ad5 vectors, which contained the chimeric fiber in the endogenous fiber locus and expressed an EGFP transgene (234). The *lacZ* transgene was ideal for the purposes of this study because it enables the quantification of vector transduction both *in vitro* and in muscle lysates using a chemiluminescent assay. Therefore, the following cloning strategy was used for the generation of all three fiber-modified FG-Ad vectors expressing *lac*Z under the control of the CMV promoter. First, the AgeI-MfeI (New England Biolabs, NEB) fragment corresponding to the chimeric fiber construct (Ad5s: 1069bp, Ad5/9s 1093bp, Ad5/35s: 992bp) was isolated from the original plasmids. Using the same restriction sites, the AgeI-MfeI fragment was cloned in place of the endogenous fiber locus in a 'shuttle' plasmid containing only the endogenous Ad5 fiber and flanking Ad5 DNA sequences within in pBluescriptII backbone (pRP2397). The resulting

shuttle plasmid provided the necessary flanking Ad5 DNA required for the subsequent homologous recombination as described in Chartier *et al.* (235)(following linearization with XbaI (NEB)) of the chimeric fiber into the E1/E3 deleted Ad5 vector backbone (pRP2468). The pRP2468 plasmid is a derivative of pRP2014, which is an E1/E3 deleted FGAd5 vector backbone that is commonly used in the Parks lab. pRP2468 has been deleted from the wild-type Ad5 fiber locus (nt 31042 to 32787 of the conventional Ad5 genome). In place of fiber is a unique BstBI site that allows for linearization for homologous recombination with the pRP2397 derivatives described above. The resulting plasmids with the chimeric fiber in the FGAd5 backbone were then linearized with Bsu15I (MBI Fermentas) and recombined with pCA38 (236) (linearized with EheI, (NEB)) in order to insert the CMV-*lac*Z transgene expression cassette into the E1 region.

### *2.1.2 Cloning of mSEAPΔ*

pBS-mSEAP (225) was used as a template for the amplification of mSEAPΔ by polymerase chain reaction (PCR). Synthetic oligonucleotides were designed to remove 14 amino acids (510-542) from the C-terminus of mSEAP. The sense primer used was 5'-CAG *GAA TTC* GTA CAC CAT GAT CTC ACC ATT TTT AG- and the antisense primer used was 5'-GCG *AAG CTT* TAC CCT GGG GAG GGT GCG CTC CC (EcoRI and HindIII sites are shown in italics). The resulting PCR product was digested with EcoRI and HindIII and cloned into pBluescript II KS (+) and designated pKW4. The mSEAPΔ sequenced was verified (Stemcore, Ottawa, Ont), and cloned into pcDNA3-Ubc under the control of the ubiquitin C (Ubc) promoter and the bovine growth hormone (BGH) polyadenylation sequence, and designated pKW8. To generate AdmSEAPΔ, the mSEAPΔ sequence in pKW8 (a BamHI and XbaI 1665bp fragment)

was ligated into pShuttle-Ubc-mSEAP (digested with BamHI and XbaI), replacing the mSEAP sequence, where the resulting plasmid was termed pKW14. The pShuttle-Ubc-mSEAP plasmid previously generated in the Parks lab was a pShuttle derivative with Ubc promoter (kindly provided by Dr. Doug Gray, Ottawa Health Research Institute, Ottawa, Canada) driving expression of mSEAP. An infectious plasmid was generated by homologous recombination of pKW14 and pRP2014 (233). pRP2014 an E1/E3 deleted FGAd5 vector backbone that is commonly used in the Parks lab.

### *2.1.3 Cloning of mSEAPΔ-H451E*

pKW8 was used to generate the mSEAPΔ-H451E mutant construct (Figure 16 C) by site directed mutagenesis through overlap PCR. The sense primers used to generate mSEAPΔ-H451E was 5'GCG *AGC GCT* GTT CCC CTG CGC GAG GAG ACC CAC GGT GGA GAA-3' and the antisense primer was 5'-GCG *AGC GCT* CTG GGC CTG GTA GTT GTT GTG-3' (unique Eco47III restriction sites are shown in italics). PCR using these oligonucleotides amplified around the plasmid in both directions, and resulted in a linear DNA molecule which was digested with Eco47III and re-circularized. The sequence of the mutant mSEAPΔ gene was verified (Stemcore, Ottawa, Ont), and cloned into pcDNA3-Ubc under the control of the Ubc promoter and the BGH polyadenylation sequence, termed pKW22. To generate AdmSEAPΔ-H541E, the mSEAPΔ-H551E sequence in pKW22 (a SgrAI and EheI 5339bp fragment) was ligated into pShuttle-Ubc-mSEAP (digested with SgrAI and EheI), replacing the mSEAP sequence, the resulting plasmid was termed pKW28. An infectious plasmid was generated by homologous recombination of pKW28 and pRP2014 (233).

### *2.1.4 Cloning of AdmSEAP, AdhSEAP*

The previously described E1/E3 deleted vector expressing mSEAP and hSEAP (AdmSEAP and AdhSEAP, respectively) in Maelandsmo *et al.,* (225) encoded the CMV promoter and SV40 polyadenylation signal. Therefore, analogous E1/E3 deleted vectors were generated expressing hSEAP and mSEAP under the regulation of the Ubc promoter and the BGH polyadenylation sequence using a similar cloning strategy used for AdmSEAPΔ and AdmSEAPΔ-H451E. The infectious AdmSEAP plasmid was generated by homologous recombination of pShuttle-Ubc-mSEAP (linearized with Bst1107I) with pRP2014 (linearized with Bsu15I). To generated AdhSEAP, the hSEAP sequence within pRP2618 (SpeI and XhoI 1665bp fragment) was ligated into pShuttle-Ubc-mSEAP (digested with SpeI and XhoI); the resulting plasmid was termed pKW15. pRP2618 was previously produced in the Parks lab and is a pCDNA3 derivative (Invitrogen) with the CMV promoter replaced by an Ubc promoter that drives expression of hSEAP. pKW15 was homologously recombined with pRP2014 to generate the infectious hSEAP plasmid.

## *2.2 Cell and Virus Culture*

### *2.2.1 Virus culture*

Infectious plasmids were digested with PacI (NEB) to release the viral genomes and were transiently transfected into 293 cells (62). The cells were then overlaid with agarose so that the corresponding viruses could be rescued from individual plaques. Viral vectors were rescued, propagated, and purified by standard methods (237). The genomic content of the fiber-modified viruses was verified by isolating the viral DNA and verifying appropriate banding pattern by electrophoresis after digestion with appropriate restriction

enzymes. Viruses were titrated in infectious units by plaque-forming unit (pfu) assay and β-galactosidase (β-gal) forming units assay (BFU) (237). The number of viral particles/ml was also determined using two methods: (i) determining $OD_{260}$ with a spectrophotometer (237) and (ii) the FluoStar method using the Quanti-iT PicoGreen dsDNA reagent (Invitrogen) according to the manufacturer's instructions. Briefly, serial dilutions (1/10, 1/100, and 1/1000) of the virus were compared to a DNA standard (Herring Sperm DNA, Invitrogen) of 50ng/100ul dilutions of ½, ¼, up to 1/2054 in 10mM Tris and 0.1% SDS that were individually aliquotted in duplicate into a 96 well plate (Corning). Before reading the fluorescence intensity (FLUOStar, BMG Labtech, Gmbh, Durham, NC), a solution containing the PicoGreen dsDNA reagent (Molecular probes) diluted 1/200 in 10mM Tris and 0.1% SDS was added to the samples in the 96 well plate in a proportion of 1:1 v/v. To determine the number of virus particles in the serial dilutions, the fluorescence intensity values were plotted on a DNA standard curve using the known concentrations of DNA dilutions vs. the fluorescence readings where 1ug of DNA equals $2.2x10^{10}$ virus particles.

### *2.2.2 Cell culture*

Human alveolar epithelial cells (A549, human lung carcinoma ATCC CCL 185) and HEK 293 cells (62) were maintained on 150mm plates (Sarstedt) in minimal essential medium (MEM, Sigma) supplemented with 10% fetal bovine serum (FBS, Hyclone), 1% antibiotic/antimycotic (Invitrogen), and 1% glutamax (Invitrogen). A549 cells were passaged when confluent by washing twice with Dulbecco's phosphate buffered saline (DPBS) (Hyclone) and incubating with 2ml of 1X trypsin for 10 min at 37°C, 5% $CO_2$. The 293 cell line was passaged when confluent by rinsing twice with 1X citric saline and incubating for 10

minutes at 37°C, 5% $CO_2$ in a minimal volume of 1X citric saline. Undifferentiated $C_2C_{12}$ cells (CRL-1772) were maintained in Dulbecco's minimal essential medium (DMEM, Sigma) supplemented with 10% FBS, 1% antibiotic/antimycotic (Invitrogen), and 1% glutamax (Invitrogen) and passaged when 75% confluent by washing twice with DPBS and incubating with 2ml of 1X trypsin for 10 min at 37°C , 5% $CO_2$. $C_2C_{12}$ cells were differentiated by plating $1x10^6$ cells on a 35mm tissue culture dish (Sarstedt), and the next day the media was discarded and the monolayer was rinsed twice with DPBS and the differentiation medium (0.5% FBS DMEM supplemented with 1% antibiotic/antimycotic and 1% glutamax) was added to the monolayer (Day 0). On day 3, the medium was removed and replaced with fresh differentiation medium. The differentiation time course was complete by day 4 when *in vitro* experiments began.

## *2.3 In vitro Analysis*

### *2.3.1 Ad Infection*

Frozen viral stocks in 200µl aliquots were thawed at room temperature. Using the following calculation, a volume of virus corresponding to a multiplicity of infection (MOI) of 20 virus particles per cell was diluted in 100ul of DPBS.

$$Volume\ of\ virus = \frac{(total\ \#\ of\ cells)(MOI)}{(Virus\ particles/ml)}$$

This innoculum was vortexed and added to a monolayer of $1x10^6$ cells plated on a 35mm dish after the media was removed and discarded. Cells were incubated in the innoculum for

1 hour at 37°C, redistributing the virus by gentle rocking of the dish every 15 minutes. After 1 hour, fresh maintenance media (either MEM or DMEM supplemented with 10% FBS, 1% antibiotic/antimycotic and 1% glutamax) was added to the dish. The infection was terminated 24 hours later and cells were prepared either for β-gal staining or harvested for a β-gal chemiluminescent assay.

### *2.3.2 In vitro β-gal Stain*

At 24 hours post-infection, media was removed from the 35mm tissue culture dish and 1ml of β-gal fixative was gently added over the monolayer. After 10 minutes at room temperature, the β-gal fixative was discarded and 1ml of β-gal stain supplemented with 1mg/ml of X-gal was added over the monolayer. Tissue culture dishes were incubated at room temperature in the dark over night and representative photomicrographs were taken of the stained monolayers (Axioplan2, AxioCam, Zeiss).

### *2.3.3 AP Activity Assay*

Thirty-five millimeter dishes of HEK 293 cells were transfected in duplicate with 1.5 μg of the various mSEAP or hSEAP constructs and 0.5 μg of pCA35 expressing β-gal using the Superfect reagent (Qiagen). At 18 hours post-transfection, 500μl of media was harvested from the tissue culture dish. The remaining media was discarded and the cell monolayer was incubated with 300μl of reporter lysis buffer (Promega) for 10 minutes; the resulting cell lysate was scraped from the plate and harvested. The media and cell lysate samples were stored at -80°C until assaying for AP activity and β-gal activity to normalize for transfection efficiency (using a chemiluminescent kit (Roche) according to the manufacturer's instructions).

To examine the effect of heating on native mSEAP and its derivatives, samples were incubated at 55 or 65°C for 30 minutes prior to assaying for AP activity using a commercially available chemiluminescent kit (Roche) according to the manufacturer's protocol with the following modifications: the incubation step with the inactivation buffer was omitted. Endogenous AP and mSEAP was sensitive to the L-homoarginine included in the inactivation buffer (data not shown). The inactivation buffer was subsequently excluded from further analysis in order to compare the susceptibility of the mutant mSEAP construct to heat inactivation.

To test function of the mSEAP constructs expressed from the Ad5 vector, A549 cells were infected with a multiplicity of infection (MOI, in plaque forming units per cell) of 20 for 1 hour and at 18 hours post-infection, media was harvested, treated at 55°C for 30 min to inactivate endogenous AP and assayed for AP activity as described above.

### *2.3.4 Chemiluminescent β-gal Assay*

Cells were prepared for the chemiluminescent assay by removing the media and incubating the monolayer for 10 minutes at room temperature with 1X reporter lysis buffer (Promega). The monolayer was scraped with plastic scrapers (Corning) and the cell lysate was dispensed into sterile microfuge tubes, and stored at -80°C. Samples were thawed on ice prior to the β-gal assay. To insure the A549 and 293 cell lysate readings were within the β-gal linear range of the luminometer (5,000 to 5,000,000 relative light units (RLU)) (Lumat LB 9507, Berthold Technologies, Mandel Scientific, Guelph, Ont) these samples were diluted 1 in 100 in 1X reporter lysis buffer. Differentiated and undifferentiated $C_2C_{12}$ cell lysates

were undiluted and assayed directly. All samples were centrifuged at 20,000xg for 2 minutes at room temperature then processed using the GalactoStar β-gal assay kit (Applied Biosystems) as per the manufacturer's instructions.

## *2.4 In vivo analysis*

### *2.4.1 Mouse Injections*

All animal experiments were performed in accordance with the Canadian Council of Animal Care Guidelines and the University of Ottawa Animal Care Committee, with the aid of the University of Ottawa Animal Care and Veterinary Service (ACVS). Adult (up to 23 weeks of age) or 2-5 week old female C57Bl/6J mice (Charles River Laboratories, Wilmington, MA) and 2-5 week old female *mdx* mice (Jackson Laboratories, Bar Harbor, ME) were obtained and quarantined for 1 week prior to manipulation. The specific age at which mice were obtained was designed to coincide with massive muscle degeneration observed at 3-5 weeks of age in *mdx* mice (97, 98, 238). Therefore, 2-5 week old *mdx* mice were ordered such that mice could be administered viral vectors at 3 to 6 weeks of age then sacrificed either two or ten days later at approximately 3-6 weeks or 4-7 weeks of age, respectively.

Respiration and cardiac function were monitored and the mice were marked for identification by the ACVS. Prior to injection, experimental animals were anesthetized by halothane (10ml/kg/hour of anesthesia) and received a warm saline IP injection for hydration; sterile ophthalmic ointment was applied around the eyes to avoid corneal desiccation while under anesthesia. The hind limb was shaved and sterilized with iodine.

Using 3/10cc syringes (BD Biosciences) with the bevel side down, 25ul of the injection solution ($1x10^9$, $3x10^9$, or $1x10^{10}$ virus particles or $1x10^9$ 190nm fluorescent polystyrene beads (Bangs Laboratories Inc., Fishers, IN) in PBS) was carefully administered at an approximate 60° angle into the belly of the TA muscle, penetrating 2mm below the skin (depth was measured using a plastic injection guard). Both TA mouse muscles were injected with the same solution and animals were returned to their cage for recovery.

### *2.4.2 Tissue preparation*

#### *2.4.2.1 Tissue Removal*

At two or ten days post-injection, mice were euthanized by an overdose of sodium pentobarbital followed by cervical dislocation. Livers were removed, wrapped in tin foil and immediately frozen in liquid nitrogen. The TA muscle was removed and either prepared for homogenization or sectioning. In preparation for homogenization, TA muscles were placed in a liquid nitrogen cooled cryovial (Sarstedt) and the liquid nitrogen was carefully decanted out of the cryovial and capped. In preparation for sectioning, muscles were embedded in OTC mounting medium (Tissue-Tek, Elkhart, IN) within a mould (made from a longitudinally cut 1ml disposable pipette tip). Using forceps, the sample was lowered into liquid nitrogen cooled isopentane (Sigma) to gradually freeze the muscle tissue, maintaining its structural integrity. Once frozen, the muscle contained within the OTC medium was placed in a cryovial. All samples were stored at -80°C until use.

### *2.4.2.2 Tissue Homogenization*

Homogenization of liver and TA muscle was performed as previously described (239). Briefly, samples were removed from storage at -80°C and thawed on ice in 3ml of PBS in 13ml tubes. Samples were processed with a tissue homogenizer (Fisher) for 15s, sonicated (Vibra cell, Sonics & Materials Inc., Newton, CT) twice for 15s each, and then centrifuged at 700xg for 5 minutes. The resulting supernatant was decanted into new 13ml tubes that were heated for 15 min in a 50°C water bath to reduce background activity. The liquid was transferred into 1.5ml microfuge tubes and centrifuged at 20,000xg for 10 minutes at room temperature. Finally, the resulting supernatant was decanted into fresh microfuge tubes that were subsequently stored at -80°C until assayed for β-gal activity.

### *2.4.2.3 Sectioning*

Ten micrometer thick longitudinal or cross sections of TA muscle were prepared at -16°C using a cryostat (CM 1850, Leica Microsystems, Wetzlar, Germany). Sections were dry mounted on a series of 4 microscope slides (termed A, B, C, and D series) (SuperFrost Plus, Fisher) through the entirety of the muscle. For example, to generate four series of slides with representative sections throughout the whole of the muscle, the first section was mounted on slide A, the second on slide B, third on slide C, fourth on slide D, and the fifth on slide A etc. Slides were stored in air tight slide boxes at -80°C containing a filter paper moistened in 50% glycerol solution to maintain humidity of the chamber upon thawing. Subsequent histochemical processing was performed on an entire series (ie. A or B) of muscle sections.

### *2.4.3 Detection of transgene expression*

Two methods were used to detect transgene expression. To quantify the overall amount of transgene expression achieved in the entire tissue, β-gal chemiluminescent assay was performed on undiluted tissue homogenates as described above. Histochemistry was performed on frozen sections to assess viral dispersion.

#### *2.4.3.1 Histochemistry*

The slides were thawed at room temperature within their humidified storage containers. Once equilibrated, the slides were transferred to a humidified chamber for subsequent staining procedures and immediately fixed with β-gal fixative (See Appendix I: Reagents). After 5 minutes, slides were washed 3 times for 5 minutes with PBS. Two milliliters of β-gal stain supplemented with 1mg/ml of X-gal was added to each slide; the humidified chamber was sealed and set in the dark for 4-5 hours. The slides were washed twice for 5 minutes with PBS, and twice in distilled water prior to counterstaining with eosin alone or eosin and Hoechst. The slides that were counterstained with eosin alone were dipped in eosin for 10 seconds, dehydrated through a series of ethanol washes (70%, 95%, and two 100% ethanol) for two minutes each, followed by two washes with xylene. Excess xylene was removed by blotting the slides prior to addition of 3 drops of Permount (Fisher) and a glass coverslip (Fisher). The slides were stored at room temperature.

The slides were counterstained with eosin and Hoechst as follows: the slides were washed twice for 5 minutes with distilled water prior to application of Hoechst stain. Hoechst stain (0.05mg/ml, Fisher) was applied per slide and incubated for 10 minutes at room temperature. The slides were washed twice with distilled water for 5 minutes and

transferred to a slide rack for subsequent counterstaining in Wheaton staining dishes (Sigma). The slides were stained with eosin for 10 seconds then rinsed twice for 5 minutes in distilled water. The slides were removed from the slide rack, excess water was removed from the slides, and Dako fluorescent mounting medium (Dako) was applied directly to the slide prior to the addition of a coverslip. The slides were stored at -20°C.

### *2.4.3.1 Immunohistochemistry*

The slides were thawed at room temperature within their humidified storage containers. Once equilibrated, the slides were transferred to a humidified chamber and immediately fixed with 2.5% paraformaldehyde in PBS for 5 minutes at room temperature. The slides were rinsed twice with PBS, and incubated with blocking solution (1% bovine serum albumin (BSA, Sigma) and 0.5% Triton X-100 in PBS) for 1 hour at room temperature. The blocking solution was removed and a solution of primary antibodies was added and incubated for 1 hour at room temperature. The primary antibody solution contained a mixture of mouse anti-embryonic MHC (MHC (F1.652): sc-53091, Santa Cruz Biotechnology) and rabbit anti-B-gal (A-11132, Molecular Probes), diluted to 1:200 in blocking solution. After the primary incubation, the slides were washed twice with PBS for 10 minutes followed by 10 minute incubation with blocking solution. Next, slides were incubated for an hour in a secondary antibody solution in the dark; subsequent steps were also carried out in the dark. The secondary antibody solution contained a mixture of Rhodamine (TRITC) conjugated goat anti-mouse (115-025-044, Jackson ImmunoResearch) and Alexa fluor 448 conjugated Donkey Anti-rabbit (A21206, Invitrogen) diluted 1:200 in blocking solution. After

the secondary incubation, the slides were rinsed twice with PBS for each and stained with Hoechst as described above.

### *2.4.4 Microscopy*

Photomicrographs of stained muscle sections were obtained with a light microscope (Axioplan2, Zeiss) and a color camera (AxioCam, Zeiss). Muscle sections that contained fluorescent polystyrene beads were imaged directly, without fixation using a fluorescent microscope (Axioplan2, Zeiss) and a color camera (AxioCam, Zeiss). Images of entire muscle sections were compiled using Photoshop software (Adobe). The injection sites of the polystyrene beads were interpreted by examining a complete series of longitudinal muscle sections. Scoring criteria used in this study was developed as a combination of generally accepted protocols (240-242). Briefly, three of the largest sections through the belly of the muscle were randomly chosen for scoring since this portion of sections has the most muscle fibers and would effectively display transduced muscle fibers originating throughout the length of the muscle. ImageJ program was used to quantify the area of muscle cross section (243). The cell counter plugin written by Kurt De Vos (University of Sheffield) was downloaded from the ImageJ website and used to score the total number of muscle fibers and the number of muscle fibers stained with β-gal.

## *2.6 Statistical Analysis*

Data were averaged for each vector group and graphed with the standard error of the mean. All data were analyzed using SigmaStat software (Systat Software Inc., San Diego, CA) for subsequent analyses. If data were derived from a normal population with equal

variances, groups were compared using a one way Analysis Of Variance (ANOVA) where multiple comparisons were made using Tukey's test. In some cases, data differed by several orders of magnitude, making analysis of the data easily detectable by eye; these extreme conditions of data distribution are not appropriate for ANOVA analysis. In these cases, individual groups of data were directly compared using an unpaired t-test. If data displayed a non-normal population or populations with unequal variances, individual groups of data were compared with a Mann-Whitney rank sum test.

# *Chapter 3: Improvement of Ad vectors for muscle-directed gene therapy*

## *3.1 Introduction*

DMD is a debilitating muscle wasting disease affecting 1 in 3500 boys worldwide (1, 2). Currently, there are no effective treatments or a cure for this severe disease (16). Gene therapy is a promising option for the treatment of DMD and other genetic disorders. Of the many gene therapy vectors, Ad is the most commonly used in the field of gene therapy (48). Ad is an ideal vector for gene therapy because it has a large cloning capacity, it can transduce a wide variety of tissue types at a high efficiency (49), and it can be made replication defective, thus reducing immunogenicity (54). However, the major challenge of muscle-directed gene therapy is improving Ad transduction in muscle. Ad does not efficiently transduce mature muscle due a developmental down regulation of its primary receptor, CAR (202-204, 218). It was previously shown that retargeting Ad to a receptor highly prevalent on mature muscle can improve transduction by 4-fold *in vitro*, but this effect was attenuated *in vivo* (208). It is hypothesized that the basal lamina acts as a physical barrier preventing efficient Ad transduction in muscle (209). The basal lamina is a molecular mesh composed of laminin and collagen that surrounds and supports muscle fibers that serves to organize and orient muscle regeneration (212, 213). In addition, the basal lamina acts as a passive molecular sieve that may restrict the passage of molecules to mature muscle. It was previously found in the Parks lab that, at 30 minutes post-IM injection, the Ad particles remain at the site of injection and do not disperse along the length of the muscle (198). Since the average mesh size of the basal lamina that Ad must cross to achieve transduction in muscle is 40nm in diameter and Ad is 162nm in diameter

(212), the basal lamina is likely a significant barrier to Ad transduction in muscle (218). Therefore, it is hypothesized that decreasing the overall size of the virus will improve transduction in muscle.

Attempts to decrease the size of the Ad capsid are restricted by structural symmetry requirements of the virion (219). Complete elimination of the Ad5 fiber failed to produce viable vectors because the elimination of the Ad5 fiber reduces the stability of the capsid (220). Therefore, generating chimeric viruses with shorter fibers decreased the overall size of the Ad virion by 30%. The transduction efficacy of fiber-modified viruses was first characterized *in vitro* and then their efficacy was compared in wild type and *mdx* muscle.

### *3.1.1 Experimental Approach for Assessment of Fiber-modified viruses in vivo*

As previously mentioned, the primary goal in treating DMD is to replace DYS expression in skeletal muscle of the limbs, diaphragm, and cardiac tissue. As a first step, the efficacy of the fiber-modified viruses was tested in skeletal muscle, specifically the tibialis anterior (TA) muscle, because it is easily accessible for injections and for removal by dissection.

The animal models used to compare vector transduction *in vivo* were C57Bl/6 and *mdx* mice. C57Bl/6 mice were chosen for the wild type muscle because of their availability and they are commonly used in FGAd gene therapy studies. In comparison with other immunocompetent animal strains, C57Bl/6 mice do not produce neutralizing antibodies against immunogenic transgenes like human factor XI (hFIX) or human $\alpha_1$-antitrypsin (AAT), despite a CTL response to the FGAd delivery vectors (244-246). The fiber-modified viruses

used in this study express the β-galactosidase (β-gal) antigen, the expression of which declines rapidly within 3 weeks post-administration due to a cellular immune response to the antigen in the C57Bl/6 model (245). Therefore, C57Bl/6 was an adequate model for assessing early transgene expression. In this study, *mdx* mice were chosen to model early stage human DMD pathology because experimentation would coincide with the massive muscle necrosis and degeneration observed in the TA muscle at 3-5 weeks of age (97, 98, 238).

The delivery route and vector dose are important parameters affecting the transduction efficiency of FGAds (247). The majority of FGAd studies for muscle-directed gene therapy employ IM injection because IV delivery is generally not as efficient, transducing less than 12% of muscle fibers in the hind limb (205). Therefore, in this study, the vectors were administered intramuscularly to the TA. In general, efficient muscle transduction can be achieved by local administration using lower doses of Ad vector than are required for systemic delivery (248). For this reason, a low dose of $1x10^9$ virus particles was initially chosen to assess viral transduction in muscle. Vector efficacy at low doses is ideal because the innate arm of the immune system becomes activated in a dose-dependent manner such that, at high titers, systemically delivered Ad can trigger significant amounts of local inflammation and cause a rapid loss of transgene expression (76, 80, 84). Although the bulk of IM-delivered Ad vector remains in the muscle, a small portion of the Ad dose may circulate systemically post-IM delivery and transduce the liver (249). As hepatotoxicity was a concern, transgene expression was assessed in the liver as well as in muscle. Taken

together, a conservative approach was taken to testing the hypothesis by directly delivering a low dose of an FGAd vector.

## *3.2 Results*

### *3.2.1 Generation of fiber-modified viruses*

To decrease the overall size of the Ad virion, Ad5 based vectors with shorter fibers were generated. Using the same cloning strategy, fiber-modified viruses were constructed by cloning the short fiber shafts into the endogenous fiber locus of an E1/E3 deleted FG-Ad5 vector expressing *lac*Z under the control of the CMV promoter (Figure 6A). For the purposes of this study, the CMV promoter was chosen because CMV-driven expression is consistently higher than muscle specific muscle creatine kinase (MCK) driven expression of *lac*Z from an FGAd in muscle (250). The fiber-modified Ad5 vectors are schematically represented in Figure 6B. The Ad fiber consists of two parts: the knob and the shaft. The fiber knob binds the primary cellular receptor and is thought to be the main determinant of viral tropism (251). The fiber shaft consists of a number of 14 amino acid repeats that form a β-sheet secondary structure (252). The number of β-sheet repeats in a fiber shaft determines its length. For example, Ad5 contains 22 β-sheets and is 37nm in length while the shorter fibers of Ad9 and Ad35 contain 8 and 6 β-sheets and are 11nm and 9nm in length, respectively (252). Fiber-modified viruses were compared in all experiments to Ad5 as a control. The Ad5 fiber is 37nm long and consists of the full length Ad5 shaft and the Ad5 knob. Fibers protrude out from vertices of the 90nm capsid and extend the diameter of the Ad5 virion to 162nm. The following fiber-modified vectors decrease the overall

**Figure 6: Schematic representation of fiber-modified viruses used in this study**

(A) Fiber cassettes were cloned into an Ad5 backbone containing a CMV promoter and *lac*Z reporter gene. Shown in black is the polyadenylation sequence. (B) Three modified viruses were generated: Ad5s has an Ad5 knob and a short shaft derived from Ad9 of 11nm. Ad5/9s has the same short shaft as Ad5s but with Ad9 knob. Ad5/35s has the shortest shaft of all the fiber-modified viruses at 9nm in length with an Ad35 knob. Ad5, Ad5s and Ad5/9s bind CAR, whereas Ad5/35s binds CD46. Figure adapted from (234).

A


B

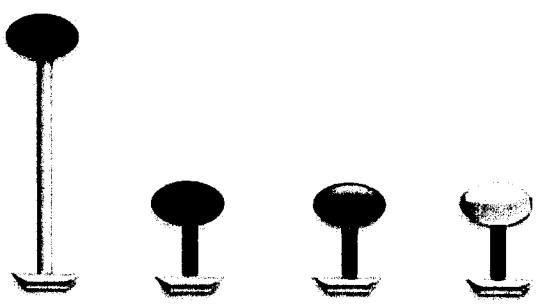

| Ad Vector | Ad5 | Ad5s | Ad5/9s | Ad5/35s |
|---|---|---|---|---|
| Fiber Length (nm) | 37 | 11 | 11 | 9 |
| Receptor Binding | CAR | CAR | CAR | CD46 |

diameter of the Ad5 vector by 30%. Ad5s consists of a short Ad9 fiber that is 11nm in length together with an Ad5 knob. Ad5/9s has the same Ad9 short fiber (11nm in length) but with an Ad9 knob. Finally, Ad5/35s fiber consists of the short Ad35 shaft (9 nm in length) terminating with an Ad35 knob. All viruses primarily bind CAR, except for Ad5/35s which binds CD46.

### *3.3.2 In vitro Characterization of fiber-modified viruses*

Fiber-modified virus transduction was compared in A549 cells and in undifferentiated and differentiated $C_2C_{12}$ cells. $1x10^6$ cells per 35mm dish were infected with an MOI of 20 virus particles/cell and transduction was measured using a chemiluminescent β-gal assay. The mean β-gal activity in cell lysates and the standard error of the means were calculated and graphed; a one way ANOVA test was performed to determine statistical significance between treatment groups where multiple comparisons were made using Tukey's test.

The A549 cell line was chosen as a control because they are adenovirus permissive and express a high level of CAR and CD46 (201). When directly comparing the levels of transduction in A549 cells, all viruses were equally as efficient except for Ad5/9s which transduced A549 cells more efficiently than Ad5s (Figure 7A). Ad5/9s and Ad5s have the same the short Ad9 fiber but with different knobs, both of which bind CAR. This observation that the Ad9 knob may confer an advantage over the Ad5 knob in fiber-modified viruses in A549s was surprising. It has been established that the Ad9 knob binds CAR with a lesser affinity than the Ad5 knob resulting in less internalization and transduction of 293 cells

**Figure 7: *In vitro* characterization of fiber-modified viruses**

Fiber-modified viruses have a similar level of transduction in differentiated and undifferentiated $C_2C_{12}$ cells. (A) A549 cells, (B) undifferentiated, and (C) differentiated $C_2C_{12}$ cells ($1x10^6$ cells per 35mm dish) were infected with Ad5 or fiber-modified Ad5 vectors at an MOI of 20 virus particles/cell. At 24 hours post-infection, cell lysates were harvested and measured for β-Gal activity by a chemiluminescent assay (n=4). Graphs plot the mean ± the standard error of the mean. An asterisk (*) denotes a significant difference from Ad5s. A double asterisk (**) denotes a significant difference from Ad5.

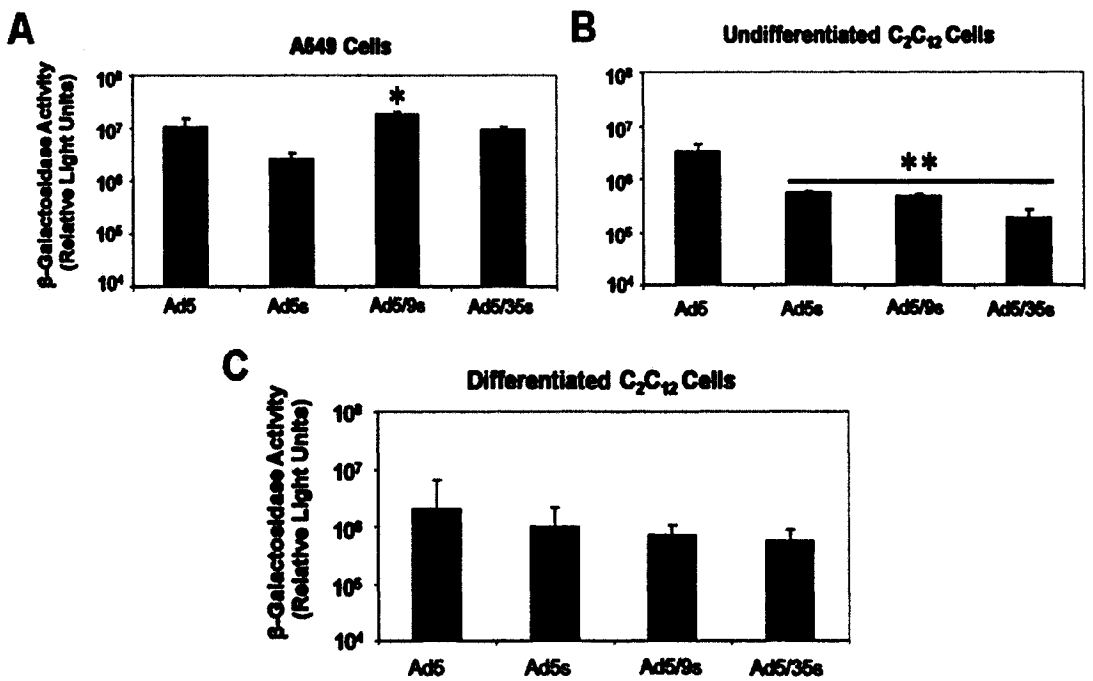
A
A549 Cells
β-Galactosidase Activity (Relative Light Units)
*
Ad5
Ad5s
Ad5/9s
Ad5/35s
B
Undifferentiated C2C12 Cells
**
C
Differentiated C2C12 Cells

D

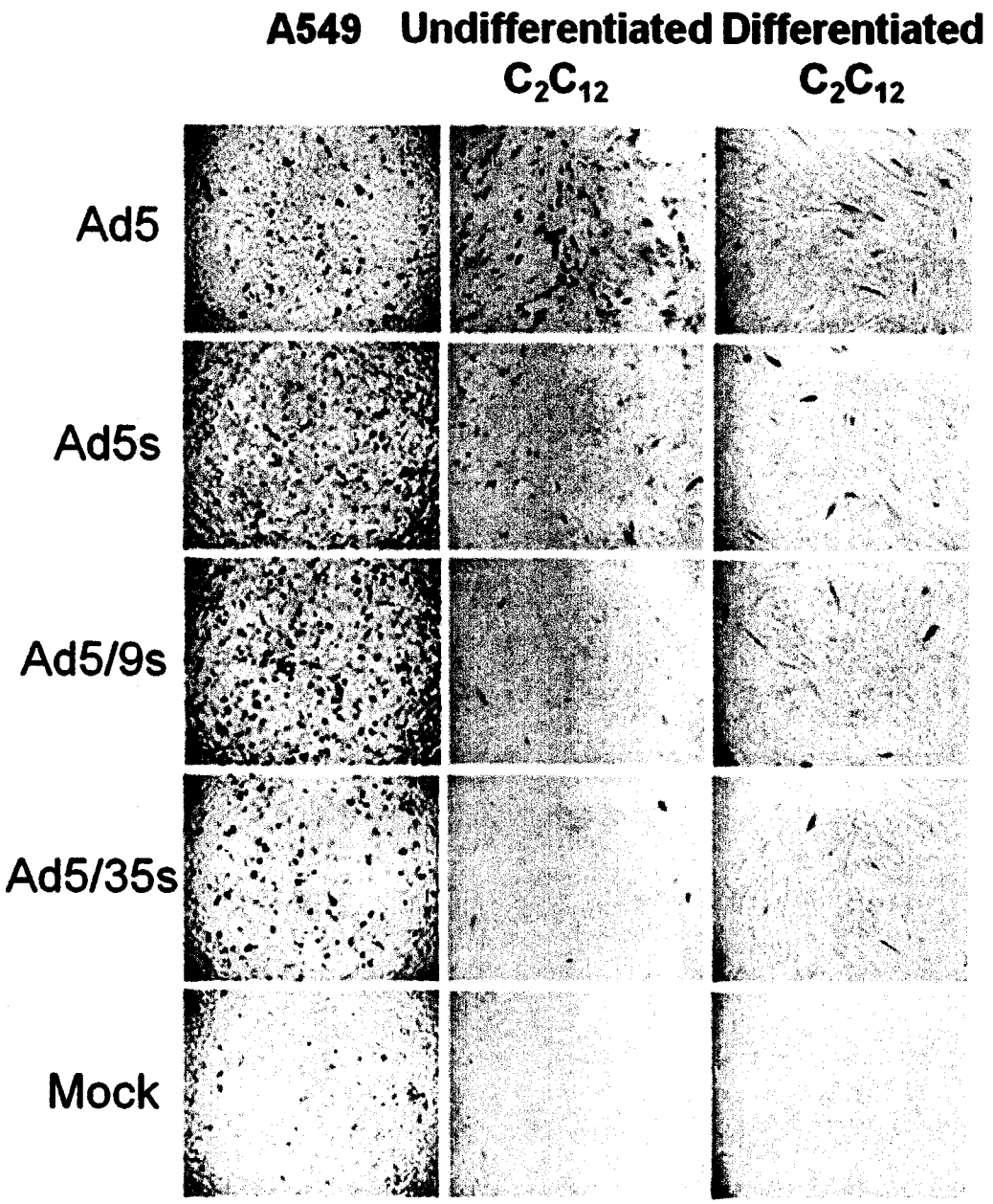
A549
Undifferentiated $C_2C_{12}$
Differentiated $C_2C_{12}$
Ad5
Ad5s
Ad5/9s
Ad5/35s
Mock

(234, 253). In summary, all vectors efficiently transduced A549 cells and the uniformly high vector transduction was likely due to the high presence of cellular receptors.

$C_2C_{12}$ cells are a mouse myoblast cell line that can be induced to differentiate into myotubes. It was expected that all viruses would infect A549 cells more efficiently than $C_2C_{12}$ cells (Figure 7A, 7B, 7C) because both CD46 and CAR are differentially expressed in $C_2C_{12}$ cells (203, 254, 255). Specifically, as differentiation proceeds from confluent $C_2C_{12}$ myoblasts to myotubes at 4 days, CAR expression decreases by 3.5-4-fold as determined by quantitative polymerase chain reaction (qPCR) (J. Nalbantoglu, McGill, Montreal, Canada, personal communication). Consistent with previous studies, Ad5 transduction of undifferentiated $C_2C_{12}$ cells was 2-fold more efficient than in differentiated $C_2C_{12}$ cells (Figure 7B, C) suggesting that Ad5 transduction *in vitro* was dependent on the presence of cellular receptors (203, 240). Fiber-modified viruses transduced undifferentiated $C_2C_{12}$ cells less efficiently than Ad5 (Figure 7B). Taken together, efficient transduction was dependent on fiber length.

All viruses transduced differentiated $C_2C_{12}$ cells with a similar efficiency (Figure 7C). Ad5 transduced differentiated $C_2C_{12}$ cells 2-fold less efficiently than undifferentiated $C_2C_{12}$ cells; fiber-modified viruses transduced differentiated $C_2C_{12}$ cells between 1 .5-and 3-fold more efficiently than undifferentiated $C_2C_{12}$ cells. Representative photomicrographs of β-gal staining confirm that even though the differentiated $C_2C_{12}$ cell population was heterogeneous, vectors primarily transduced myotubes (Figure 7D).

### *3.2.3 Distribution of 190nm polystyrene beads in muscle*

Before testing fiber-modified viruses *in vivo*, the effect of particle size on distribution in muscle was examined. The hypothesis that decreasing the overall size of the Ad virion would improve transduction in muscle was, in part, based on observations that the distribution of Ad vectors in muscle was primarily restricted to the injection site post-IM delivery (198). Was this observation unique to the Ad virion itself? This question was addressed by examining the distribution of inert polystyrene beads, approximately the size of Ad (190nm), after injection into muscle. After 30 minutes PI, the bulk of the 190nm beads remained concentrated around the injection site in the middle of the muscle and did not fully distribute by 48 hours post-injection (Figure 8A, B). Therefore, the limited dispersion of Ad virus particles in muscle was common to other particles of the same size, thus a size sensitive physical barrier may be restricting their passage in muscle.

### *3.2.4 Characterization of fiber-modified viruses in wild type muscle*

Next, the effect of decreasing the overall size of the Ad virion was examined *in vivo*. Ad vectors were directly injected into the hind limb of 3-5 week old wild type mice, and vector transduction was assessed at either 2 days or 10 days post-injection. Two methods were employed to describe vector transduction *in vivo*. The total transgene expression was quantified by measuring β-gal expression in whole muscle lysates using a chemiluminescent assay (n=8). A descriptive analysis was also preformed to qualitatively asses vector transduction in muscle cross sections in order to determine if any enhancement in transduction was due to the transduction of more muscle fibers or the co-infection of the same number of muscle fibers (n=2). Both measures of gene expression were important

**Figure 8: Distribution of 190nm polystyrene beads *in vivo***

Photomicrographs of fresh frozen longitudinal sections of adult female C57BL/6 murine TA muscles that were injected with $1x10^9$ 190nm diameter fluorescent beads (Bangs Laboratories Inc., Fishers, IN) visualized by fluorescence microscopy at 30 minutes post-injection and 48 hours post-injection. The perimeter of the muscle sections are outlined in white. White arrows indicate the location and direction of the injection site. Representative photomicrographs were taken at 50X magnification.

A

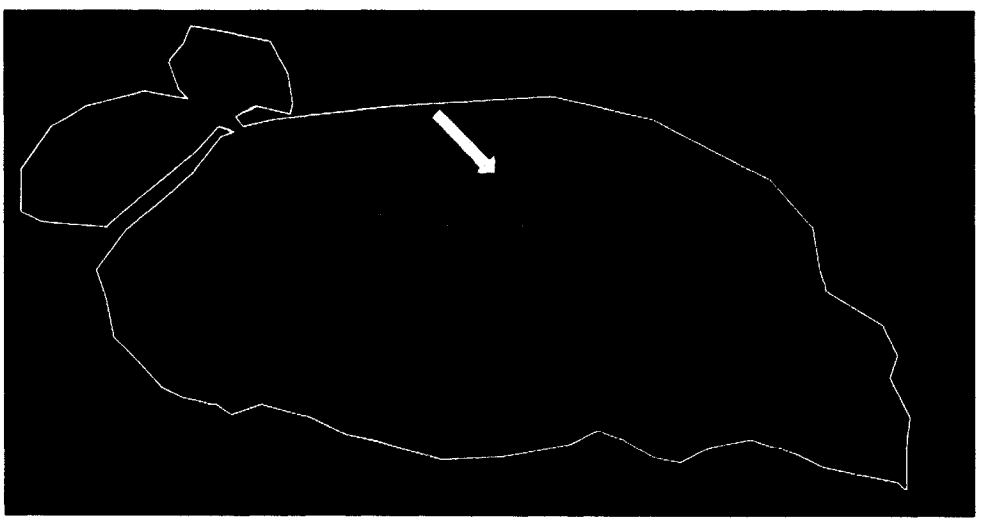

**30 minutes post-injection**

B

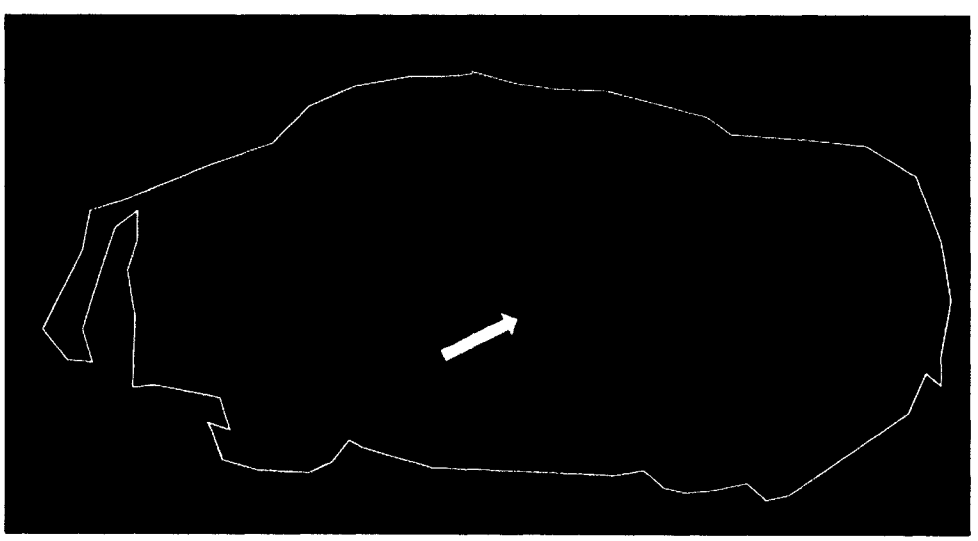

**48 hours post-injection**

since an effective gene therapy strategy for DMD aims for a high level of transgene expression in a large proportion of muscle fibers (113, 114). These complimentary methods were used to examine whether fiber-modified viruses conferred an advantage over Ad5 in muscle.

For the first *in vivo* experiment, a low dose of vector ($1x10^9$ virus particles) was injected into adult wild type TA muscle and β-gal expression was assayed at 2 days PI using a chemiluminescent assay. The mean β-gal expression in whole muscle (Figure 9A) and liver (Figure 9B) lysates and the standard error of the means were calculated and graphed; Mann-Whitney rank sum tests were performed between each treatment group to determine statistical significance. Fiber-modified viruses improved transduction in muscle over Ad5 by 30-fold in muscle (Figure 9A) and negligibly transduced the liver (Figure 9B). However, preliminary *in vitro* characterization of the Ad5 viral stocks before and after this first *in vivo* experiment indicated that the stock was compromised. Prior to the first *in vivo* experiment, Ad5s transduced 293 cells 100-fold more efficiently than Ad5 (Figure 9C). These same viral stocks were used in the first *in vivo* experiment (Figure 9A, B). However, immediately following the first *in vivo* experiment, Ad5 expression was undetectable (Figure 9D). A new viral stock of Ad5 was prepared and tested *in vitro*; Ad5s transduced 293 cells 2.5-fold more efficiently than Ad5 (Figure 9E). These preliminary data raised a question about the infectivity of the Ad5 stock used in the first *in vivo* experiment that described a 30-fold difference in transduction between fiber-modified viruses and Ad5. Therefore, a newly prepared Ad5 stock was used for all subsequent experiments.

**Figure 9: Preliminary data on the infectivity of the Ad5 viral stock used in the first *in vivo* experiment**

The infectivity of the Ad5 viral stock used in the first *in vivo* experiment (A, B) was compromised. 293 cells were infected Ad5 or Ad5s at an MOI of 5 β-gal forming units (BFU) per cell before (C) and after (D) the first *in vivo* experiment using the same viral stocks and (E) with a newly prepared Ad5 viral stock thereafter. At 24 hours post-injection, cell lysates were harvested and measured for β-Gal activity by a chemiluminescent assay (n=2). Three to five week old female C57BL/6 mice were injected intramuscularly with $1x10^9$ virus particles. At 2 days post-injection, (A) TA muscles and (B) liver were dissected, flash frozen, then assayed for β-gal expression by a chemiluminescent assay (n=4 mice, 8 muscles). Graphs plot the mean ± the standard error of the mean. An asterisk (*) denotes a significant difference from Ad5/9s and Ad5/35s.

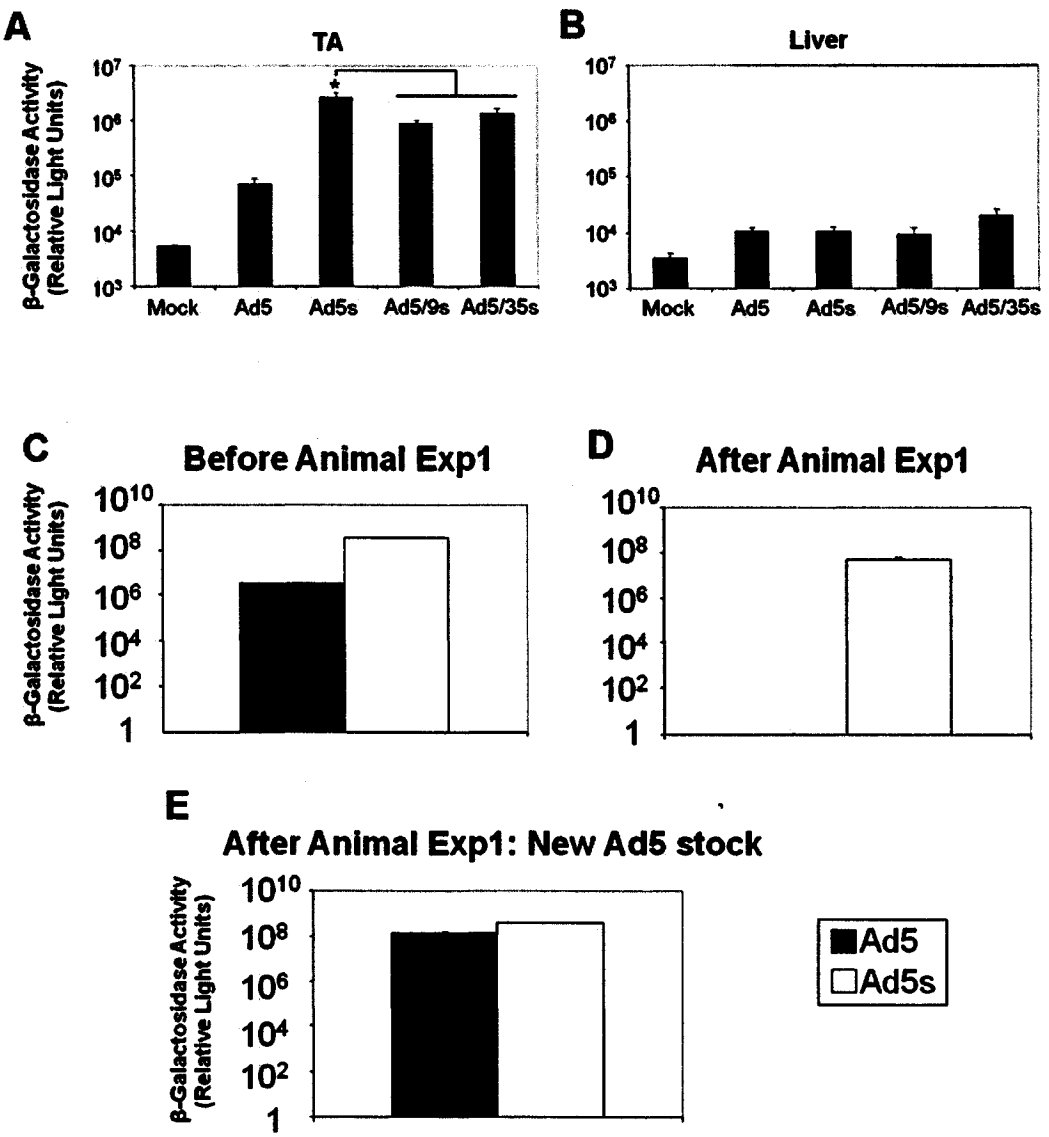
A
TA
β-Galactosidase Activity (Relative Light Units)
10^7
10^6
10^5
10^4
10^3
Mock
Ad5
Ad5s
Ad5/9s
Ad5/35s
B
Liver
C
Before Animal Exp1
10^10
10^8
10^6
10^4
10^2
1
D
After Animal Exp1
E
After Animal Exp1: New Ad5 stock
Ad5
Ad5s

The next experiment compared a low dose of vector ($1x10^9$ virus particles) transduction in 3-5 week old wild type muscle, assayed at 10 days PI using a chemiluminescent assay. The mean β-gal activity for whole muscle and liver lysates and the standard error of the mean were calculated and graphed; Mann-Whitney rank sum tests were performed to determine statistical significance between treatment groups. All fiber-modified viruses improved transduction in muscle by 10-fold over Ad5 (Figure 10A) and negligibly transduced the liver (Figure 10B) as measured by a chemiluminescent β-gal assay. Descriptive analysis was performed by scoring every muscle fiber for β-gal activity in three of the largest, randomly selected muscle fibers (Figure 10 C). The mean β-gal positive muscle fibers and the standard error of the means were graphed (Figure 10 D); Mann-Whitney rank sum tests were performed to determine statistical significance between treatment groups. In representative cross sections of muscle, fiber-modified viruses had a more favorable pattern of transduction and dispersed further throughout the width of the muscle (Figure 10 C). In addition, fiber- modified viruses transduced up to 4.5-fold more muscle fibers than Ad5 (Figure 10 D), although very few muscle fibers were transduced overall.

The goal of muscle directed gene therapy studies is to transduce the most muscle fibers possible. Therefore, a dose escalation experiment was performed to describe the maximal muscle transduction possible by fiber-modified viruses. Previous experiments indicated that Ad5s transduced muscle more efficiently than other fiber-modified viruses (Figure 9A) therefore; Ad5s was directly compared to Ad5 in this experiment. Three incremental doses

**Figure 10: Characterization of fiber-modified viruses in wild type muscle at 10 days post-injection**

Decreasing Ad fiber length improves transduction in wild type muscle by infecting more muscle fibers. Three to five week old female C57BL/6 mice were injected intramuscularly with $1x10^9$ virus particles. At 10 days post-injection, (A) TA muscles and (B) livers were dissected, flash frozen, then assayed for β-gal expression by a chemiluminescent assay (n=4 mice, 8 muscles) or (C) TA muscles were preserved in embedding compound and were cross sectioned then co-stained with X-gal and eosin. Scale bar = 100μm. (C) The number of B-gal positive muscle fibers were calculated by randomly selecting and scoring all the muscle fibers in 3 of the largest muscle cross sections (n= 2 muscles). Graphs plot the mean ± the standard error of the mean. An asterisk (*) denotes a significant difference from mock and Ad5.

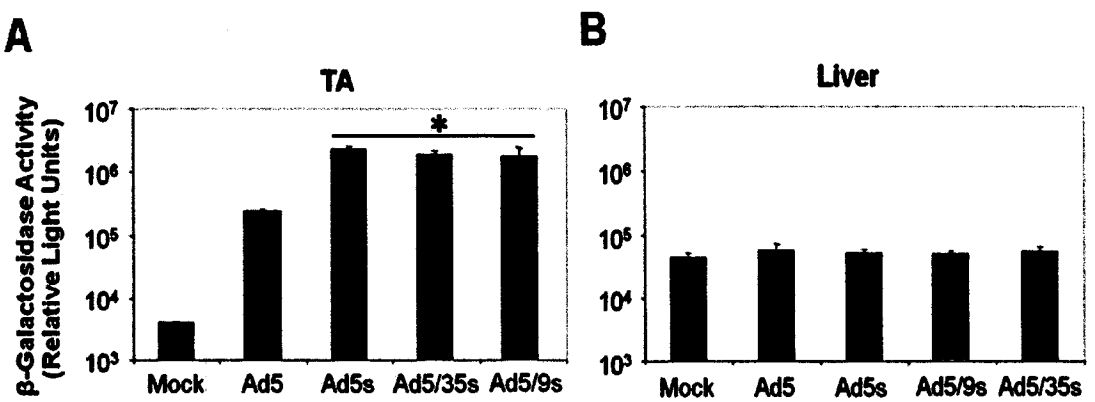
A
TA
β-Galactosidase Activity (Relative Light Units)
10^7
10^6
10^5
10^4
10^3
*
Mock
Ad5
Ad5s
Ad5/35s
Ad5/9s
B
Liver
10^7
10^6
10^5
10^4
10^3
Mock
Ad5
Ad5s
Ad5/9s
Ad5/35s

C

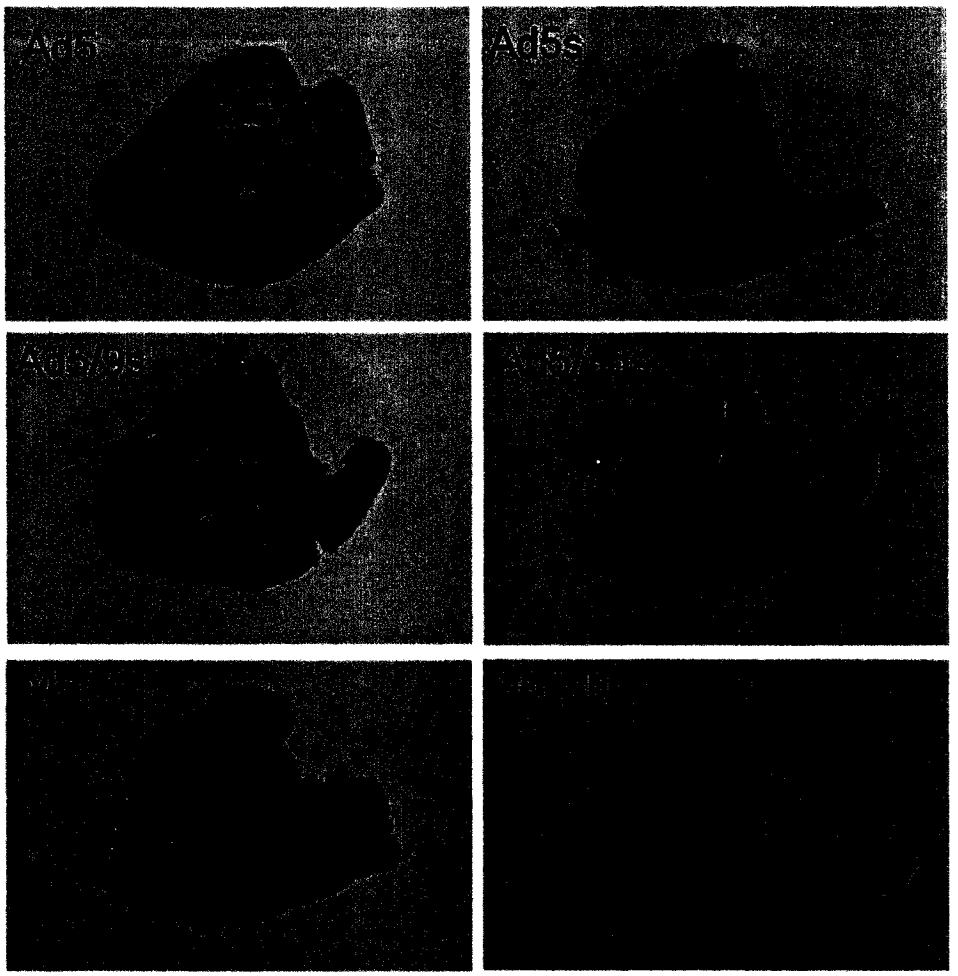
Ad5
Ad5s

D

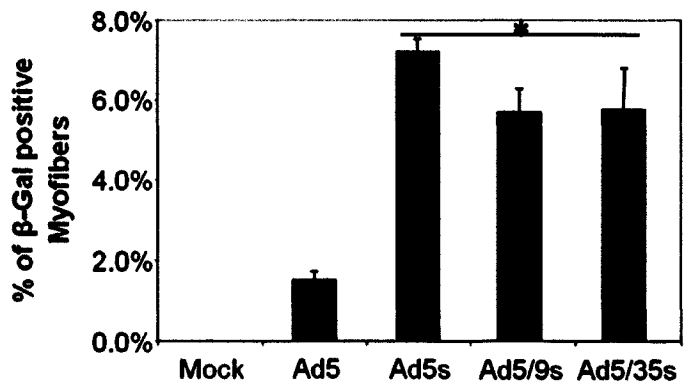
% of β-Gal positive Myofibers
8.0%
6.0%
4.0%
2.0%
0.0%
Mock
Ad5
Ad5s
Ad5/9s
Ad5/35s

were chosen based on limitations imposed by the viral titer and injection volume of 25ul. Either with a low ($1x10^9$ virus particles), medium ($3.3x10^9$ virus particles) or a high dose ($1x10^{10}$ virus particles) was injected into wild type TA muscle then assayed for vector transduction at 2 days PI. The mean β-gal activity in whole muscle (Figure 11A) and liver lysates (Figure 11B) and the standard error of the means were calculated and graphed; unpaired t-tests were performed to determine statistical significance between treatment groups. Although the level of transduction in the liver was high, a greater transduction was observed in the muscle than in the liver. High and medium doses of Ad5s showed significantly greater muscle transduction than the low dose (Figure 11A). In comparison, the muscle transduction, resulting from only the high dose of Ad5, was significantly greater than the low dose (Figure 11A). Therefore, a significant dose-dependent increase in vector transduction was observed in muscle, in contrast, an overall dose escalation trend was observed in the liver. Descriptive analysis for the high vector dose was performed in muscle (Figure 11C). Every muscle fiber in three of the largest randomly selected cross sections was scored for β-gal expression. The mean β-gal positive muscle fibers and the standard error of the mean were graphed (Figure 11D); an un-paired t-test was performed to determine statistical significance between treatment groups. Examining representative muscle cross sections of the high dose of vector, Ad5s had a more favorable pattern of muscle transduction (Figure 11C) and transduced up to 14% of muscle fibers, compared to Ad5 which transduced only 6% (Figure 11D).

The level of Ad5 and Ad5s transduction in wild type muscle from both experiments were directly compared (Figure 12). The mean β-gal activity in whole muscle lysates and the

**Figure 11: Characterization of fiber-modified viruses in wild type muscle at 2 days post-injection**

A high dose of Ad5s transduced 14% of total muscle fibers. Three to five week old female C57BL/6 mice were injected intramuscularly with either a low ($1x10^9$ virus particles), medium ($3.3x10^9$ virus particles), or high dose ($1x10^{10}$ virus particles). At 2 days post-injection, (A) TA muscles and (B) livers were dissected, flash frozen, then assayed for β-gal expression by a chemiluminescent assay (n=4 mice, 8 muscles) or (C) TA muscles were preserved in embedding compound and were cross sectioned then co-stained with X-gal and eosin. Scale bar = 100μm. (D) The number of B-gal positive muscle fibers were calculated by randomly selecting and scoring every muscle fiber in 3 of the largest muscle cross sections (n= 2 muscles). Graphs plot the mean ± the standard error of the mean. An asterisk (*) denotes a significant difference from the low dose within a treatment group. A double asterisk (**) denotes a significant difference from Ad5.

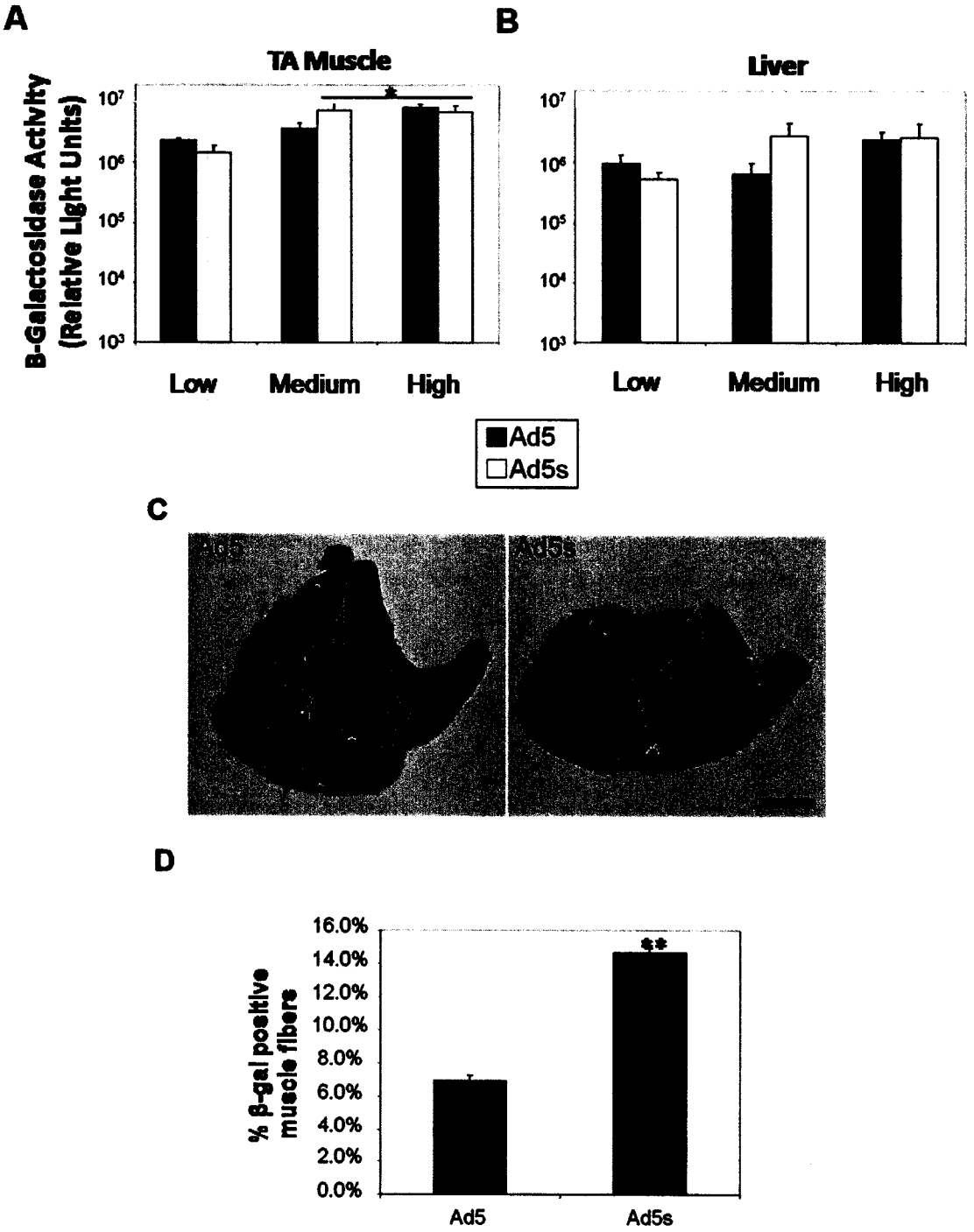
A
TA Muscle
B-Galactosidase Activity (Relative Light Units)
$10^7$
$10^6$
$10^5$
$10^4$
$10^3$
Low
Medium
High
B
Liver
Low
Medium
High
Ad5
Ad5s
C
Ad5
Ad5s
D
% β-gal positive muscle fibers
16.0%
14.0%
12.0%
10.0%
8.0%
6.0%
4.0%
2.0%
0.0%
**
Ad5
Ad5s

**Figure 12: Comparison of Ad5 and Ad5s in wild type muscle at 2 and 10 days post-injection**

The transduction of Ad5s was stable over 10 days. This figure plots the level of Ad5 and Ad5s transduction in muscle from Figure 11 and Figure 10 (low dose) such that viral transduction at 2 and 10 days post-injection can be compared. The graph displays the mean ± the standard error of the mean. An asterisk (*) denotes a significant difference between transduction at 2 and 10 days post-injection.

## Comparison of Ad5 and Ad5s in wild type muscle

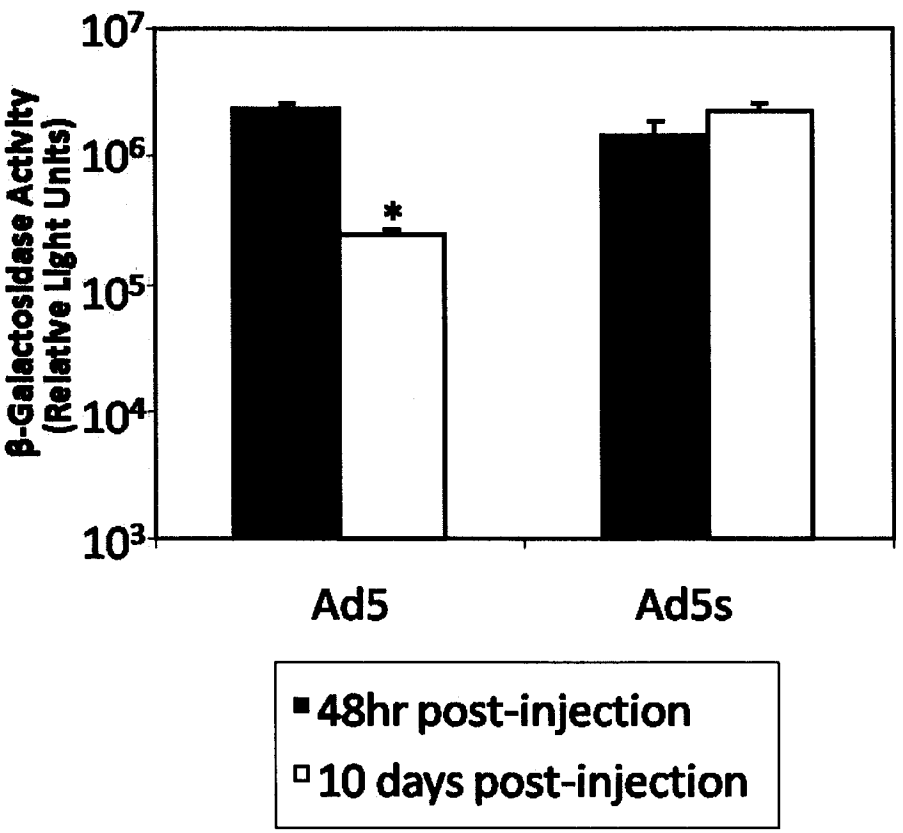

standard error of the mean were graphed; Mann-Whitney rank sum tests were performed to describe statistical significance between treatment groups. The level of Ad5 transduction was comparable to Ad5s at 2 days PI but at 10 days PI, where the level of Ad5 transduction was significantly lower than Ad5s. Considering that these viral vectors encode identical expression cassettes, these data suggest a possible selective clearance of Ad5 transduced muscle fibers over 10 days PI.

### *3.2.5 Characterization of fiber-modified viruses in mdx muscle*

Finally, in order to evaluate fiber-modified viruses as candidates for gene therapy vectors for DMD, their efficacies were tested in a model of the disease. A low dose of fiber-modified viruses were directly injected into the TA muscle of 3-5 week old *mdx* mice and vector transduction was assessed both quantitatively (in the whole muscle lysate using a chemiluminescent β-gal assay) and qualitatitively (by analyzing β-gal expression in muscle sections) at 10 days PI. The mean β-gal activity in whole muscle (Figure 13A) and liver Figure 13B) lysates and the standard error of the means were calculated and graphed; unpaired t-tests were performed to determine statistical significance between treatment groups. Ad5 transduced *mdx* muscle significantly more efficiently than fiber-modified viruses (Figure 13A) and all viruses negligibly transduced the liver (Figure 13B). Descriptive histological analysis was performed by scoring every muscle fiber for β-gal activity and central nucleation present in 3 of the largest, randomly selected muscle cross sections (Figure 13 C). The mean centrally nucleated muscle fibers and β-gal positive muscle fibers were calculated with the standard error of the means, which were then graphed (Figure

**Figure 13: Characterization of fiber-modified viruses in *mdx* muscle at 10 days post-injection**

Adenoviruses with shorter fibers transduce *mdx* muscle less efficiently than Ad5. Three to five week old female mdx mice were injected intramuscularly with $1x10^9$ virus particles. At 10 days post-injection, (A) TA muscles and (B) livers were dissected, flash frozen, and assayed for β-gal expression by a chemiluminescent assay (n=4 mice, 8 muscles) or (C) TA muscles were preserved in embedding compound and were cross sectioned and co-stained with X-gal, eosin, and Hoechst (shown in green). Scale bar = 100μm. (D) The number of centrally nucleated myofibers were calculated and (E) the β-gal positive muscle fibers were calculated by randomly selecting and scoring every muscle fiber in 3 of the largest muscle cross sections (n= 2 muscles). The graphs display the mean ± the standard error of the mean. An asterisk (*) denotes a significant difference from Ad5. A double asterisk (**) denotes a significant difference.

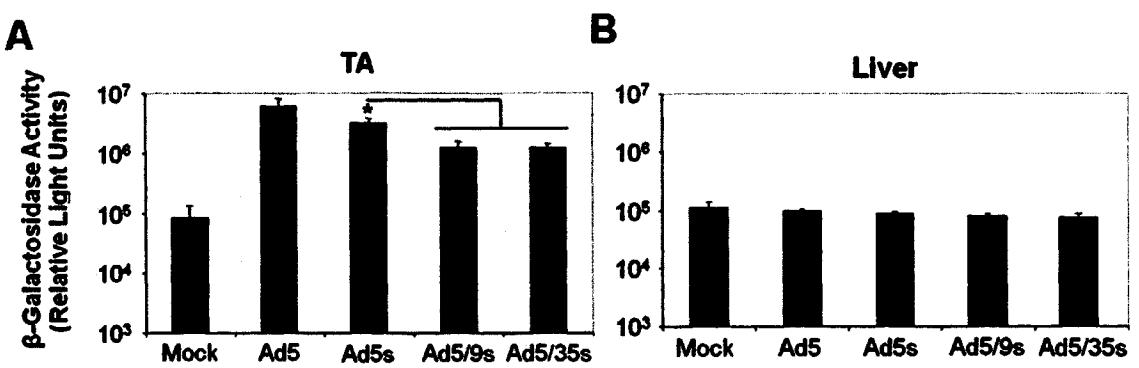
A
TA
β-Galactosidase Activity
(Relative Light Units)
10^7
10^6
10^5
10^4
10^3
Mock
Ad5
Ad5s
Ad5/9s
Ad5/35s
B
Liver
10^7
10^6
10^5
10^4
10^3
Mock
Ad5
Ad5s
Ad5/9s
Ad5/35s

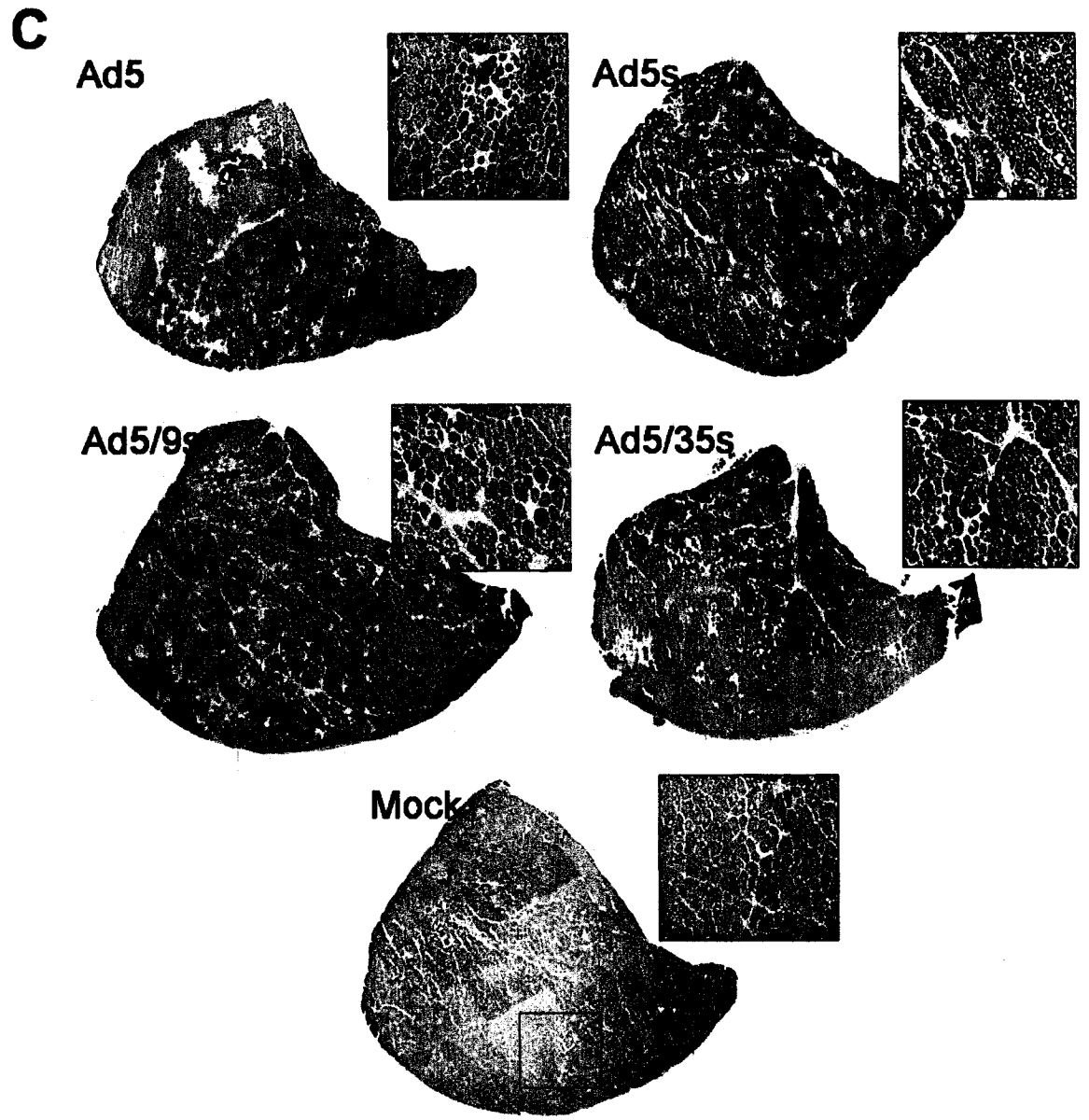
C
Ad5
Ad5s
Ad5/9s
Ad5/35s
Mock

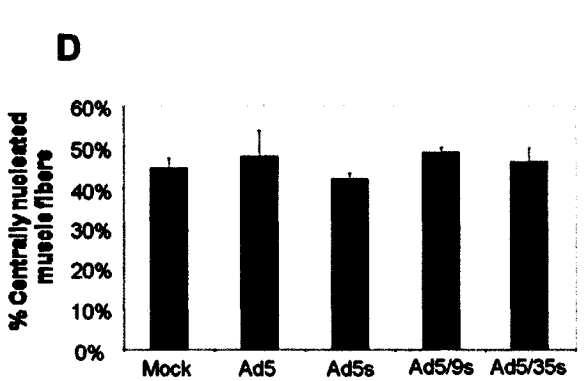
D
% Centrally nucleated muscle fibers
60%
50%
40%
30%
20%
10%
0%
Mock
Ad5
Ad5s
Ad5/9s
Ad5/35s

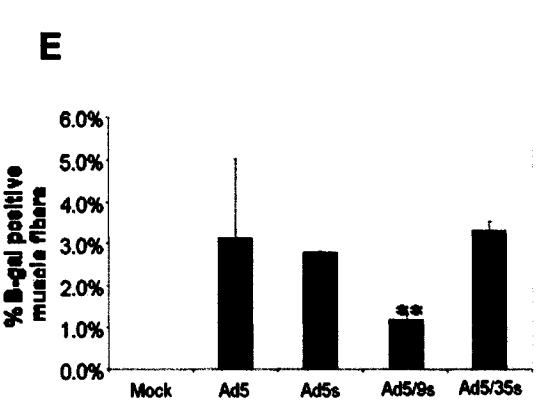
E
% B-gal positive muscle fibers
6.0%
5.0%
4.0%
3.0%
2.0%
1.0%
0.0%
**
Mock
Ad5
Ad5s
Ad5/9s
Ad5/35s

13D, E); un-paired t-tests were performed to determine statistical significance. The pattern of viral dispersion in *mdx* muscle was difficult to assess due to the low number of muscle fibers transduced (Figure 13 C, E). Therefore, it was also difficult to assess if fiber-modified viruses were preferentially infecting dividing muscle fibers, marked by central nucleation, even though approximately half of the *mdx* muscle fibers were centrally nucleated (Figure 13 D).

Descriptive immunohistochemical analysis was employed to identify and further break down the actively regenerating muscle fiber population and examine whether vectors were preferentially transducing newly regenerating muscle fibers. Transduced muscle fibers were stained using anti-β-gal (shown in green), newly regenerating fibers were stained using anti-embryonic-MHC (e-MHC, shown in red), and nuclei were stained with Hoechst (shown in blue) (Fig. 14 A). All muscle fibers in three of the largest, randomly chosen muscle sections were scored appropriately. The mean values for centrally nucleated ad β-gal positive muscle fibers, as well as the proportion of centrally nucleated β-gal positive muscle fibers and the number of e-MHC positive muscle fibers were calculated and graphed along with the standard error of the mean (Figure 14 B,C,D,E); unpaired t-tests were performed to determine statistical significance between treatment groups. Immunohistochemical staining and analysis of % central nucleation and % β-gal positive myofibers in Figure 14A, B, and C reaffirmed histological data, specifically the low percentage of muscle fibers transduced (Figure 13C, D, E). The immunohistochemical data on the preferential

**Figure 14: Preliminary data on the infectivity of fiber-modified viruses in regenerating muscle**

Three to five week old female mdx mice were injected intramuscularly with $1x10^9$ virus particles. At 10 days post-injection, (A) TA muscles were preserved in embedding compound and were cross sectioned and stained using immunohistochemical techniques for β-gal (green), embryonic-MHC (red) and Hoechst (blue). Scale bar = 100μm. (B) The number of centrally nucleated muscle fibers, (C) β-gal positive muscle fibers and (E) embryonic-MHC muscle fibers were calculated by randomly selecting and scoring all muscle fibers in 3 of the largest muscle cross sections (n= 2 muscles). From this analysis, (D) the proportion of β-gal-positive, centrally nucleated and mature muscle fibers were calculated. The graphs display the mean ± the standard error of the mean. An asterisk (*) denotes a statistically significant difference from all other treatment groups.

A

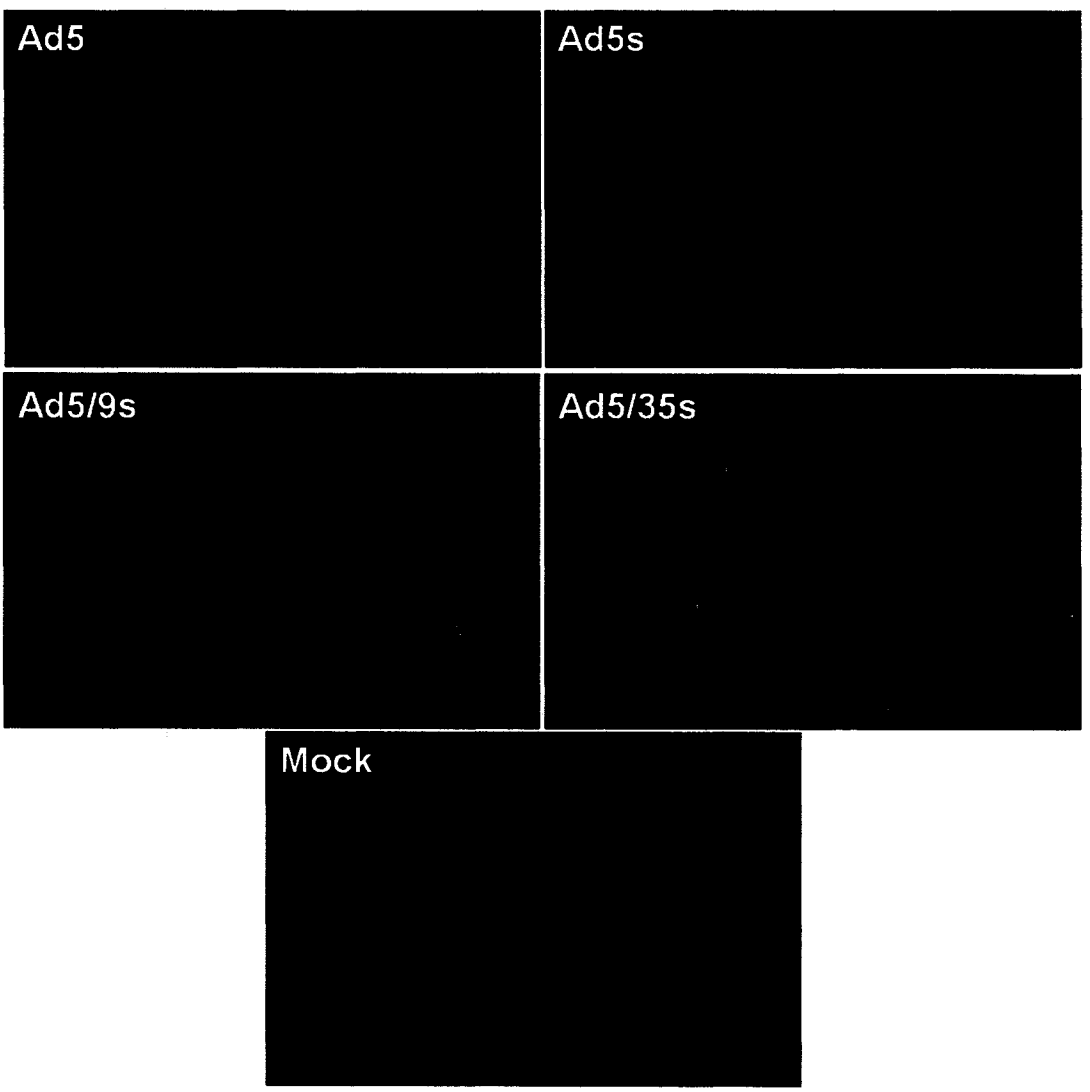

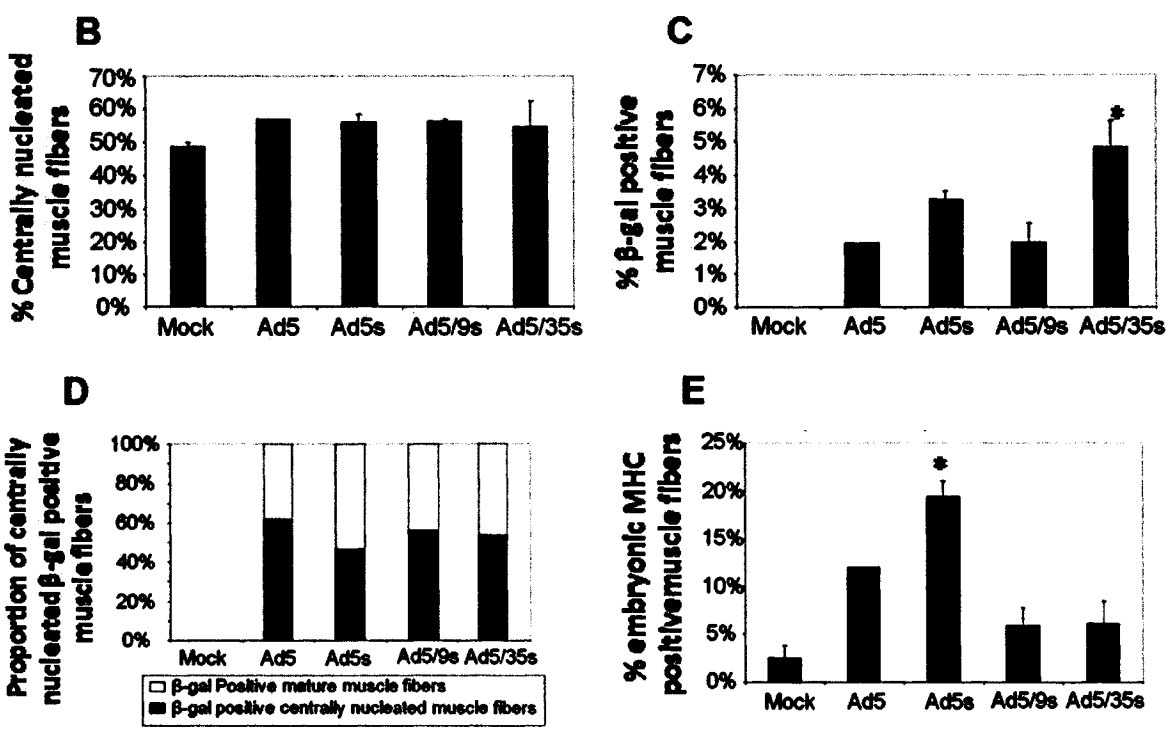
B
% Centrally nucleated muscle fibers
70%
60%
50%
40%
30%
20%
10%
0%
Mock
Ad5
Ad5s
Ad5/9s
Ad5/35s
C
% β-gal positive muscle fibers
7%
6%
5%
4%
3%
2%
1%
0%
*
Mock
Ad5
Ad5s
Ad5/9s
Ad5/35s
D
Proportion of centrally nucleated β-gal positive muscle fibers
100%
80%
60%
40%
20%
0%
Mock
Ad5
Ad5s
Ad5/9s
Ad5/35s
β-gal Positive mature muscle fibers
β-gal positive centrally nucleated muscle fibers
E
% embryonic MHC positivemuscle fibers
25%
20%
15%
10%
5%
0%
*
Mock
Ad5
Ad5s
Ad5/9s
Ad5/35s

infectivity of fiber-modified viruses remains preliminary because this and other descriptive analysis was performed using an n value of only two. Although these data indicate viruses infected centrally nucleated and non-centrally nucleated muscle fibers in equal proportion (Figure 14 D), this conclusion cannot be conclusively supported without follow up analysis. Furthermore, infection of newly regenerating muscle fibers was not observed (Figure 14A). It was unknown why it appeared that *mdx* muscle transduced with Ad5s exhibited a greater proportion of newly regenerating fibers at 10 days PI (Figure 14E); follow up experimentation would be required to conclusively validate this observation.

Ad5 and Ad5s transduction was compared in wild type and *mdx* muscle at 10 days PI. The mean β-gal activity in whole muscle lysates and the standard error of the mean were graphed (Figure 15); un-paired t-tests were performed to determine statistical significance between treatment groups. Ad5 transduced *mdx* muscle 10-fold more efficiently than wild type, where Ad5s transduced both types of muscle with similar efficiency (Figure 15).

## *3.3 Discussion*

Inefficient Ad transduction of muscle is thought to be due, at least in part, to restrictions imposed on the virus particles by the basal lamina *in vivo*. The goal of this study was to investigate whether decreasing the size of the Ad virion would improve transduction in muscle. FGAd fiber-modified viruses were generated expressing *lacZ* from the CMV promoter and their transduction efficacy was examined *in vitro* and *in vivo*. Although efficient transduction may be dependent on fiber length in some cell lines and in *mdx*

**Figure 15: Comparison of Ad5 and Ad5s in wild type and *mdx* muscle at 10 days post-injection.**

Ad5 transduced *mdx* muscle more efficiently than wild type muscle. This figure plots the level of Ad5 and Ad5s transduction wild type muscle from Fig. 4A and in *mdx* muscle Fig. 7A such that viral transduction between muscle types at 10 days post-injection could be compared. The graph plots the mean ± the standard error of the mean. An asterisk (*) denotes a significant difference in transduction compared to wild type muscle.

**Comparison of Ad5 and Ad5s**
**10 days post-injection in wild type and *mdx* muscle**

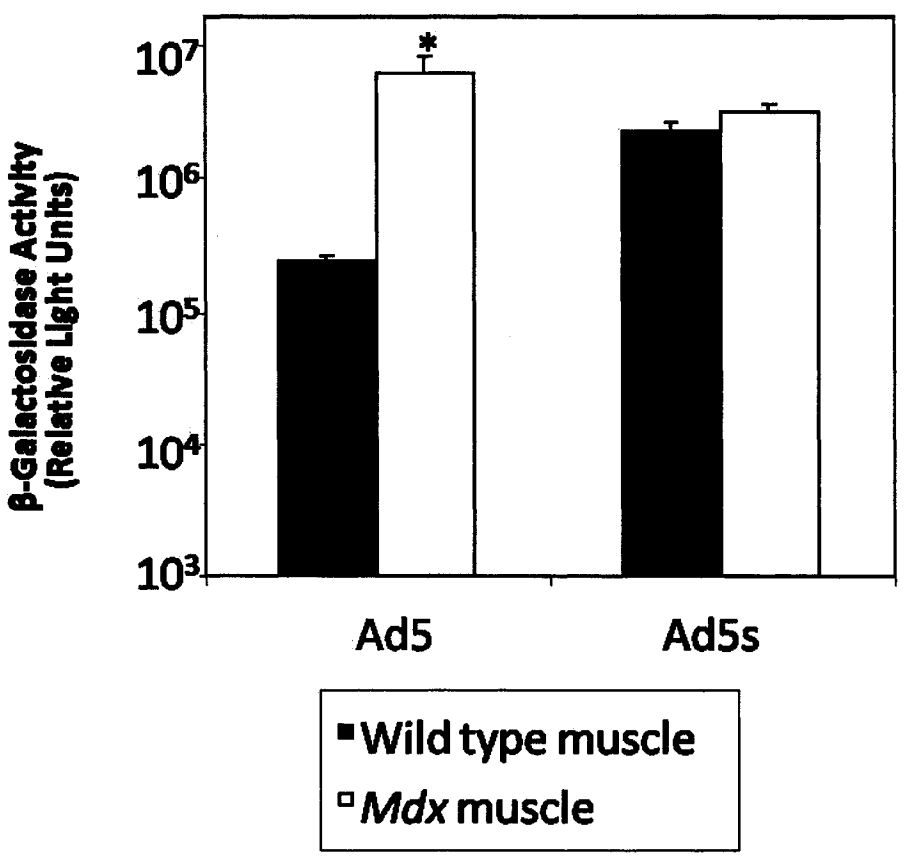

muscle, fiber-modified viruses improved transduction in muscle at 10 days PI in wild type muscle, although not at 2 days PI.

### *3.3.1 Viral infectivity was dependent on fiber length in vitro*

There have been conflicting reports in the literature about how viruses with shorter fibers compare to their long shafted counter parts *in vitro*. One of the first of such accounts described that although Ad9 (with a short fiber length of 11nm) competes for CAR binding with Ad2 (which has a long shaft of 37nm), the short Ad9 fiber was uniquely able to bind $\alpha_v$ integrins (256). It was later shown that an Ad5 based vector with a short fiber and Ad9 knob, was subject to a saturation effect *in vitro* (257). The authors described that the Ad9 chimeric vector improved transduction over Ad5 in human primary fibroblasts, which are deficient in CAR. However, when CAR was expressed in these cells, Ad5 transduction was increased, but the level of transgene expression from the chimeric Ad9 vector remained unchanged. The authors described that vectors with short fibers were binding and entering cells through a direct interaction with $\alpha_v$ integrin receptors (257). Although both the Ad9 chimeric vector and Ad5 are able to bind $\alpha_v$ integrin receptors, the shorter length of Ad9 chimeric fiber enhanced the ability to do so, which was actually favored over the fiber-knob CAR binding capability (257). These results were quite provocative; could changing only the fiber length affect the receptor binding Ad tropism? A major focus in the field of Ad vectorology has been concentrated on ablating and re-directing the Ad the liver tropism, to expand the utility of Ad vectors for gene therapy. Thus, Shayakhmetov and Lieber set out to investigate this possibility by applying different short chimeric fiber constructs to Ad5 based vectors, as Ad5 is the most commonly applied serotype in Ad vectorology. They found fiber-

modified Ad5 based vectors resulted in lower transduction *in vitro* compared to their long-shafted counter parts, irrespective of the level of $\alpha_v$ integrin and CAR present *in vitro* (234). The authors determined that vectors with shorter fibers created a charge repulsion between the acidic cell surface and the negatively charged Ad capsid *in vitro,* while the long shaft of the Ad5 fiber was of a sufficient length to separate both charged surfaces and not impact CAR binding (234). In fact, the authors described that Ad5 fiber is optimized for CAR binding, and fiber-modified viruses are disadvantaged in comparison (234). As a result, their fiber-modified vectors were unable to bypass the necessity of the knob-mediated CAR binding with efficient $\alpha_v$ integrin binding (234). In summary, the literature describes that Ad viruses with shorter fibers may bind $\alpha_v$ integrin to overcome CAR binding, independent of the fiber knob, or their transduction may be universally hindered by a charge repulsion. Even though the fiber-modified vectors used in this study were more similar to those used by Shayakhmetov and Lieber, the *in vitro* results in this work were not necessarily in complete agreement with their findings, therefore the *in vitro* results herein were evaluated with these two possibilities in mind.

In this study, fiber-modified viruses were applied to a muscle-directed gene therapy approach, and thus compared in a relevant *in vitro* model, specifically undifferentiated and differentiated $C_2C_{12}$ cells, and A549s as a control.

In A549 cells, fiber-modified viruses showed no evidence of a charge repulsion that would reduce the efficacy of CAR-mediated transduction because Ad5 and Ad5s had similar transduction efficiency. To conclusively eliminate the effect of a charge repulsion, all viruses

would have to respond equally to the presence of polycations. Fiber-modified viruses may have transduced A549s by a direct interaction with $\alpha_v$ integrin, since both CAR and $\alpha_v$ $\beta_1$ integrin are highly expressed on these cells (201, 258). Competition assays for CAR or $\alpha_v$ $\beta_1$ integrin binding could also be performed to determine if fiber-modified viruses were able to bind $\alpha_v$ $\beta_1$ integrin on A549s. The unexpected observation that Ad5/9s conferred an statistically significant advantage over Ad5s in A549 cells would be supportive of alternate receptor binding, because according to the literature the Ad5 knob is more efficient at binding CAR than Ad9 (234, 253). This observation would be also supported if the amount of CAR and $\alpha_v$ $\beta_1$ integrin were comparable on A549s, however this direct comparison and measurement of receptors by flow cytometry does not exist in the literature. It was expected that all viruses would infect A549 cells more efficiently than $C_2C_{12}$ cells because both CD46 and CAR are differentially expressed in $C_2C_{12}$ cells (203, 254, 255). Since all vectors transduced A549s with a similarly efficiency, the high amount of CAR and $\alpha_v$ integrin must have been responsible for the overall high vector transduction in these cells relative to $C_2C_{12}$ cells.

In undifferentiated $C_2C_{12}$ cells, optimal infectivity was dependent on fiber length, which may have been due to a charge repulsion effect on all fiber-modified viruses. It is of interest to note Shayakhmetov and Leiber initially described that Ad5/35s (which binds the host cell by interaction with CD46) was not subject to a charge repulsion effect *in vitro*; specifically Ad5/35s conferred no disadvantage in terms of attachment and internalization compared to Ad5/35L, with a full length shaft (234). Yet, in this work, Ad5/35s appeared to be subject to a charge repulsion effect, similar to Ad5s and Ad5/9s, which enter by binding CAR. This

could suggest that there are fewer CD46 receptors present on these cell lines than CAR receptors, although this has not been conclusively measured by flow cytometry approach in the literature. To identify that a charge repulsion effect was observed, only fiber-modified vector transduction would be affected by incubation with polycations. As previous literature suggests, Ad5 transduction in $C_2C_{12}$ cells decreases along with differentiation consistent with the down regulation of CAR (203, 240). However, this trend was not observed for fiber-modified viruses. Fiber-modified viruses could have bound $\alpha_v$ integrin instead of CAR, which was supported by the observation that all fiber-modified vectors transduced these cells with a similar efficiency, independent of knob-receptor binding. If this were the case then the level of $\alpha_v$ integrin would have to be substantially lower than the levels of CAR in undifferentiated $C_2C_{12}$ cells. Even though a limited amount of $\alpha_v$ integrin is present on undifferentiated $C_2C_{12}$ cells (259), its amount relative to CAR is unknown. If fiber-modified viruses were responding to a decreased level of integrin, and not charge repulsion, then competition with integrin binding antibodies would determine what role integrin binding plays in fiber-modified vector transduction of undifferentiated $C_2C_{12}$ cells. Therefore, the level of fiber-modified transduction was likely subject to a charge repulsion effect when low levels of receptors were present, in undifferentiated $C_2C_{12}$ cells.

All viruses transduced differentiated $C_2C_{12}$ cells with a similar efficiency (Figure 7C) and therefore were not indicative of a robust charge repulsion effect, as previously described in cells with low CAR (234). This finding may be explained by comparing relative reporter gene expression levels between undifferentiated and differentiated $C_2C_{12}$ cell lines. While Ad5 transduced undifferentiated $C_2C_{12}$ cells 2-fold more efficiently than differentiated $C_2C_{12}$

cells, the trend for fiber-modified viruses was the opposite. Fiber-modified viruses transduced differentiated $C_2C_{12}$ cells between 1.5-and 3-fold more efficiently than undifferentiated $C_2C_{12}$ cells. As previously mentioned the decrease in Ad5 transduction over $C_2C_{12}$ cells differentiation was likely the result of the down regulation of CAR (203, 240), however what caused the increase in fiber-modified vector transduction throughout the $C_2C_{12}$ differentiation? If fiber-modified vectors were binding $\alpha_v$ integrin, which is down regulated throughout the process of myoblast differentiation (260), then lower transduction would be expected in differentiated $C_2C_{12}$ cells than in undifferentiated $C_2C_{12}$ cells, which was not observed. Another possibility for explaining these results is that differentiated $C_2C_{12}$ myotubes have a fully formed basal lamina compared to undifferentiated myoblasts (261, 262), and the presence of a basal lamina may have afforded fiber-modified viruses an advantage over Ad5 *in vitro*. The smaller, fiber-modified viruses may be able to access the receptors present on myotubes more effectively through the basal lamina and achieve transduction compared to the larger Ad5 particles. It may be expected that the presence of a physical barrier, like the basal lamina, would have a larger impact on viral transduction *in vitro*, however this effect was likely diluted by the heterogeneous nature of the differentiated $C_2C_{12}$ cell population. As differentiation proceeds, some myoblasts do not fuse into myotubes. Representative photomicrographs of cell monolayers show that primarily myotubes were transduced in the differentiated $C_2C_{12}$ cell population (Figure 7D). The generation of a homogeneous population of differentiated $C_2C_{12}$ myotubes, complete with formed basal laminas, may result in a more dramatic impact on transduction. Although a method for selective enrichment of myotubes has been

described (263), technical difficulties and time constraints precluded the ability to test this hypothesis directly. Therefore, in differentiated $C_2C_{12}$ cells where the presence of a basal lamina and fewer Ad receptors create conditions that improve the transduction of fiber-modified viruses such that they are equally as efficient as Ad5.

### *3.3.2 Size dependent physical barrier* in vivo

The migration of Ad in muscle is limited (198). Using an Ad5 vector expressing an EGFP-pIX fusion protein, it was shown that at 30 min PI in adult TA muscle, Ad remains primarily at the site of injection (198). Here, polystyrene beads that approximate the size of the Ad virion (190nm) have the same restricted pattern of dispersion in muscle at 30 minutes PI (Figure 8A). The limited distribution of polystyrene beads was maintained at 48 hours PI (Figure 8B) suggesting a physical barrier exists *in vivo* that was not specific to the Ad virion. The physical barrier restricting the migration of the polystyrene beads and Ad particles in muscle was likely the basal lamina, which is a size-specific, passive molecular sieve (209-211). The basal lamina easily permits the passage of the 20nm AAV virion to muscle (217), but restricts particles the size of Ad (162nm -190nm). Therefore, it was hypothesized that decreasing the overall size of the Ad virion may permit the passage through this physical barrier which is necessary for the transduction of muscle fibers.

### *3.3.3 Fiber modified viruses in vivo*

#### *3.3.3.1 Loss of Ad5 infectivity affected first in vivo experiment*

The results of the first *in vivo* experiment were questioned in light of *in vitro* data suggesting that the infectivity of the Ad5 viral stock was compromised. The Ad5 stock used

for the first *in vivo* experiment (Figure 9A, B) was initially verified *in vitro* (Figure 9C). However, immediately after this *in vivo* experiment, Ad5 became undetectable *in vitro* (Figure 9D). The physical stability and titer of Ad preparations are influenced by many factors including temperature (264, 265), how quickly the stock was cooled, and what buffers and cryoprotectants the vector was suspended in (266, 267). Particularly, the physical stability of the Ad virion becomes compromised in conditions of acidic pH (267, 268). Ad stored in PBS is uniquely unstable because the pH decreases with each freeze-thaw cycle, regardless of cryoprotectant used (267). This phenomena is observed because components of the phosphate buffer (specifically, disodium hydrogen phosphate dodecahydrate) precipitate out of solution at low temperatures, thus significantly changing the composition of the buffer (269). The original Ad5 stock that was used in the first *in vivo* experiment was prepared years ago, with no records of how many freeze thaws it underwent. Even though the original Ad5 stock was likely purified in 10mM Tris and not PBS, which more effectively maintains pH over the freeze-thaw cycle (267), Ad stocks prepared in 10mM Tris can still lose infectivity with freeze-thaw activity. Therefore, when *in vitro* experiments determined the Ad5 stock was evidently compromised, the vector was re-prepared and verified.

The transduction of the new viral stock was compared using β-gal forming units (BFU) *in vitro*. BFU assays normalize for differential infectivity *in vitro*, thus similar gene expression between viruses was expected when BFU titers were compared. The infectivity of the newly prepared Ad5 stock was confirmed, typical of a BFU assay result (Figure 9 E). Although these data were obtained from an n value of only two, these preliminary results sufficiently bring

into question the integrity of the initial Ad5 virus stock and results obtained from the first *in vivo* experiment. In this experiment, fiber-modified viruses showed almost a 30-fold improvement over Ad5 transduction in adult muscle (Figure 9A). Likely, this large difference observed between fiber-modified vectors and Ad5 transduction in muscle was due to the loss of infectivity of the Ad5 viral stock. Therefore, the newly prepared Ad5 stock was utilized for subsequent experiments.

### *3.3.3.2 Fiber-modified viruses improve transduction in wild type muscle*

The record in the literature of how fiber-modified viruses are characterized *in vivo* is also subject to interpretation. Various studies describe that fiber-modified viruses result in an attenuated immune response compared to their long shafted counter parts (270, 271). However, these findings were largely the result of a decreased infectivity of these viruses. In this work, fiber-modified viruses do not exhibit a decreased infectivity compared to Ad5 in wild type muscle and may be able to circumvent or delay the immune mediate clearance of vector transduction in wild type muscle after 10 days post-injection.

The smaller overall size of the fiber-modified viruses conferred a 10-fold advantage over Ad5 *in vivo* at 10 days PI. Fiber-modified viruses transduced more muscle fibers than Ad5 and displayed an improved pattern of dispersion *in vivo*. The smaller size of the fiber-modified viruses may have permitted further dispersion of the virus particles throughout the muscle, creating the potential to transduce more muscle fibers than Ad5, the large size of Ad, which limits its dispersion to around the injection site. Although an improved pattern of transduction was evident from the muscle sections, further characterization of this

observation was hindered by two experimental limitations. Firstly, a higher dose of administered vectors would be required to quantitatively characterize if the pattern of fiber-modified vectors dispersions differs from Ad5 *in vivo*. The conservative dose of $1x10^9$ virus particles transduced too few muscle fibers (between 2-8% of muscle fibers for all vectors) and thus did not permit embarking on a meaningful analysis of overall area distribution. Secondly, this type of analysis would require more muscles to be analyzed to account for experimental variability as an n value of only two would not produce results of meaningful statistical power. Since increasing the n value for the tissue analysis portion of *in vivo* experimentation was not possible due to financial implications, a dose escalation experiment was performed in order to qualitatively assess an appropriate vector dose for assessing viral dispersion *in vivo*.

The dose escalation experiment directly comparing Ad5 and Ad5s at 2 days PI was performed to determine if vector transduction in muscle increased proportionate to vector dose. A higher level of transgene expression in the muscle than in the liver was anticipated because the vector was directly delivered to muscle. Surprisingly, at two days post-injection, the level of liver transduction was comparable to that of muscle. Although quite dramatic, this result speaks to the well characterized liver tropism of the Ad vector (84). It is speculated that the high level of liver transduction observed at 2 days PI (Figure 11 B) compared to 10 days PI (Figure 10 B) captured the process whereby circulating Ad vectors become entrapped within the fenestrations of the liver resulting in transduction of hepatocytes (190).

Although statistically insignificant, vector transduction of the liver displayed a dose-dependent trend. This observation was in line with a previous study that described escalating Ad vector doses of less than $3x10^{10}$ virus particles produce a modest increase in liver transduction and doses beyond that threshold (up to $1x10^{11}$ virus particles) result in a disproportionately high level of liver transduction (193). The authors explained the threshold effect: Kupffer cells sequester of Ad vectors by acting as a biological filter, inhibiting transduction of hepatocytes (193).

Generally, Ad transduction in muscle is dose-dependent (169). Results showed that the high dose of Ad5 resulted in muscle transduction that was significantly higher than the low dose. For Ad5s, the high and medium doses resulted in significantly higher transduction than the low dose. Although this effect was not directly proportional to the increase in vector dose, the results indicate Ad5 and Ad5s produce a dose-dependent increase in muscle transduction. Despite similar overall transduction levels with the high dose of vector, Ad5s transduced more muscle fibers than Ad5. One explanation for this observation is that Ad5 delivery produces more co-infection of muscle compared to Ad5s. Since only two muscles were examined per condition, additional experimentation would be needed to account for potential injection variability.

Comparing both wild type experiments, the data suggests that Ad5 transduction was selectively cleared over 10 days PI (Figure 12), in comparison to Ad5s transduction which was stable over this time course. Using similar experimental methods, elimination of Ad5CMV-*lac*Z transduction in *mdx* and normal muscle has been previously described (250).

The methods used by Hartigan-O'Connor *et al.* (250) differ from this body of work in the following ways: (1) the Ad5 vector included a minx intron to enhance splicing and a nuclear targeted β-gal sequence (272), (2) a higher dose of vector was used at $2.5x10^{10}$ virus particles, (3) β-gal was quantified in terms of unit enzyme/kg of muscle, (4) C57Bl/10 was used as the control normal muscle strain. Hartigan-O'Connor *et al.* observed a 5-fold decrease in Ad5 transduction in normal muscle between 3 and 10 days PI. In congruence with this data, a 10-fold decrease in Ad5 transduction was observed in this study between 2 and 10 days PI. Hartigan-O'Connor *et al.* describe this decrease in Ad5 transduction as an effect specific to the CMV promoter. The CMV promoter immediately produces a high amount of β-gal protein in a non-muscle specific manner such that the resident immune cells in the muscle tissue can efficiently recognize and eliminate the immunogenic protein and vector. Although this work by Hartigan-O'Connor *et al.* described the likely mechanism by which Ad transduction was eliminated in normal muscle, further studies of fiber-modified viruses have provided insight as to why this effect was not observed with fiber-modified viruses. The Ad5 shaft contains a specific KKTK domain that mediates the targeting to DCs through heparin sensitive receptor binding (273). Fiber-modified viruses do not contain this domain and thus may elicit an attenuated adaptive immune response, delaying the clearance of vector transduction. Taken together, this body of work suggests Ad5 was a selectively cleared in normal muscle. Likely, fiber-modified viruses are cleared by a similar mechanism as Ad5, only with a difference in the kinetics. Further research would be necessary to determine if higher gene expression by fiber-modified vectors at later time

points post-administration was due to their evasion of the immune-mediated clearance of transduced cells.

The factor in this work that challenges this conclusion of a selective clearance of Ad5 in wild type muscle is that it was reached by comparing two separate experiments that were performed on separate days; the primary concern is a matter of injection variability. The comparison between experiments was justified because injection variability was consistent across all experiments. The quantitative analysis of vector transduction (n=8) showed similar levels of fiber-modified vector transduction across all *in vivo* experiments (Figure 9A, 10A, 11A, 13A), which speaks to a consistent experimental method when an n value of 8 was utilized. Therefore, the comparison between experiments was valid, thus supporting a selective clearance of Ad5 in wild type muscle, the mechanism of which warrants further investigation.

### *3.3.3.3 Ad5 transduces mdx muscle more efficiently than fiber-modified viruses*

When developing an appropriate vector system for the treatment of DMD, it must be effective in an experimental model of the disease. *Mdx* muscle contains three unique muscle fiber populations: normal, regenerating, and degenerating (274). Electron microscopy (EM) of *mdx* tissue at 4 weeks and 28 weeks of age reveals that the basal lamina and sarcolemma are present surrounding normal and regenerating muscle fiber but may be incomplete surrounding degenerating muscle fibers (95). Muscle degeneration and inflammation does not occur uniformly throughout the entire length of muscle fibers, rather degeneration is segmental (95), affecting between 50-90% of the muscle fiber length

(274). Segments of necrotic muscle fibers can be divided into three populations: mild, moderate and severely degenerated. At 28 weeks of age in *mdx* tissue, moderately degenerated muscle fibers are the most prevalent (274). The basal lamina and sarcolemma are intact surrounding mildly degenerated muscle fibers. In contrast, moderately degenerated myofibers, which are coagulated in areas of necrosis, completely lacked a sarcolemma in these regions even though portions of the basal lamina are preserved (274). Severely degenerated regions of muscle fibers taper to empty basal lamina tube lacking a sarcolemma (274). The basal lamina of degenerated muscle fibers is left behind in the interstitial space (213), accumulating multiple layers of laminin (95). In summary, the structural integrity of the basal lamina is quite different in *mdx* mice than in normal muscle and it was questioned whether fiber-modified viruses would confer an advantage over Ad5 in this environment.

In 3-5 week old *mdx* muscle, Ad5 transduced *mdx* muscle more efficiently than fiber-modified viruses, independent of receptor binding (Figure 13B). In comparison, fiber-modified viruses were able to transduce wild type and *mdx* muscle at a similar efficiency, but Ad5 was able to transduce *mdx* muscle 20-fold more efficiently than wild type muscle (Figure 15). Hartigan-O'Connor et al. showed that a similar vector (Ad5CMV-*lacZ*) expressed 14-fold more β-gal at 7 days PI in *mdx* muscle compared to in normal muscle, which was consistent with these results (250). The authors indicate that Ad transduced *mdx* muscle with a greater efficiency than wild type because a greater proportion of regenerating muscle fibers was found in *mdx* tissue (204, 207), and Ad preferentially transduces regenerating muscle fibers.

In these studies, immunohistochemical (IHC) analysis was performed in attempt to describe if vectors were preferentially transducing regenerating muscle fibers in *mdx* tissue. Actively regenerating muscle fibers were identified with a centrally located nucleus and normal muscle fibers were identified by the absence of central nucleation. Newly regenerating muscle fibers were identified by e-MHC staining. Two distinct morphologies of the e-MHC positive fibers may indicate muscle in two separate points along the continuum of muscle regeneration and repair. Strong e-MHC staining was described in small muscle fibers, thought to be differentiated satellite cells while larger muscle fibers that stained weaker for e-MHC were older muscle fibers, further along in the differentiation pathway (275). In rat muscle, it takes 2 weeks for regenerating muscle fibers to reach maturity and completely lose e-MHC expression (276). The IHC analysis revealed that e-MHC positive muscle fibers were predominantly of the small, darker stained morphology indicative of differentiated satellite cells (data not shown). In general, all vectors transduced very few muscle fibers in total (Figure 13E, 14C), and there was no evidence of transduction of e-MHC positive muscle fibers by any of the vectors tested (Figure 14 A). As expected, 50% of muscle fibers were centrally nucleated (Figure 13D, 14B) (98), but preferential infectivity for newly regenerating muscle by Ad vectors was not observed (Figure 14D) (206). Because so few muscle fibers were transduced, it was difficult to assess viral dispersion and conclusively determine if vectors preferentially transduced or had access to certain types of muscle fibers.

Ad5 transduction was highly efficient in mdx muscle and was not indicative of a selective clearance as observed in wild type muscle. It is hypothesized that Ad5 is able to

highly transduce *mdx* muscle because of the high prevalence of CAR on regenerating muscle (250). Therefore, a high amount of receptor binding may be able to overcome the loss of transduction Ad5 due to immune cell clearance. However, this effect was not observed with fiber-modified viruses, which had similar transduction regardless of vector binding in both wild type and *mdx* muscle.

In wild type and *mdx* muscle, the transduction of fiber-modified vector was equally as efficient, independent of knob-receptor binding. This effect was supportive of the direct binding fiber-modified viruses to $\alpha_v$ integrin, and not the primary receptor as defined by the knob-receptor binding affinity. It should be noted that the level of fiber-modified vector transduction was consistent between wild type and *mdx* muscle even though 50% of the muscle fibers in *mdx* muscle was actively regenerating. This significant amount of regenerating muscle fibers in the tissue would be expected to affect the overall $\alpha_v$ integrin levels in the *mdx* muscle since $\alpha_v$ integrin expression decreases with muscle differentiation (260). In turn, if fiber-modified viruses were binding $\alpha_v$ integrin directly, higher transduction would be expected in *mdx* muscle compared to wild type. The possibility of $\alpha_v$ integrin binding *in vivo* could be addressed by examining a preferential infectivity for fiber-modified viruses for muscle fibers that highly express $\alpha_v$ integrin, however this was not possible in these studies since so few muscle fibers were transduced.

In summary, this body of work explored the utility of fiber-modified viruses as tool for the field of muscle-directed gene therapy. Although the hypothesis that fiber-modified viruses improve transduction in muscle was demonstrated only at 10 days PI in wild type

muscle, this finding is still of significant importance. The implications of this work raised important questions that warrant further investigation. For example, is there a spatial difference between the dispersion of fiber-modified viruses Ad5 *in vivo*, what is the mechanism by which fiber-modified vectors maintain transduction over 10 days, and do fiber-modified viruses preferentially transduce mature muscle fibers? The outcome of this work would shape the design of future studies such that the utility of fiber-modified viruses can be further described.

# *Chapter 4: Optimization of the murine secreted embryonic alkaline phosphatase (mSEAP) reporter gene*

## *4.1 Introduction*

Gene therapy is a versatile experimental approach that can be applied to the treatment of many human diseases. However, current challenges in developing vectors for specific gene therapy application require attenuating their toxicity to the host and improving transgene expression in target tissues. To sensitively analyze vector efficacy, reporter genes are used in place of a therapeutic transgene. Most experimental studies use murine models of human disease, yet the available reporter genes that are commonly used for these applications elicit an immune response in mice, like human secreted placental alkaline phosphatase (hSEAP). The Parks lab previously described the murine placental-derived SEAP (mSEAP) as a non-immunogenic alternative to the hSEAP reporter gene. Although mSEAP is non-immunogenic, it is not efficiently secreted from transduced cells, nor is it heat-stable. Herein, mSEAP has been rationally modified to improve the ease of sampling and the sensitivity of mSEAP detection by addressing these drawbacks.

## *4.2 Results*

### *4.2.1 Plasmid expression of mSEAP in vitro*

In order to improve the release of mSEAP from the cell, the same approach used to generate the hSEAP reporter construct was employed (230). Specifically, the C-terminal transmembrane domain that localizes the enzyme to the membrane was removed (Figure 16 A,B). Plasmids were generated to first assess the nature of reporter gene expression *in*

**Figure 16: Schematic representation of SEAP constructs used in this study**

(A) SEAP constructs consist of an N-terminal sequence peptide (shown in dark grey), a crown domain (shown in light grey) and a C-terminal transmembrane domain (shown in black). (B) The secretion of mSEAPΔ was enhanced by truncating the C-terminal transmembrane domain. (C) The heat stability of hSEAP is due to a key histidine residue at the 445 position in the crown domain near the active site of the enzyme (277). Since mSEAPΔ has gultamic acid at this key site, mSEAPΔ-H451E was constructed with the analogous residues of the hSEAP construct. Expression of all constructs was driven by the ubiquitin C promoter.

A

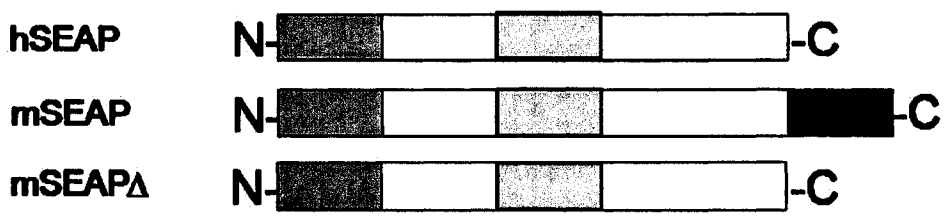


B

```
mSEAP    500 AGSGSAPSPGALLLPLAVLSLP
mSEAPΔ   500 AGSGSAPSPG----------
```

C

```
mSEAPΔ           443 QSAVPRLHETHHGGE 458
hSEAP            437 ******RE****A** 453
mSEAPΔ-H451E     443 *******E****A** 458
```

*vitro*. Plasmids were transiently transfected into 293 cells and the resulting AP activity associated with the cell membranes and the media was compared (Figure 17). As expected, hSEAP was not highly cell-associated (7%) as compared to mSEAP (77%). The truncated mSEAPΔ had a similar amount of cell-associated AP activity compared to hSEAP (6%). Examination of the conditioned media showed that the majority of hSEAP was released (93%). In contrast, mSEAP was less efficiently released from the cell. Therefore, removal of the hydrophobic tail in the mSEAPΔ construct improves its release from the cell (94%) similar to that of hSEAP.

Next, key residues on mSEAPΔ were mutated to match analogous residues on hSEAP that facilitate its heat stability (Figure 16 C). The mutant construct, mSEAPΔ-H451E, was compared to hSEAP in a heat inactivation time course experiment so that the extent and duration of heat stability could be identified (Figure 18). Over 30 minutes at 65°C, mSEAP, mock, and the pcDNA-Ubc control lost more than 97% of enzymatic activity while hSEAP maintained the majority of its activity. At 55°C, mSEAPΔ-H451E maintained its AP activity over the duration of the time course. mSEAP, mSEAPΔ, and mock pcDNA-Ubc control lost more than 89% of their enzymatic activity at 55°C, where as hSEAP and mSEAPΔ-H451E lost 37% and 41% of their activity, respectively. Therefore, mSEAPΔ-H451E exhibits similar heat stability to hSEAP at 55°C.

**Figure 17: The Release of SEAP activity from the cell**

One and a half micrograms of plasmid DNA were transiently transfected into 293 cells and at 24 hrs post-transfection, media and cell lysates were harvested and assayed for AP activity using a chemiluminescent assay. Graphs plot the mean ± the standard error of the mean. The percentage AP activity that was released from the cell was calculated and listed at the bottom of the figure (n=5).

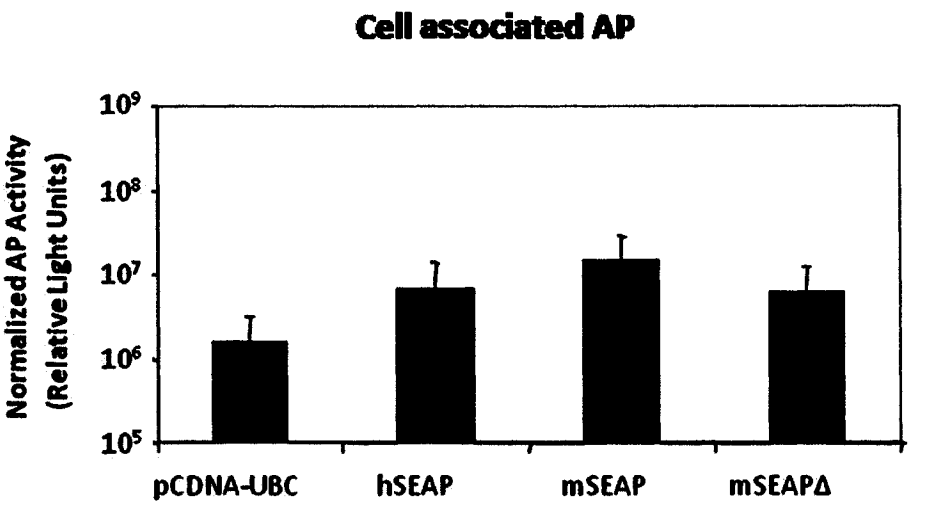


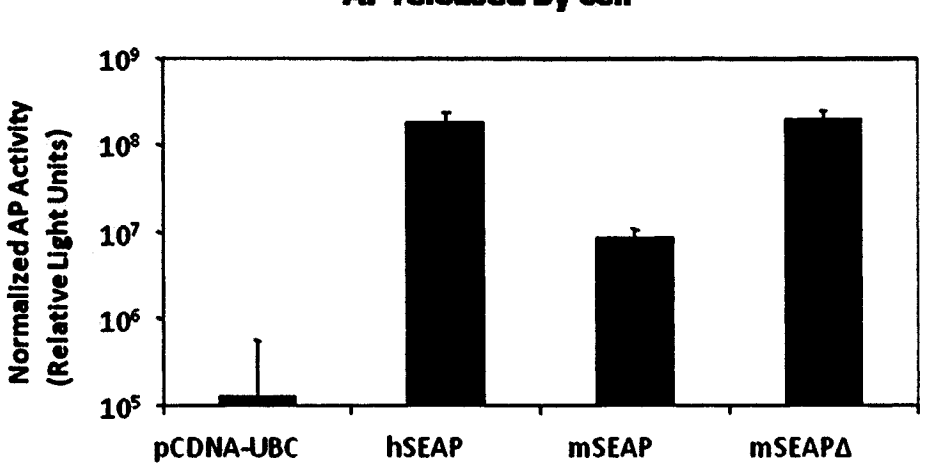


| % AP Secreted | – | 93 | 23 | 94 |
|---|---|---|---|---|

**Figure 18: Heat Stability of SEAP**

mSEAPΔ-H451E was heat stable at 55°C. Two micrograms of the indicated plasmid DNA were transiently transfected into 293 cells and at 24 hrs post-transfection, media was harvested and incubated at (A) 65°C or (B) 55°C for 0, 5, 10, 20 and 30 minutes and assayed for AP activity using a chemiluminescent assay (n=3). Graphs plot the mean ± the standard error of the mean.

A

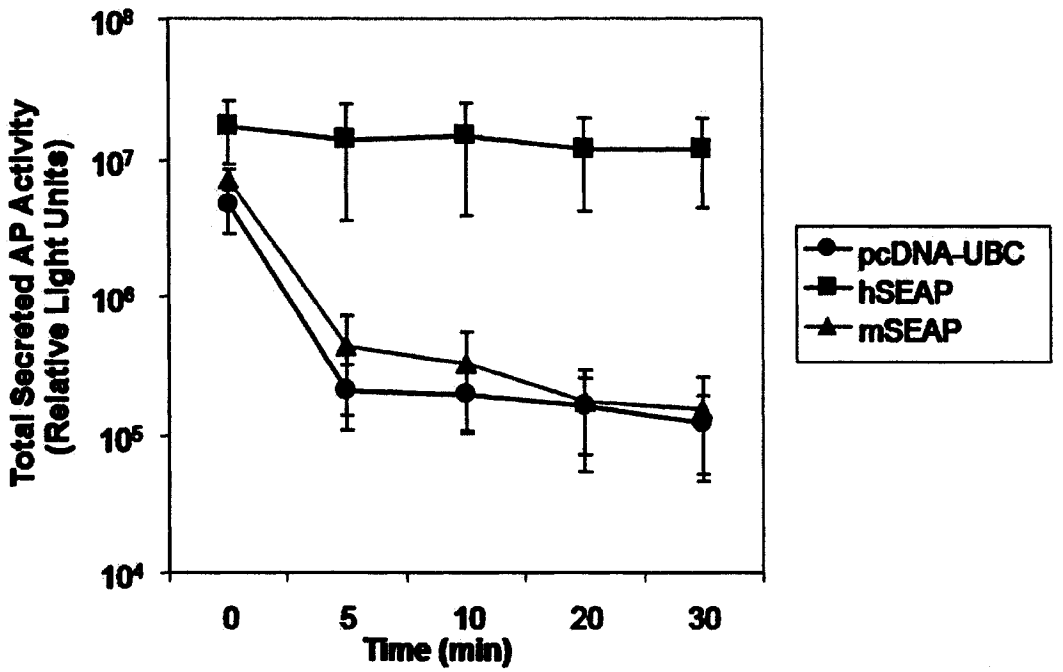
Total Secreted AP Activity (Relative Light Units)
10⁸
10⁷
10⁶
10⁵
10⁴
0
5
10
20
30
Time (min)
pcDNA-UBC
hSEAP
mSEAP

B

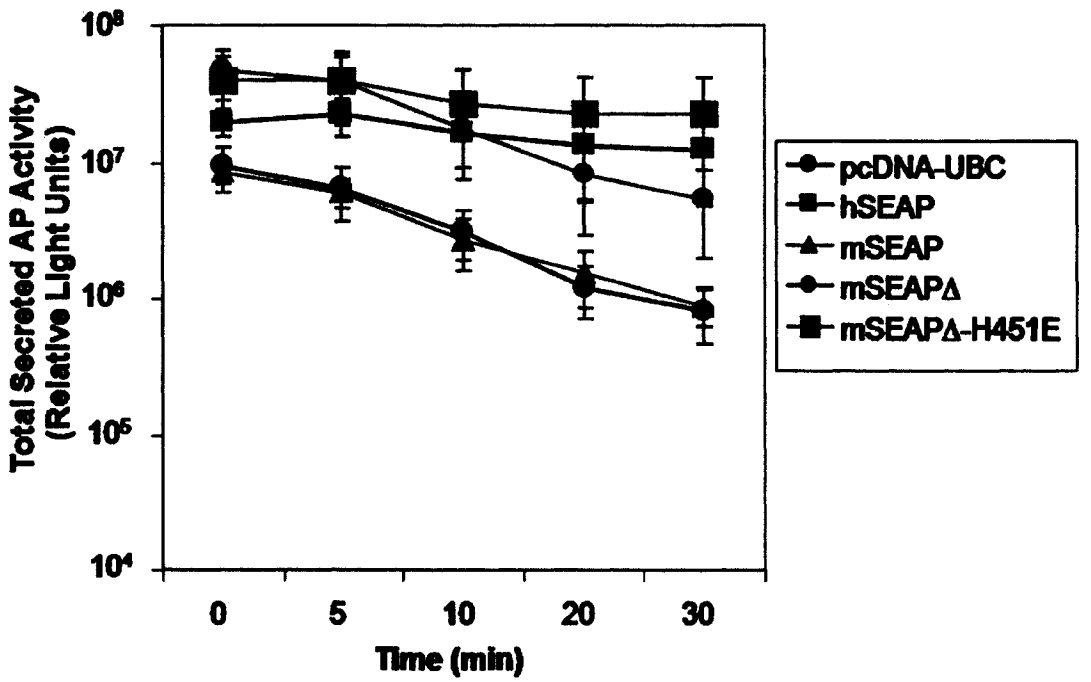
Total Secreted AP Activity (Relative Light Units)
10⁸
10⁷
10⁶
10⁵
10⁴
0
5
10
20
30
Time (min)
pcDNA-UBC
hSEAP
mSEAP
mSEAPΔ
mSEAPΔ-H451E

### *4.2.2 Ad vector expression of mSEAP in vitro*

In order to confirm the efficacy of the mSEAPΔ-H451E reporter gene for gene therapy vector studies, first generation Ad5 vectors expressing mSEAPΔ and mSEAPΔ-H451E were generated and transgene secretion was measured *in vitro*. An MOI of 20 virus particles per cell was used to infect A549 cells; at 24 hours post-infection media was harvested and assayed for AP activity using a chemiluminescent assay. At a relatively low MOI, hSEAP and mSEAP expression was indistinguishable from background (Figure 19). Heat inactivation of hSEAP was required to discern endogenous AP activity from reporter gene expression. Because mSEAP was not heat stable, AP activity post-heat inactivation was indistinguishable from background. Modifications made to mSEAPΔ improved its release from the cell by 4-fold, this improvement was sufficient to discern between transgene expression and background AP activity with and without heat inactivation. Because mSEAPΔ-H451E was heat stable at 55°C, transgene expression was clearly discerned from background AP activity after heat inactivation (Figure 19). Therefore, mSEAPΔ-H451E was effectively expressed from an Ad vector and its heat stability is advantageous for *in vitro* gene therapy studies.

In summary, the remaining drawbacks of the mSEAP reporter gene were addressed by rationally modifying the mSEAP construct in order to improve its ease of sampling and the sensitivity of its detection. The release of mSEAP from the cell was improved by 71% by removing the C-terminal hydrophobic transmembrane domain that allows mSEAP to remain cell-associated. Furthermore, key residues in the crown domain were mutated to make the mSEAP protein heat stable; heating to 55°C resulted in a 91% decrease in background AP

**Figure 19: Heat stability of SEAP expressed from an Ad vector**

AdmSEAPΔ-H451E was heat stable at 55°C. First generation E1/E3 deleted Ad5 based vectors were generated encoding either hSEAP (AdhSEAP), mSEAP (AdmSEAP), mSEAPΔ (AdmSEAPΔ), mSEAPΔ-H451E (AdmSEAPΔ-H451E) under the control of the ubquitin C promoter and bovine growth hormone polyadenylation sequence. A549 cells ($1x10^6$ cells per 35mm dish) were infected with the respective Ad vectors at an MOI=20. At 24 hours post-infection, media was harvested incubated at 0°C and 55°C for 30 minutes and assayed for AP activity using a chemiluminescent assay (n=5). Graphs plot the mean ± the standard error of the mean.

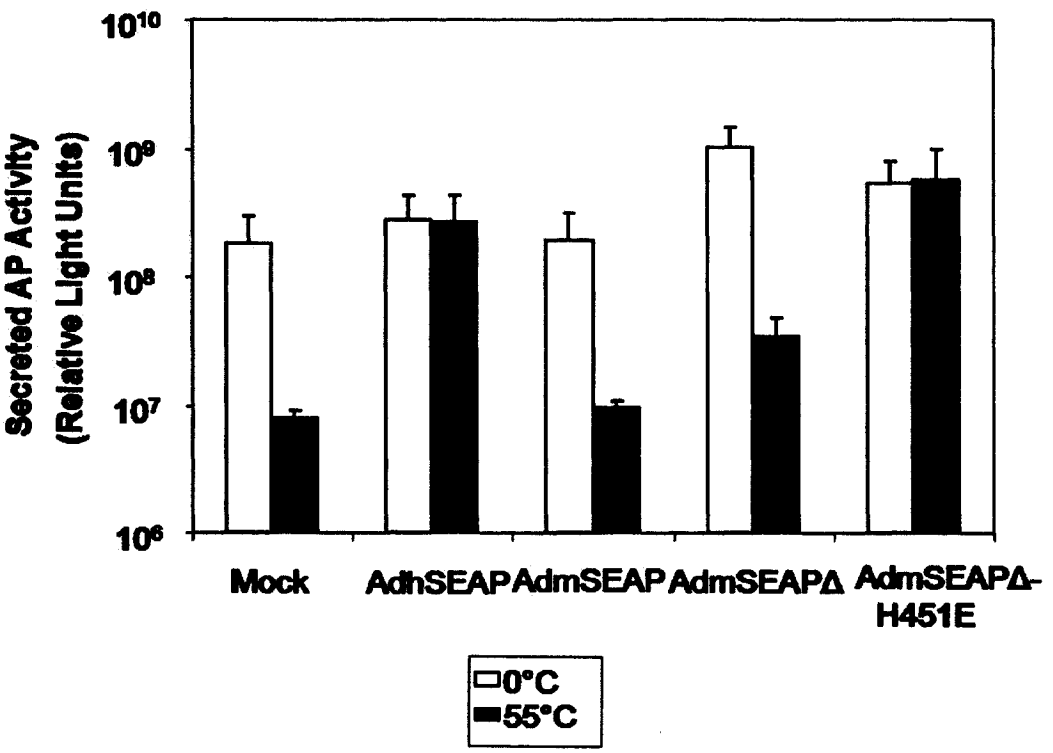
Secreted AP Activity
(Relative Light Units)
10^10
10^9
10^8
10^7
10^6
Mock
AdhSEAP
AdmSEAP
AdmSEAPΔ
AdmSEAPΔ-H451E
0°C
55°C

activity. Therefore, the modifications to mSEAP improved the secretion and heat stability of the reporter construct as expressed from DNA plasmid vectors and FGAd vectors. However, this work did not examine the function of the improved mSEAPΔ-H451E reporter construct *in vivo,* which would be required to fully realize the utility of the reporter construct as a tool for gene therapy vector studies.

## *4.3 Discussion*

### *4.3.1 mSEAPΔ was released from the cell similar to hSEAP*

Most mammalian AP encode a hydrophobic tail resulting in predominantly cell-associated protein (278). The hSEAP reporter protein was engineered for more efficient release from the cell by removal of the hydrophobic tail that participates in the process of phoshatidylinositol-glycan anchoring (GPI) of the enzyme to the plasma membrane (230, 279, 280). Therefore, truncating the C-terminus of hSEAP converted a primarily cell-associated enzyme to one that is primarily released into the media. The same approach was used to improve the release of mSEAP from the cell, where the construct was termed mSEAPΔ. Truncating the C-terminal transmembrane domain improved the release of mSEAP from the cell similar to that of hSEAP.

### *4.3.2 mSEAPΔ-H451E confers heat stability*

The heat stability of hSEAP as well as resistance to EDTA and L-leucine has been linked to a key residue located in the crown domain, Glu-429 (231). The negatively charged residue stabilizes the protein homodimer and metal binding, which is essential for catalytic activity. Furthermore, Le Du and Milan reported that substitution of this hSEAP residue

(E429G) eliminates its heat stability properties (277). Even though substitutions at Glu-429 affect the conformation of the surface of the protein, significant structural changes to the active site are not incurred (281, 282). Although hSEAP and mSEAP are relatively conserved throughout the crown domain, mSEAP contains a histidine residue at this key site. Therefore, the analogous residue (H451E) on mSEAPΔ was mutated, making the mSEAPΔ sequence similar to hSEAP.

A heat inactivation time course experiment was performed to examine the extent and duration of the potential heat stability of the secreted mutant mSEAPΔ constructs. hSEAP was used as a control because it is heat stable. AP activity was first assessed at 65°C because typical hSEAP reporter assays suggest a heat inactivation step at this temperature for 30 minutes to effectively eliminate background AP activity. Over the 30 minute time course examined, mSEAP lost the majority of its activity while hSEAP did not. A 55°C incubation time course was then performed to determine if the mSEAPΔ-H451E construct could confer heat resistance over a longer incubation time, as mSEAPΔ-H451E was not able to maintain AP activity at 65°C or 60°C (data not shown). mSEAPΔ-H451E maintained its AP activity at 55°C over 30 minutes, which was an ideal incubation period for a heat inactivation assay.

### *4.3.3 mSEAPΔ-H451E expression from an adenoviral vector*

The data thus far was based on transient transfections of reporter constructs in 293 cells. To assess whether the improved mSEAP expression cassettes performed equally well in a second vector system, the various expression cassettes were cloned into Ad vectors

and the expression and stability of the resulting AP protein was examined. mSEAPΔ and mSEAPΔ-H451E were cloned into a first generation Ad5 vector, which was made replication defective due to the deletion of the E1 early gene. Reporter gene expression was under the control of the Ubc promoter and the BGH polyadenylation sequence. AdmSEAPΔ and AdmSEAPΔ-H451E were compared to AdmSEAP and AdhSEAP *in vitro*. A549 cells were infected at an MOI of 20, and at 18 hours post-infection the AP activity in the media was assayed. Heat inactivation was required to distinguish endogenous AP activity in A549 cells from hSEAP expressed from an Ad vector at a low MOI of 20 (Figure 19). Because mSEAP and mSEAPΔ were sensitive to heat inactivation, levels of AP activity expressed from AdmSEAP were not clearly discerned from background post-heat inactivation. As expected, the deletion of the tail domain of mSEAP resulted in a 4-fold increase in AP in the medium. AdmSEAPΔ-H451E maintained AP activity post-heat inactivation at levels well above background, similar to AdhSEAP. Therefore mSEAPΔ-H451E performed equally well as expressed from plasmid expression system and an adenoviral vector.

This report described an improved reporter gene designed as a rapid, effective tool for the assessment of vector function. The secretion of mSEAP was improved by removing the C-terminal hydrophobic tail and heat stability was achieved by mutating a key residue, more closely mimicking its heat stable human homolog. The improved secretion of mSEAPΔ shown *in vitro* would translate to enhanced secretion into serum, if applied *in vivo*, and would permit sequential sampling of experimental animals by analyzing blood samples. Improved heat stability proved essential for discerning reporter gene expression from endogenous AP *in vitro*, which would also be an asset when applied *in vivo*. If the

modifications to mSEAPΔ-H451E prove to be non-immunogenic, then its utility as an ideal reporter gene for long-term mouse studies would truly be realized.

# *Chapter 5: Conclusions*

Efficient vector transduction was dependent on fiber length in myoblasts *in vitro* and in *mdx* muscle, but fiber-modified viruses improved transduction in wild type muscle by 10-fold at 10 days PI. This finding is significant to the field of gene therapy because it is well established that Ad vectors poorly transduce normal mature muscle due to the low level of CAR expression (202, 203). Improving the efficiency of gene delivery to wild type muscle alone is actually relevant to DMD pathology. In late stage DMD pathology the regenerative capacity of muscle becomes exhausted, and as a result, there are fewer regenerating muscle fibers (97, 105). It is advantageous to optimize vectors towards older DMD pathology because diagnosis typically occurs at this point in disease progression (207). However, treating late stage DMD involves the challenge of delivering Ad vectors to non-regenerating muscle fibers. Although we were unable to conclusively show that Ad preferentially infects regenerating muscle fibers, as shown in the literature, some strategies actually employ the use of crush injury or neurotoxin administration that damage the few existing muscle fibers, forcing regeneration in order to improve Ad transduction (205-207). The benefits of therapeutic gene delivery to late stage DMD pathology may outweigh the risks of further damaging the already fragile muscle population (207). Here, multiple Ad vectors with enhanced delivery to non-regenerating muscle fibers were described, without the use of damaging methods to force muscle regeneration.

The fact that chimeric Ad vectors with different serotypes were described in muscle is clinically significant. Wild-type Ad infections are relatively common and the majority of the

North American population has circulating antibodies against Ad5, 55% of which are neutralizing (161). Upon re-exposure to Ad in the form of a therapeutic Ad vector, both CD8 T cells and neutralizing antibodies produce an anti-Ad immune response eliminating therapeutic transduction and limiting the efficacy of treatment (283, 284). Although a high neutralizing antibody titer may not limit the efficacy of a locally administered Ad vector, they are a significant concern for systemically circulating Ad which does occur despite local administration (249, 285). Switching the knob domain on fiber sufficiently shields the vectors from pre-existing neutralizing antibodies even though these Abs are typically raised against hexon (283, 286). The chimeric fiber-modified vectors in this study had knobs from three different serotypes, Ad5, Ad9, and Ad35. All three fiber-modified vectors were effective gene delivery tools to wild type muscle, especially if repeated administration of gene therapy vectors is required for a cure for DMD to be achieved. Although DYS has a long half life *in vivo* (109), it is unrealistic to presume that one treatment alone will be sufficient for a therapeutic level of gene expression. Applying chimeric fibers to the HDAd system may convey an additional advantage by evading the humoral immune response, as HDAds can be repeatedly administered in the presence of neutralizing antibodies raised against an alternate serotype of Ad (287). Therefore, chimeric fiber-modified Ad vectors are of significant importance to the field of DMD gene therapy as they could be applied to the HDAd system for the repeated delivery of therapeutic vectors to normal muscle.

In wild type muscle, fiber-modified viruses disperse further and transduce mature muscle more efficiently than Ad5 at 10 days PI. Viral transduction observed at the earlier time point of 2 days PI indicates that the advantage of fiber-modified viruses have over Ad5

at 10 days PI may not be related to an increased ability to overcome physical barriers, like the basal lamina, but instead possibly a decreased susceptibility to clearance by immune cells. It has been shown that the Ad5 fiber contains the specific KKTK domain, which targets Ad5 to DCs (273). Additional experiments are required to examine the potential role of APCs in fiber-modified vector transduced muscle. Straightforward end point assays could be used to examine the role of the adaptive immune system on fiber-modified viral transduction in muscle. The efficiency of clearance of transduced cells could be inferred by transgene persistence over time, and humoral immunity could be described by the presence of neutralizing antibodies against the viral capsid as well as the transgene (271).

In *mdx* muscle, Ad5 was more efficient than fiber-modified viruses. Ad5 transduces *mdx* muscle more efficiently than wild type muscle likely because CAR is up regulated in regenerating mouse muscle (189) and Ad5 is optimized for CAR binding over the fiber-modified viruses because the shorter fibers cause a charge repulsion between Ad capsid and cell surface proteins (234). However, the number of transduced muscle fibers was too low to conclusively determine if fiber-modified viruses preferentially infect regenerating fibers. These results are important for guiding future investigation of fiber-modified viruses *in vivo*. For example, higher doses (of at least $1x10^{10}$ virus particles) would be required to achieve high enough transduction in muscle to determine if fiber-modified viruses preferentially infect actively dividing muscle fibers. In addition, higher doses would be needed to examine the role of the innate and adaptive immune response on fiber-modified viral transduction *in vivo*. Generally, a dose of $1x10^{10}$ virus particles per animal is recommended for many measures of immunological response like transcriptional induction

of cytokine and chemokine and subsequent cellular recruitment as well as serum ELISAs and Replication protein A (RPA) assays (271). A dose within the limits of sensitivity for measuring immediate cytokine gene expression (ie. 6 hrs PI) is $1x10^{11}$ particles/ animal (288). Therefore, this body of work will guide future experimentation to fully characterize fiber-modified viruses *in vivo*.

Further examination of fiber-modified viruses *in vivo* would require the evaluation of transgene expression over a longer period of time in wild type and *mdx* mice. As this work raised important questions regarding the immunological interaction of fiber-modified vectors *in vivo*, further characterization of vector function would require substituting the immunogenic β-gal reporter gene used in these studies with a non-immunogenic one, so the effects of the vector could be isolated and properly studied. Since the majority of available reporter genes are immunogenic, a complementary approach was used to develop a non-immunogenic reporter gene, ideal for the follow up studies on the fiber-modified vector system. Although the mSEAPΔ-H451E reporter construct demonstrated improved secretion and heat stability as expressed from a plasmid DNA vector and a FGAd vector, its efficacy and function *in vivo* remains unknown. If FGAd vectors expressing mSEAPΔ-H451E were systemically delivered *in vivo*, efficient transduction of the liver would result. Theoretically, a portion of the produced mSEAP reporter gene would be released from the transduced hepatocytes and would be detectable in the serum of animals, allowing for sequential sampling of the same animals. Although mSEAPΔ-H451E release from the cell was efficient *in vitro*, that does not necessarily infer an efficient process *in vivo*. High endogenous AP activity would be expected to reduce the sensitivity of the mSEAP

reporter gene *in vivo*. Additional investigation would be required to determine if the modifications made to mSEAP are, in fact, immunogenic. It is generally assumed that truncating the C-terminal transmembrane domain would not result in an immunogenic effect. However, the point mutations that were introduced into the crown domain of the protein may have immunogenic consequences. This would be easily assessed by comparing long persistence of transgene expression *in vivo* as described in (225). The mSEAPΔ-H451E is of significant value to the scientific community and completing the suggested *in vivo* characterization experiments would be crucial for the utilization of this new research tool in the future.

Taken together, this body of work described a gene therapy vector system efficacious in normal muscle and introduced a reporter gene ideal continuing the study of this vector system, which is needed to fully elucidate its utility towards developing a cure for DMD.

# *References*


1. England, S.B., L.V. Nicholson, M.A. Johnson, S.M. Forrest, D.R. Love, E.E. Zubrzycka-Gaarn, D.E. Bulman, J.B. Harris, and K.E. Davies. 1990. Very mild muscular dystrophy associated with the deletion of 46% of dystrophin. *Nature* 343:180-182.
2. Zhou, G.Q., H.Q. Xie, S.Z. Zhang, and Z.M. Yang. 2006. Current understanding of dystrophin-related muscular dystrophy and therapeutic challenges ahead. *Chin Med J (Engl)* 119:1381-1391.
3. Emery, A.E. 1998. The muscular dystrophies. *BMJ* 317:991-995.
4. Emery, A. 1993. Duchenne Muscular Dystrophy. Oxford University Press, Oxford.
5. Aartsma-Rus, A., J.C. Van Deutekom, I.F. Fokkema, G.J. Van Ommen, and J.T. Den Dunnen. 2006. Entries in the Leiden Duchenne muscular dystrophy mutation database: an overview of mutation types and paradoxical cases that confirm the reading-frame rule. *Muscle Nerve* 34:135-144.
6. Ibraghimov-Beskrovnaya, O., J.M. Ervasti, C.J. Leveille, C.A. Slaughter, S.W. Sernett, and K.P. Campbell. 1992. Primary structure of dystrophin-associated glycoproteins linking dystrophin to the extracellular matrix. *Nature* 355:696-702.
7. Ervasti, J.M. 2007. Dystrophin, its interactions with other proteins, and implications for muscular dystrophy. *Biochim Biophys Acta* 1772:108-117.
8. Ervasti, J.M., and K.J. Sonnemann. 2008. Biology of the striated muscle dystrophin-glycoprotein complex. *Int Rev Cytol* 265:191-225.
9. Hutter, O.F., F.L. Burton, and D.L. Bovell. 1991. Mechanical properties of normal and mdx mouse sarcolemma: bearing on function of dystrophin. *J Muscle Res Cell Motil* 12:585-589.
10. Petrof, B.J., J.B. Shrager, H.H. Stedman, A.M. Kelly, and H.L. Sweeney. 1993. Dystrophin protects the sarcolemma from stresses developed during muscle contraction. *Proc Natl Acad Sci U S A* 90:3710-3714.
11. Wakayama, Y., D.L. Schotland, E. Bonilla, and E. Orecchio. 1979. Quantitative ultrastructural study of muscle satellite cells in Duchenne dystrophy. *Neurology* 29:401-407.
12. Ervasti, J.M., K. Ohlendieck, S.D. Kahl, M.G. Gaver, and K.P. Campbell. 1990. Deficiency of a glycoprotein component of the dystrophin complex in dystrophic muscle. *Nature* 345:315-319.
13. Straub, V., F. Duclos, D.P. Venzke, J.C. Lee, S. Cutshall, C.J. Leveille, and K.P. Campbell. 1998. Molecular pathogenesis of muscle degeneration in the delta-sarcoglycan-deficient hamster. *Am J Pathol* 153:1623-1630.
14. Hogan, A., L. Shepherd, J. Chabot, S. Quenneville, S.M. Prescott, M.K. Topham, and S.H. Gee. 2001. Interaction of gamma 1-syntrophin with diacylglycerol kinase-zeta. Regulation of nuclear localization by PDZ interactions. *J Biol Chem* 276:26526-26533.
15. Roberts, R.G. 2001. Dystrophins and dystrobrevins. *Genome Biol* 2:REVIEWS3006.
16. Manzur, A.Y., M. Kinali, and F. Muntoni. 2008. Update on the management of Duchenne muscular dystrophy. *Arch Dis Child*
17. Ciafaloni, E., and R.T. Moxley. 2008. Treatment options for duchenne muscular dystrophy. *Curr Treat Options Neurol* 10:86-93.

18. Heckmatt, J.Z., V. Dubowitz, S.A. Hyde, J. Florence, A.C. Gabain, and N. Thompson. 1985. Prolongation of walking in Duchenne muscular dystrophy with lightweight orthoses: review of 57 cases. *Dev Med Child Neurol* 27:149-154.
19. Cox, G.F., and L.M. Kunkel. 1997. Dystrophies and heart disease. *Curr Opin Cardiol* 12:329-343.
20. Simonds, A.K., F. Muntoni, S. Heather, and S. Fielding. 1998. Impact of nasal ventilation on survival in hypercapnic Duchenne muscular dystrophy. *Thorax* 53:949-952.
21. Radley, H.G., A. De Luca, G.S. Lynch, and M.D. Grounds. 2007. Duchenne muscular dystrophy: focus on pharmaceutical and nutritional interventions. *Int J Biochem Cell Biol* 39:469-477.
22. DeSilva, S., D.B. Drachman, D. Mellits, and R.W. Kuncl. 1987. Prednisone treatment in Duchenne muscular dystrophy. Long-term benefit. *Arch Neurol* 44:818-822.
23. Khan, M.A. 1993. Corticosteroid therapy in Duchenne muscular dystrophy. *J Neurol Sci* 120:8-14.
24. Wehling-Henricks, M., J.J. Lee, and J.G. Tidball. 2004. Prednisolone decreases cellular adhesion molecules required for inflammatory cell infiltration in dystrophin-deficient skeletal muscle. *Neuromuscul Disord* 14:483-490.
25. Kolodziejczyk, S.M., G.S. Walsh, K. Balazsi, P. Seale, J. Sandoz, A.M. Hierlihy, M.A. Rudnicki, J.S. Chamberlain, F.D. Miller, and L.A. Megeney. 2001. Activation of JNK1 contributes to dystrophic muscle pathogenesis. *Curr Biol* 11:1278-1282.
26. St-Pierre, S.J., J.V. Chakkalakal, S.M. Kolodziejczyk, J.C. Knudson, B.J. Jasmin, and L.A. Megeney. 2004. Glucocorticoid treatment alleviates dystrophic myofiber pathology by activation of the calcineurin/NF-AT pathway. *FASEB J* 18:1937-1939.
27. Angelini, C. 2007. The role of corticosteroids in muscular dystrophy: a critical appraisal. *Muscle Nerve* 36:424-435.
28. Bartlett, R.J., S. Stockinger, M.M. Denis, W.T. Bartlett, L. Inverardi, T.T. Le, N. thi Man, G.E. Morris, D.J. Bogan, J. Metcalf-Bogan, and J.N. Kornegay. 2000. In vivo targeted repair of a point mutation in the canine dystrophin gene by a chimeric RNA/DNA oligonucleotide. *Nat Biotechnol* 18:615-622.
29. van Deutekom, J.C., A.A. Janson, I.B. Ginjaar, W.S. Frankhuizen, A. Aartsma-Rus, M. Bremmer-Bout, J.T. den Dunnen, K. Koop, A.J. van der Kooi, N.M. Goemans, S.J. de Kimpe, P.F. Ekhart, E.H. Venneker, G.J. Platenburg, J.J. Verschuuren, and G.J. van Ommen. 2007. Local dystrophin restoration with antisense oligonucleotide PRO051. *N Engl J Med* 357:2677-2686.
30. Welch, E.M., E.R. Barton, J. Zhuo, Y. Tomizawa, W.J. Friesen, P. Trifillis, S. Paushkin, M. Patel, C.R. Trotta, S. Hwang, R.G. Wilde, G. Karp, J. Takasugi, G. Chen, S. Jones, H. Ren, Y.C. Moon, D. Corson, A.A. Turpoff, J.A. Campbell, M.M. Conn, A. Khan, N.G. Almstead, J. Hedrick, A. Mollin, N. Risher, M. Weetall, S. Yeh, A.A. Branstrom, J.M. Colacino, J. Babiak, W.D. Ju, S. Hirawat, V.J. Northcutt, L.L. Miller, P. Spatrick, F. He, M. Kawana, H. Feng, A. Jacobson, S.W. Peltz, and H.L. Sweeney. 2007. PTC124 targets genetic disorders caused by nonsense mutations. *Nature* 447:87-91.
31. Hirawat, S., E.M. Welch, G.L. Elfring, V.J. Northcutt, S. Paushkin, S. Hwang, E.M. Leonard, N.G. Almstead, W. Ju, S.W. Peltz, and L.L. Miller. 2007. Safety, tolerability,

and pharmacokinetics of PTC124, a nonaminoglycoside nonsense mutation suppressor, following single- and multiple-dose administration to healthy male and female adult volunteers. *J Clin Pharmacol* 47:430-444.

32. Peault, B., M. Rudnicki, Y. Torrente, G. Cossu, J.P. Tremblay, T. Partridge, E. Gussoni, L.M. Kunkel, and J. Huard. 2007. Stem and progenitor cells in skeletal muscle development, maintenance, and therapy. *Mol Ther* 15:867-877.
33. Skuk, D., and J.P. Tremblay. 2000. Progress in myoblast transplantation: a potential treatment of dystrophies. *Microsc Res Tech* 48:213-222.
34. Grounds, M.D., and K.E. Davies. 2007. The allure of stem cell therapy for muscular dystrophy. *Neuromuscul Disord* 17:206-208.
35. Partridge, T. 2002. Myoblast transplantation. *Neuromuscul Disord* 12 Suppl 1:S3-6.
36. Skuk, D., M. Goulet, B. Roy, P. Chapdelaine, J.P. Bouchard, R. Roy, F.J. Dugre, M. Sylvain, J.G. Lachance, L. Deschenes, H. Senay, and J.P. Tremblay. 2006. Dystrophin expression in muscles of duchenne muscular dystrophy patients after high-density injections of normal myogenic cells. *J Neuropathol Exp Neurol* 65:371-386.
37. Skuk, D., B. Roy, M. Goulet, P. Chapdelaine, J.P. Bouchard, R. Roy, F.J. Dugre, J.G. Lachance, L. Deschenes, S. Helene, M. Sylvain, and J.P. Tremblay. 2004. Dystrophin expression in myofibers of Duchenne muscular dystrophy patients following intramuscular injections of normal myogenic cells. *Mol Ther* 9:475-482.
38. Skuk, D., M. Goulet, B. Roy, V. Piette, C.H. Cote, P. Chapdelaine, J.Y. Hogrel, M. Paradis, J.P. Bouchard, M. Sylvain, J.G. Lachance, and J.P. Tremblay. 2007. First test of a "high-density injection" protocol for myogenic cell transplantation throughout large volumes of muscles in a Duchenne muscular dystrophy patient: eighteen months follow-up. *Neuromuscul Disord* 17:38-46.
39. Webster, C., and H.M. Blau. 1990. Accelerated age-related decline in replicative life-span of Duchenne muscular dystrophy myoblasts: implications for cell and gene therapy. *Somat Cell Mol Genet* 16:557-565.
40. Gussoni, E., Y. Soneoka, C.D. Strickland, E.A. Buzney, M.K. Khan, A.F. Flint, L.M. Kunkel, and R.C. Mulligan. 1999. Dystrophin expression in the mdx mouse restored by stem cell transplantation. *Nature* 401:390-394.
41. Asakura, A., P. Seale, A. Girgis-Gabardo, and M.A. Rudnicki. 2002. Myogenic specification of side population cells in skeletal muscle. *J Cell Biol* 159:123-134.
42. Asakura, A., H. Hirai, B. Kablar, S. Morita, J. Ishibashi, B.A. Piras, A.J. Christ, M. Verma, K.A. Vineretsky, and M.A. Rudnicki. 2007. Increased survival of muscle stem cells lacking the MyoD gene after transplantation into regenerating skeletal muscle. *Proc Natl Acad Sci U S A* 104:16552-16557.
43. Cerletti, M., S. Jurga, C.A. Witczak, M.F. Hirshman, J.L. Shadrach, L.J. Goodyear, and A.J. Wagers. 2008. Highly Efficient, Functional Engraftment of Skeletal Muscle Stem Cells in Dystrophic Muscles. *Cell* 134:37-47.
44. Torrente, Y., J.P. Tremblay, F. Pisati, M. Belicchi, B. Rossi, M. Sironi, F. Fortunato, M. El Fahime, M.G. D'Angelo, N.J. Caron, G. Constantin, D. Paulin, G. Scarlato, and N. Bresolin. 2001. Intraarterial injection of muscle-derived CD34(+)Sca-1(+) stem cells restores dystrophin in mdx mice. *J Cell Biol* 152:335-348.

45. Polesskaya, A., P. Seale, and M.A. Rudnicki. 2003. Wnt signaling induces the myogenic specification of resident CD45+ adult stem cells during muscle regeneration. *Cell* 113:841-852.
46. Ferrari, G., A. Stornaiuolo, and F. Mavilio. 2001. Failure to correct murine muscular dystrophy. *Nature* 411:1014-1015.
47. Verma, I.M., and M.D. Weitzman. 2005. Gene therapy: twenty-first century medicine. *Annu Rev Biochem* 74:711-738.
48. Edelstein, M.L., M.R. Abedi, and J. Wixon. 2007. Gene therapy clinical trials worldwide to 2007--an update. *J Gene Med* 9:833-842.
49. Wilson, J.M. 1996. Adenoviruses as gene-delivery vehicles. *N Engl J Med* 334:1185-1187.
50. Odom, G.L., P. Gregorevic, and J.S. Chamberlain. 2007. Viral-mediated gene therapy for the muscular dystrophies: successes, limitations and recent advances. *Biochim Biophys Acta* 1772:243-262.
51. Trentin, J.J., Y. Yabe, and G. Taylor. 1962. The quest for human cancer viruses. *Science* 137:835-841.
52. Goverdhana, S., M. Puntel, W. Xiong, J.M. Zirger, C. Barcia, J.F. Curtin, E.B. Soffer, S. Mondkar, G.D. King, J. Hu, S.A. Sciascia, M. Candolfi, D.S. Greengold, P.R. Lowenstein, and M.G. Castro. 2005. Regulatable gene expression systems for gene therapy applications: progress and future challenges. *Mol Ther* 12:189-211.
53. Shenk, T. 1996. Adenoviridae: The Viruses and Their Replication. In Fields Viriology. B.N. Fields, Knipe, D.M., Howley, P.M., Chanock, R.M., Monath, T.P., Melnick, J.,L., Roizman, B., Straus, S.E., editor Lippincott- Raven Publishers, Philadelphia.
54. Parks, R.J., L. Chen, M. Anton, U. Sankar, M.A. Rudnicki, and F.L. Graham. 1996. A helper-dependent adenovirus vector system: removal of helper virus by Cre-mediated excision of the viral packaging signal. *Proc Natl Acad Sci U S A* 93:13565-13570.
55. Muruve, D.A., M.J. Cotter, A.K. Zaiss, L.R. White, Q. Liu, T. Chan, S.A. Clark, P.J. Ross, R.A. Meulenbroek, G.M. Maelandsmo, and R.J. Parks. 2004. Helper-dependent adenovirus vectors elicit intact innate but attenuated adaptive host immune responses in vivo. *J Virol* 78:5966-5972.
56. Tworkowski, K.A., A.A. Chakraborty, A.V. Samuelson, Y.R. Seger, M. Narita, G.J. Hannon, S.W. Lowe, and W.P. Tansey. 2008. Adenovirus E1A targets p400 to induce the cellular oncoprotein Myc. *Proc Natl Acad Sci U S A* 105:6103-6108.
57. Freimuth, P., L. Philipson, and S.D. Carson. 2008. The coxsackievirus and adenovirus receptor. *Curr Top Microbiol Immunol* 323:67-87.
58. Fleischli, C., D. Sirena, G. Lesage, M.J. Havenga, R. Cattaneo, U.F. Greber, and S. Hemmi. 2007. Species B adenovirus serotypes 3, 7, 11 and 35 share similar binding sites on the membrane cofactor protein CD46 receptor. *J Gen Virol* 88:2925-2934.
59. Wang, H., Y.C. Liaw, D. Stone, O. Kalyuzhniy, I. Amiraslanov, S. Tuve, C.L. Verlinde, D. Shayakhmetov, T. Stehle, S. Roffler, and A. Lieber. 2007. Identification of CD46 binding sites within the adenovirus serotype 35 fiber knob. *J Virol* 81:12785-12792.

60. Short, J.J., A.V. Pereboev, Y. Kawakami, C. Vasu, M.J. Holterman, and D.T. Curiel. 2004. Adenovirus serotype 3 utilizes CD80 (B7.1) and CD86 (B7.2) as cellular attachment receptors. *Virology* 322:349-359.
61. Lee, T.W., D.A. Matthews, and G.E. Blair. 2005. Novel molecular approaches to cystic fibrosis gene therapy. *Biochem J* 387:1-15.
62. Graham, F.L., J. Smiley, W.C. Russell, and R. Nairn. 1977. Characteristics of a human cell line transformed by DNA from human adenovirus type 5. *J Gen Virol* 36:59-74.
63. Yang, Y., F.A. Nunes, K. Berencsi, E.E. Furth, E. Gonczol, and J.M. Wilson. 1994. Cellular immunity to viral antigens limits E1-deleted adenoviruses for gene therapy. *Proc Natl Acad Sci U S A* 91:4407-4411.
64. Yang, Y., H.C. Ertl, and J.M. Wilson. 1994. MHC class I-restricted cytotoxic T lymphocytes to viral antigens destroy hepatocytes in mice infected with E1-deleted recombinant adenoviruses. *Immunity* 1:433-442.
65. O'Neal, W.K., H. Zhou, N. Morral, E. Aguilar-Cordova, J. Pestaner, C. Langston, B. Mull, Y. Wang, A.L. Beaudet, and B. Lee. 1998. Toxicological comparison of E2a-deleted and first-generation adenoviral vectors expressing alpha1-antitrypsin after systemic delivery. *Hum Gene Ther* 9:1587-1598.
66. Engelhardt, J.F., L. Litzky, and J.M. Wilson. 1994. Prolonged transgene expression in cotton rat lung with recombinant adenoviruses defective in E2a. *Hum Gene Ther* 5:1217-1229.
67. Wang, Q., G. Greenburg, D. Bunch, D. Farson, and M.H. Finer. 1997. Persistent transgene expression in mouse liver following in vivo gene transfer with a delta E1/delta E4 adenovirus vector. *Gene Ther* 4:393-400.
68. Brusilow, S.W., and N.E. Maestri. 1996. Urea cycle disorders: diagnosis, pathophysiology, and therapy. *Adv Pediatr* 43:127-170.
69. Somia, N., and I.M. Verma. 2000. Gene therapy: trials and tribulations. *Nat Rev Genet* 1:91-99.
70. Crystal, R.G., B.G. Harvey, J.P. Wisnivesky, K.A. O'Donoghue, K.W. Chu, J. Maroni, J.C. Muscat, A.L. Pippo, C.E. Wright, R.J. Kaner, P.L. Leopold, P.D. Kessler, H.S. Rasmussen, T.K. Rosengart, and C. Hollmann. 2002. Analysis of risk factors for local delivery of low- and intermediate-dose adenovirus gene transfer vectors to individuals with a spectrum of comorbid conditions. *Hum Gene Ther* 13:65-100.
71. Ben-Gary, H., R.L. McKinney, T. Rosengart, M.L. Lesser, and R.G. Crystal. 2002. Systemic interleukin-6 responses following administration of adenovirus gene transfer vectors to humans by different routes. *Mol Ther* 6:287-297.
72. Muruve, D.A. 2004. The innate immune response to adenovirus vectors. *Hum Gene Ther* 15:1157-1166.
73. Banchereau, J., and R.M. Steinman. 1998. Dendritic cells and the control of immunity. *Nature* 392:245-252.
74. Girardin, S.E., P.J. Sansonetti, and D.J. Philpott. 2002. Intracellular vs extracellular recognition of pathogens--common concepts in mammals and flies. *Trends Microbiol* 10:193-199.
75. Taniguchi, M., K. Seino, and T. Nakayama. 2003. The NKT cell system: bridging innate and acquired immunity. *Nat Immunol* 4:1164-1165.

76. Muruve, D.A., M.J. Barnes, I.E. Stillman, and T.A. Libermann. 1999. Adenoviral gene therapy leads to rapid induction of multiple chemokines and acute neutrophil-dependent hepatic injury in vivo. *Hum Gene Ther* 10:965-976.
77. McCaffrey, A.P., P. Fawcett, H. Nakai, R.L. McCaffrey, A. Ehrhardt, T.T. Pham, K. Pandey, H. Xu, S. Feuss, T.A. Storm, and M.A. Kay. 2008. The host response to adenovirus, helper-dependent adenovirus, and adeno-associated virus in mouse liver. *Mol Ther* 16:931-941.
78. Sallusto, F., and A. Lanzavecchia. 2000. Understanding dendritic cell and T-lymphocyte traffic through the analysis of chemokine receptor expression. *Immunol Rev* 177:134-140.
79. Liu, Q., A.K. Zaiss, P. Colarusso, K. Patel, G. Haljan, T.J. Wickham, and D.A. Muruve. 2003. The role of capsid-endothelial interactions in the innate immune response to adenovirus vectors. *Hum Gene Ther* 14:627-643.
80. Zhang, Y., N. Chirmule, G.P. Gao, R. Qian, M. Croyle, B. Joshi, J. Tazelaar, and J.M. Wilson. 2001. Acute cytokine response to systemic adenoviral vectors in mice is mediated by dendritic cells and macrophages. *Mol Ther* 3:697-707.
81. Liu, Q., and D.A. Muruve. 2003. Molecular basis of the inflammatory response to adenovirus vectors. *Gene Ther* 10:935-940.
82. Stilwell, J.L., D.M. McCarty, A. Negishi, R. Superfine, and R.J. Samulski. 2003. Development and characterization of novel empty adenovirus capsids and their impact on cellular gene expression. *J Virol* 77:12881-12885.
83. McCoy, R.D., B.L. Davidson, B.J. Roessler, G.B. Huffnagle, S.L. Janich, T.J. Laing, and R.H. Simon. 1995. Pulmonary inflammation induced by incomplete or inactivated adenoviral particles. *Hum Gene Ther* 6:1553-1560.
84. Worgall, S., G. Wolff, E. Falck-Pedersen, and R.G. Crystal. 1997. Innate immune mechanisms dominate elimination of adenoviral vectors following in vivo administration. *Hum Gene Ther* 8:37-44.
85. Heath, W.R., and F.R. Carbone. 2001. Cross-presentation in viral immunity and self-tolerance. *Nat Rev Immunol* 1:126-134.
86. Kiang, A., Z.C. Hartman, R.S. Everett, D. Serra, H. Jiang, M.M. Frank, and A. Amalfitano. 2006. Multiple innate inflammatory responses induced after systemic adenovirus vector delivery depend on a functional complement system. *Mol Ther* 14:588-598.
87. Rickert, R.C. 2005. Regulation of B lymphocyte activation by complement C3 and the B cell coreceptor complex. *Curr Opin Immunol* 17:237-243.
88. Jiang, H., Z. Wang, D. Serra, M.M. Frank, and A. Amalfitano. 2004. Recombinant adenovirus vectors activate the alternative complement pathway, leading to the binding of human complement protein C3 independent of anti-ad antibodies. *Mol Ther* 10:1140-1142.
89. Kim, I.H., A. Jozkowicz, P.A. Piedra, K. Oka, and L. Chan. 2001. Lifetime correction of genetic deficiency in mice with a single injection of helper-dependent adenoviral vector. *Proc Natl Acad Sci U S A* 98:13282-13287.
90. Toietta, G., V.P. Mane, W.S. Norona, M.J. Finegold, P. Ng, A.F. McDonagh, A.L. Beaudet, and B. Lee. 2005. Lifelong elimination of hyperbilirubinemia in the Gunn

rat with a single injection of helper-dependent adenoviral vector. *Proc Natl Acad Sci U S A* 102:3930-3935.

91. Brunetti-Pierri, N., T.C. Nichols, S. McCorquodale, E. Merricks, D.J. Palmer, A.L. Beaudet, and P. Ng. 2005. Sustained phenotypic correction of canine hemophilia B after systemic administration of helper-dependent adenoviral vector. *Hum Gene Ther* 16:811-820.
92. Brunetti-Pierri, N., T. Ng, D.A. Iannitti, D.J. Palmer, A.L. Beaudet, M.J. Finegold, K.D. Carey, W.G. Cioffi, and P. Ng. 2006. Improved hepatic transduction, reduced systemic vector dissemination, and long-term transgene expression by delivering helper-dependent adenoviral vectors into the surgically isolated liver of nonhuman primates. *Hum Gene Ther* 17:391-404.
93. Hoffman, E.P., A.P. Monaco, C.C. Feener, and L.M. Kunkel. 1987. Conservation of the Duchenne muscular dystrophy gene in mice and humans. *Science* 238:347-350.
94. Sicinski, P., Y. Geng, A.S. Ryder-Cook, E.A. Barnard, M.G. Darlison, and P.J. Barnard. 1989. The molecular basis of muscular dystrophy in the mdx mouse: a point mutation. *Science* 244:1578-1580.
95. Anderson, J.E., W.K. Ovalle, and B.H. Bressler. 1987. Electron microscopic and autoradiographic characterization of hindlimb muscle regeneration in the mdx mouse. *Anat Rec* 219:243-257.
96. Bulfield, G., W.G. Siller, P.A. Wight, and K.J. Moore. 1984. X chromosome-linked muscular dystrophy (mdx) in the mouse. *Proc Natl Acad Sci U S A* 81:1189-1192.
97. DiMario, J.X., A. Uzman, and R.C. Strohman. 1991. Fiber regeneration is not persistent in dystrophic (MDX) mouse skeletal muscle. *Dev Biol* 148:314-321.
98. Torres, L.F., and L.W. Duchen. 1987. The mutant mdx: inherited myopathy in the mouse. Morphological studies of nerves, muscles and end-plates. *Brain* 110 ( Pt 2):269-299.
99. Tseng, B.S., P. Zhao, J.S. Pattison, S.E. Gordon, J.A. Granchelli, R.W. Madsen, L.C. Folk, E.P. Hoffman, and F.W. Booth. 2002. Regenerated mdx mouse skeletal muscle shows differential mRNA expression. *J Appl Physiol* 93:537-545.
100. Turk, R., E. Sterrenburg, E.J. de Meijer, G.J. van Ommen, J.T. den Dunnen, and P.A. t Hoen. 2005. Muscle regeneration in dystrophin-deficient mdx mice studied by gene expression profiling. *BMC Genomics* 6:98.
101. Lavasani, M., A. Lu, H. Peng, J. Cummins, and J. Huard. 2006. Nerve growth factor improves the muscle regeneration capacity of muscle stem cells in dystrophic muscle. *Hum Gene Ther* 17:180-192.
102. Tanabe, Y., K. Esaki, and T. Nomura. 1986. Skeletal muscle pathology in X chromosome-linked muscular dystrophy (mdx) mouse. *Acta Neuropathol* 69:91-95.
103. Durbeej, M., and K.P. Campbell. 2002. Muscular dystrophies involving the dystrophin-glycoprotein complex: an overview of current mouse models. *Curr Opin Genet Dev* 12:349-361.
104. Pastoret, C., and A. Sebille. 1995. mdx mice show progressive weakness and muscle deterioration with age. *J Neurol Sci* 129:97-105.
105. Pastoret, C., and A. Sebille. 1993. Further aspects of muscular dystrophy in mdx mice. *Neuromuscul Disord* 3:471-475.

106. Granchelli, J.A., D.L. Avosso, M.S. Hudecki, and C. Pollina. 1996. Cromolyn increases strength in exercised mdx mice. *Res Commun Mol Pathol Pharmacol* 91:287-296.
107. Harris, J.B., and C.R. Slater. 1980. Animal models: what is their relevance to the pathogenesis of human muscular dystrophy? *Br Med Bull* 36:193-197.
108. Campbell, K.P., and S.D. Kahl. 1989. Association of dystrophin and an integral membrane glycoprotein. *Nature* 338:259-262.
109. Ghahramani Seno, M.M., I.R. Graham, T. Athanasopoulos, C. Trollet, M. Pohlschmidt, M.R. Crompton, and G. Dickson. 2008. RNAi-mediated knockdown of dystrophin expression in adult mice does not lead to overt muscular dystrophy pathology. *Hum Mol Genet*
110. Reay, D.P., R. Bilbao, B.M. Koppanati, L. Cai, T.L. O'Day, Z. Jiang, H. Zheng, J.F. Watchko, and P.R. Clemens. 2008. Full-length dystrophin gene transfer to the mdx mouse in utero. *Gene Ther* 15:531-536.
111. Phelps, S.F., M.A. Hauser, N.M. Cole, J.A. Rafael, R.T. Hinkle, J.A. Faulkner, and J.S. Chamberlain. 1995. Expression of full-length and truncated dystrophin mini-genes in transgenic mdx mice. *Hum Mol Genet* 4:1251-1258.
112. Harper, S.Q., M.A. Hauser, C. DelloRusso, D. Duan, R.W. Crawford, S.F. Phelps, H.A. Harper, A.S. Robinson, J.F. Engelhardt, S.V. Brooks, and J.S. Chamberlain. 2002. Modular flexibility of dystrophin: implications for gene therapy of Duchenne muscular dystrophy. *Nat Med* 8:253-261.
113. Neri, M., S. Torelli, S. Brown, I. Ugo, P. Sabatelli, L. Merlini, P. Spitali, P. Rimessi, F. Gualandi, C. Sewry, A. Ferlini, and F. Muntoni. 2007. Dystrophin levels as low as 30% are sufficient to avoid muscular dystrophy in the human. *Neuromuscul Disord*
114. Arahata, K., T. Ishihara, K. Kamakura, T. Tsukahara, S. Ishiura, C. Baba, T. Matsumoto, I. Nonaka, and H. Sugita. 1989. Mosaic expression of dystrophin in symptomatic carriers of Duchenne's muscular dystrophy. *N Engl J Med* 320:138-142.
115. Vollestad, N.K. 1997. Measurement of human muscle fatigue. *J Neurosci Methods* 74:219-227.
116. Acsadi, G., G. Dickson, D.R. Love, A. Jani, F.S. Walsh, A. Gurusinghe, J.A. Wolff, and K.E. Davies. 1991. Human dystrophin expression in mdx mice after intramuscular injection of DNA constructs. *Nature* 352:815-818.
117. Romero, N.B., S. Braun, O. Benveniste, F. Leturcq, J.Y. Hogrel, G.E. Morris, A. Barois, B. Eymard, C. Payan, V. Ortega, A.L. Boch, L. Lejean, C. Thioudellet, B. Mourot, C. Escot, A. Choquel, D. Recan, J.C. Kaplan, G. Dickson, D. Klatzmann, V. Molinier-Frenckel, J.G. Guillet, P. Squiban, S. Herson, and M. Fardeau. 2004. Phase I study of dystrophin plasmid-based gene therapy in Duchenne/Becker muscular dystrophy. *Hum Gene Ther* 15:1065-1076.
118. Ruponen, M., P. Honkakoski, S. Ronkko, J. Pelkonen, M. Tammi, and A. Urtti. 2003. Extracellular and intracellular barriers in non-viral gene delivery. *J Control Release* 93:213-217.
119. Dow, S.W., L.G. Fradkin, D.H. Liggitt, A.P. Willson, T.D. Heath, and T.A. Potter. 1999. Lipid-DNA complexes induce potent activation of innate immune responses and antitumor activity when administered intravenously. *J Immunol* 163:1552-1561.

120. Whitmore, M., S. Li, and L. Huang. 1999. LPD lipopolyplex initiates a potent cytokine response and inhibits tumor growth. *Gene Ther* 6:1867-1875.
121. McMahon, J.M., E. Signori, K.E. Wells, V.M. Fazio, and D.J. Wells. 2001. Optimisation of electrotransfer of plasmid into skeletal muscle by pretreatment with hyaluronidase -- increased expression with reduced muscle damage. *Gene Ther* 8:1264-1270.
122. Wolff, J.A., and V. Budker. 2005. The mechanism of naked DNA uptake and expression. *Adv Genet* 54:3-20.
123. Jiao, S., P. Williams, R.K. Berg, B.A. Hodgeman, L. Liu, G. Repetto, and J.A. Wolff. 1992. Direct gene transfer into nonhuman primate myofibers in vivo. *Hum Gene Ther* 3:21-33.
124. Jooss, K., and N. Chirmule. 2003. Immunity to adenovirus and adeno-associated viral vectors: implications for gene therapy. *Gene Ther* 10:955-963.
125. Love, D.R., T.J. Flint, S.A. Genet, H.R. Middleton-Price, and K.E. Davies. 1991. Becker muscular dystrophy patient with a large intragenic dystrophin deletion: implications for functional minigenes and gene therapy. *J Med Genet* 28:860-864.
126. Dunckley, M.G., D.J. Wells, F.S. Walsh, and G. Dickson. 1993. Direct retroviral-mediated transfer of a dystrophin minigene into mdx mouse muscle in vivo. *Hum Mol Genet* 2:717-723.
127. Li, S., E. Kimura, B.M. Fall, M. Reyes, J.C. Angello, R. Welikson, S.D. Hauschka, and J.S. Chamberlain. 2005. Stable transduction of myogenic cells with lentiviral vectors expressing a minidystrophin. *Gene Ther* 12:1099-1108.
128. Quenneville, S.P., P. Chapdelaine, D. Skuk, M. Paradis, M. Goulet, J. Rousseau, X. Xiao, L. Garcia, and J.P. Tremblay. 2007. Autologous transplantation of muscle precursor cells modified with a lentivirus for muscular dystrophy: human cells and primate models. *Mol Ther* 15:431-438.
129. Fassati, A., and N. Bresolin. 2000. Retroviral vectors for gene therapy of Duchenne muscular dystrophy. *Neurol Sci* 21:S925-927.
130. Schroder, A.R., P. Shinn, H. Chen, C. Berry, J.R. Ecker, and F. Bushman. 2002. HIV-1 integration in the human genome favors active genes and local hotspots. *Cell* 110:521-529.
131. Schwarzwaelder, K., S.J. Howe, M. Schmidt, M.H. Brugman, A. Deichmann, H. Glimm, S. Schmidt, C. Prinz, M. Wissler, D.J. King, F. Zhang, K.L. Parsley, K.C. Gilmour, J. Sinclair, J. Bayford, R. Peraj, K. Pike-Overzet, F.J. Staal, D. de Ridder, C. Kinnon, U. Abel, G. Wagemaker, H.B. Gaspar, A.J. Thrasher, and C. von Kalle. 2007. Gammaretrovirus-mediated correction of SCID-X1 is associated with skewed vector integration site distribution in vivo. *J Clin Invest* 117:2241-2249.
132. Modlich, U., A. Schambach, M.H. Brugman, D.C. Wicke, S. Knoess, Z. Li, T. Maetzig, C. Rudolph, B. Schlegelberger, and C. Baum. 2008. Leukemia induction after a single retroviral vector insertion in Evi1 or Prdm16. *Leukemia*
133. Hacein-Bey-Abina, S., C. Von Kalle, M. Schmidt, M.P. McCormack, N. Wulffraat, P. Leboulch, A. Lim, C.S. Osborne, R. Pawliuk, E. Morillon, R. Sorensen, A. Forster, P. Fraser, J.I. Cohen, G. de Saint Basile, I. Alexander, U. Wintergerst, T. Frebourg, A. Aurias, D. Stoppa-Lyonnet, S. Romana, I. Radford-Weiss, F. Gross, F. Valensi, E.

Delabesse, E. Macintyre, F. Sigaux, J. Soulier, L.E. Leiva, M. Wissler, C. Prinz, T.H. Rabbitts, F. Le Deist, A. Fischer, and M. Cavazzana-Calvo. 2003. LMO2-associated clonal T cell proliferation in two patients after gene therapy for SCID-X1. *Science* 302:415-419.

134. Kotani, H., P.B. Newton, 3rd, S. Zhang, Y.L. Chiang, E. Otto, L. Weaver, R.M. Blaese, W.F. Anderson, and G.J. McGarrity. 1994. Improved methods of retroviral vector transduction and production for gene therapy. *Hum Gene Ther* 5:19-28.
135. Akkaraju, G.R., J. Huard, E.P. Hoffman, W.F. Goins, R. Pruchnic, S.C. Watkins, J.B. Cohen, and J.C. Glorioso. 1999. Herpes simplex virus vector-mediated dystrophin gene transfer and expression in MDX mouse skeletal muscle. *J Gene Med* 1:280-289.
136. Wang, Y., S. Mukherjee, C. Fraefel, X.O. Breakefield, and P.D. Allen. 2002. Herpes simplex virus type 1 amplicon vector-mediated gene transfer to muscle. *Hum Gene Ther* 13:261-273.
137. Huard, J., D. Krisky, T. Oligino, P. Marconi, C.S. Day, S.C. Watkins, and J.C. Glorioso. 1997. Gene transfer to muscle using herpes simplex virus-based vectors. *Neuromuscul Disord* 7:299-313.
138. Bueler, H. 1999. Adeno-associated viral vectors for gene transfer and gene therapy. *Biol Chem* 380:613-622.
139. Summerford, C., and R.J. Samulski. 1998. Membrane-associated heparan sulfate proteoglycan is a receptor for adeno-associated virus type 2 virions. *J Virol* 72:1438-1445.
140. Summerford, C., J.S. Bartlett, and R.J. Samulski. 1999. AlphaVbeta5 integrin: a co-receptor for adeno-associated virus type 2 infection. *Nat Med* 5:78-82.
141. Qing, K., C. Mah, J. Hansen, S. Zhou, V. Dwarki, and A. Srivastava. 1999. Human fibroblast growth factor receptor 1 is a co-receptor for infection by adeno-associated virus 2. *Nat Med* 5:71-77.
142. Yuasa, K., Y. Miyagoe, K. Yamamoto, Y. Nabeshima, G. Dickson, and S. Takeda. 1998. Effective restoration of dystrophin-associated proteins in vivo by adenovirus-mediated transfer of truncated dystrophin cDNAs. *FEBS Lett* 425:329-336.
143. Wang, B., J. Li, and X. Xiao. 2000. Adeno-associated virus vector carrying human minidystrophin genes effectively ameliorates muscular dystrophy in mdx mouse model. *Proc Natl Acad Sci U S A* 97:13714-13719.
144. Watchko, J., T. O'Day, B. Wang, L. Zhou, Y. Tang, J. Li, and X. Xiao. 2002. Adeno-associated virus vector-mediated minidystrophin gene therapy improves dystrophic muscle contractile function in mdx mice. *Hum Gene Ther* 13:1451-1460.
145. Fabb, S.A., D.J. Wells, P. Serpente, and G. Dickson. 2002. Adeno-associated virus vector gene transfer and sarcolemmal expression of a 144 kDa micro-dystrophin effectively restores the dystrophin-associated protein complex and inhibits myofibre degeneration in nude/mdx mice. *Hum Mol Genet* 11:733-741.
146. Scott, J.M., S. Li, S.Q. Harper, R. Welikson, D. Bourque, C. DelloRusso, S.D. Hauschka, and J.S. Chamberlain. 2002. Viral vectors for gene transfer of micro-, mini-, or full-length dystrophin. *Neuromuscul Disord* 12 Suppl 1:S23-29.

147. Yan, Z., Y. Zhang, D. Duan, and J.F. Engelhardt. 2000. Trans-splicing vectors expand the utility of adeno-associated virus for gene therapy. *Proc Natl Acad Sci U S A* 97:6716-6721.
148. Duan, D., Y. Yue, and J.F. Engelhardt. 2001. Expanding AAV packaging capacity with trans-splicing or overlapping vectors: a quantitative comparison. *Mol Ther* 4:383-391.
149. Lai, Y., Y. Yue, M. Liu, A. Ghosh, J.F. Engelhardt, J.S. Chamberlain, and D. Duan. 2005. Efficient in vivo gene expression by trans-splicing adeno-associated viral vectors. *Nat Biotechnol* 23:1435-1439.
150. Xu, Z., Y. Yue, Y. Lai, C. Ye, J. Qiu, D.J. Pintel, and D. Duan. 2004. Trans-splicing adeno-associated viral vector-mediated gene therapy is limited by the accumulation of spliced mRNA but not by dual vector coinfection efficiency. *Hum Gene Ther* 15:896-905.
151. Lai, Y., Y. Yue, M. Liu, and D. Duan. 2006. Synthetic intron improves transduction efficiency of trans-splicing adeno-associated viral vectors. *Hum Gene Ther* 17:1036-1042.
152. Messina, S., A. Mazzeo, A. Bitto, M. Aguennouz, A. Migliorato, M.G. De Pasquale, L. Minutoli, D. Altavilla, L. Zentilin, M. Giacca, F. Squadrito, and G. Vita. 2007. VEGF overexpression via adeno-associated virus gene transfer promotes skeletal muscle regeneration and enhances muscle function in mdx mice. *Faseb J*
153. Townsend, D., M.J. Blankinship, J.M. Allen, P. Gregorevic, J.S. Chamberlain, and J.M. Metzger. 2007. Systemic administration of micro-dystrophin restores cardiac geometry and prevents dobutamine-induced cardiac pump failure. *Mol Ther* 15:1086-1092.
154. Gregorevic, P., M.J. Blankinship, J.M. Allen, R.W. Crawford, L. Meuse, D.G. Miller, D.W. Russell, and J.S. Chamberlain. 2004. Systemic delivery of genes to striated muscles using adeno-associated viral vectors. *Nat Med* 10:828-834.
155. Rodino-Klapac, L.R., P.M. Janssen, C.L. Montgomery, B.D. Coley, L.G. Chicoine, K.R. Clark, and J.R. Mendell. 2007. A translational approach for limb vascular delivery of the micro-dystrophin gene without high volume or high pressure for treatment of Duchenne muscular dystrophy. *J Transl Med* 5:45.
156. Cordier, L., G.P. Gao, A.A. Hack, E.M. McNally, J.M. Wilson, N. Chirmule, and H.L. Sweeney. 2001. Muscle-specific promoters may be necessary for adeno-associated virus-mediated gene transfer in the treatment of muscular dystrophies. *Hum Gene Ther* 12:205-215.
157. Yuasa, K., M. Yoshimura, N. Urasawa, S. Ohshima, J.M. Howell, A. Nakamura, T. Hijikata, Y. Miyagoe-Suzuki, and S. Takeda. 2007. Injection of a recombinant AAV serotype 2 into canine skeletal muscles evokes strong immune responses against transgene products. *Gene Ther* 14:1249-1260.
158. Wang, Z., J.M. Allen, S.R. Riddell, P. Gregorevic, R. Storb, S.J. Tapscott, J.S. Chamberlain, and C.S. Kuhr. 2007. Immunity to adeno-associated virus-mediated gene transfer in a random-bred canine model of Duchenne muscular dystrophy. *Hum Gene Ther* 18:18-26.

159. Manno, C.S., G.F. Pierce, V.R. Arruda, B. Glader, M. Ragni, J.J. Rasko, M.C. Ozelo, K. Hoots, P. Blatt, B. Konkle, M. Dake, R. Kaye, M. Razavi, A. Zajko, J. Zehnder, P.K. Rustagi, H. Nakai, A. Chew, D. Leonard, J.F. Wright, R.R. Lessard, J.M. Sommer, M. Tigges, D. Sabatino, A. Luk, H. Jiang, F. Mingozzi, L. Couto, H.C. Ertl, K.A. High, and M.A. Kay. 2006. Successful transduction of liver in hemophilia by AAV-Factor IX and limitations imposed by the host immune response. *Nat Med* 12:342-347.
160. Mingozzi, F., and K.A. High. 2007. Immune responses to AAV in clinical trials. *Curr Gene Ther* 7:316-324.
161. Chirmule, N., K. Propert, S. Magosin, Y. Qian, R. Qian, and J. Wilson. 1999. Immune responses to adenovirus and adeno-associated virus in humans. *Gene Ther* 6:1574-1583.
162. Mingozzi, F., M.V. Maus, D.J. Hui, D.E. Sabatino, S.L. Murphy, J.E. Rasko, M.V. Ragni, C.S. Manno, J. Sommer, H. Jiang, G.F. Pierce, H.C. Ertl, and K.A. High. 2007. CD8(+) T-cell responses to adeno-associated virus capsid in humans. *Nat Med* 13:419-422.
163. Vandenberghe, L.H., and J.M. Wilson. 2007. AAV as an immunogen. *Curr Gene Ther* 7:325-333.
164. Clemens, P.R., T.L. Krause, S. Chan, K.E. Korb, F.L. Graham, and C.T. Caskey. 1995. Recombinant truncated dystrophin minigenes: construction, expression, and adenoviral delivery. *Hum Gene Ther* 6:1477-1485.
165. Ragot, T., N. Vincent, P. Chafey, E. Vigne, H. Gilgenkrantz, D. Couton, J. Cartaud, P. Briand, J.C. Kaplan, M. Perricaudet, and et al. 1993. Efficient adenovirus-mediated transfer of a human minidystrophin gene to skeletal muscle of mdx mice. *Nature* 361:647-650.
166. Vincent, N., T. Ragot, H. Gilgenkrantz, D. Couton, P. Chafey, A. Gregoire, P. Briand, J.C. Kaplan, A. Kahn, and M. Perricaudet. 1993. Long-term correction of mouse dystrophic degeneration by adenovirus-mediated transfer of a minidystrophin gene. *Nat Genet* 5:130-134.
167. Gardner, K.L., J.A. Kearney, J.D. Edwards, and J.A. Rafael-Fortney. 2006. Restoration of all dystrophin protein interactions by functional domains in trans does not rescue dystrophy. *Gene Ther* 13:744-751.
168. Deconinck, N., T. Ragot, G. Marechal, M. Perricaudet, and J.M. Gillis. 1996. Functional protection of dystrophic mouse (mdx) muscles after adenovirus-mediated transfer of a dystrophin minigene. *Proc Natl Acad Sci U S A* 93:3570-3574.
169. Yang, L., H. Lochmuller, J. Luo, B. Massie, J. Nalbantoglu, G. Karpati, and B.J. Petrof. 1998. Adenovirus-mediated dystrophin minigene transfer improves muscle strength in adult dystrophic (MDX) mice. *Gene Ther* 5:369-379.
170. Chen, H.H., L.M. Mack, R. Kelly, M. Ontell, S. Kochanek, and P.R. Clemens. 1997. Persistence in muscle of an adenoviral vector that lacks all viral genes. *Proc Natl Acad Sci U S A* 94:1645-1650.
171. Acsadi, G., H. Lochmuller, A. Jani, J. Huard, B. Massie, S. Prescott, M. Simoneau, B.J. Petrof, and G. Karpati. 1996. Dystrophin expression in muscles of mdx mice after adenovirus-mediated in vivo gene transfer. *Hum Gene Ther* 7:129-140.
172. Lochmuller, H., B.J. Petrof, C. Allen, S. Prescott, B. Massie, and G. Karpati. 1995. Immunosuppression by FK506 markedly prolongs expression of adenovirus-

delivered transgene in skeletal muscles of adult dystrophic [mdx] mice. *Biochem Biophys Res Commun* 213:569-574.

173. Zhao, J.E., H. Lochumuller, J. Nalbantoglu, C. Allen, S. Prescott, B. Massie, and G. Karpati. 1997. Study of adenovirus-mediated dystrophin minigene transfer to skeletal muscle by combined microscopic display of adenoviral DNA and dystrophin. *Hum Gene Ther* 8:1565-1573.
174. Guibinga, G.H., H. Lochmuller, B. Massie, J. Nalbantoglu, G. Karpati, and B.J. Petrof. 1998. Combinatorial blockade of calcineurin and CD28 signaling facilitates primary and secondary therapeutic gene transfer by adenovirus vectors in dystrophic (mdx) mouse muscles. *J Virol* 72:4601-4609.
175. Ebihara, S., G.H. Guibinga, R. Gilbert, J. Nalbantoglu, B. Massie, G. Karpati, and B.J. Petrof. 2000. Differential effects of dystrophin and utrophin gene transfer in immunocompetent muscular dystrophy (mdx) mice. *Physiol Genomics* 3:133-144.
176. Gilbert, R., J. Nalbanoglu, J.M. Tinsley, B. Massie, K.E. Davies, and G. Karpati. 1998. Efficient utrophin expression following adenovirus gene transfer in dystrophic muscle. *Biochem Biophys Res Commun* 242:244-247.
177. Gilbert, R., J. Nalbantoglu, B.J. Petrof, S. Ebihara, G.H. Guibinga, J.M. Tinsley, A. Kamen, B. Massie, K.E. Davies, and G. Karpati. 1999. Adenovirus-mediated utrophin gene transfer mitigates the dystrophic phenotype of mdx mouse muscles. *Hum Gene Ther* 10:1299-1310.
178. Kochanek, S., P.R. Clemens, K. Mitani, H.H. Chen, S. Chan, and C.T. Caskey. 1996. A new adenoviral vector: Replacement of all viral coding sequences with 28 kb of DNA independently expressing both full-length dystrophin and beta-galactosidase. *Proc Natl Acad Sci U S A* 93:5731-5736.
179. Kumar-Singh, R., and J.S. Chamberlain. 1996. Encapsidated adenovirus minichromosomes allow delivery and expression of a 14 kb dystrophin cDNA to muscle cells. *Hum Mol Genet* 5:913-921.
180. Haecker, S.E., H.H. Stedman, R.J. Balice-Gordon, D.B. Smith, J.P. Greelish, M.A. Mitchell, A. Wells, H.L. Sweeney, and J.M. Wilson. 1996. In vivo expression of full-length human dystrophin from adenoviral vectors deleted of all viral genes. *Hum Gene Ther* 7:1907-1914.
181. Clemens, P.R., S. Kochanek, Y. Sunada, S. Chan, H.H. Chen, K.P. Campbell, and C.T. Caskey. 1996. In vivo muscle gene transfer of full-length dystrophin with an adenoviral vector that lacks all viral genes. *Gene Ther* 3:965-972.
182. Gilbert, R., R.W. Dudley, A.B. Liu, B.J. Petrof, J. Nalbantoglu, and G. Karpati. 2003. Prolonged dystrophin expression and functional correction of mdx mouse muscle following gene transfer with a helper-dependent (gutted) adenovirus-encoding murine dystrophin. *Hum Mol Genet* 12:1287-1299.
183. Dudley, R.W., Y. Lu, R. Gilbert, S. Matecki, J. Nalbantoglu, B.J. Petrof, and G. Karpati. 2004. Sustained improvement of muscle function one year after full-length dystrophin gene transfer into mdx mice by a gutted helper-dependent adenoviral vector. *Hum Gene Ther* 15:145-156.
184. Kawano, R., M. Ishizaki, Y. Maeda, Y. Uchida, E. Kimura, and M. Uchino. 2008. Transduction of full-length dystrophin to multiple skeletal muscles improves motor

performance and life span in utrophin/dystrophin double knockout mice. *Mol Ther* 16:825-831.

185. Matecki, S., R.W. Dudley, M. Divangahi, R. Gilbert, J. Nalbantoglu, G. Karpati, and B.J. Petrof. 2004. Therapeutic gene transfer to dystrophic diaphragm by an adenoviral vector deleted of all viral genes. *Am J Physiol Lung Cell Mol Physiol* 287:L569-576.
186. DelloRusso, C., J.M. Scott, D. Hartigan-O'Connor, G. Salvatori, C. Barjot, A.S. Robinson, R.W. Crawford, S.V. Brooks, and J.S. Chamberlain. 2002. Functional correction of adult mdx mouse muscle using gutted adenoviral vectors expressing full-length dystrophin. *Proc Natl Acad Sci U S A* 99:12979-12984.
187. Gilchrist, S.C., M.P. Ontell, S. Kochanek, and P.R. Clemens. 2002. Immune response to full-length dystrophin delivered to Dmd muscle by a high-capacity adenoviral vector. *Mol Ther* 6:359-368.
188. Tinsley, J., N. Deconinck, R. Fisher, D. Kahn, S. Phelps, J.M. Gillis, and K. Davies. 1998. Expression of full-length utrophin prevents muscular dystrophy in mdx mice. *Nat Med* 4:1441-1444.
189. Deol, J.R., G. Danialou, N. Larochelle, M. Bourget, J.S. Moon, A.B. Liu, R. Gilbert, B.J. Petrof, J. Nalbantoglu, and G. Karpati. 2007. Successful Compensation for Dystrophin Deficiency by a Helper-dependent Adenovirus Expressing Full-length Utrophin. *Mol Ther*
190. Snoeys, J., J. Lievens, E. Wisse, F. Jacobs, H. Duimel, D. Collen, P. Frederik, and B. De Geest. 2007. Species differences in transgene DNA uptake in hepatocytes after adenoviral transfer correlate with the size of endothelial fenestrae. *Gene Ther* 14:604-612.
191. Smith, T.A., N. Idamakanti, J. Marshall-Neff, M.L. Rollence, P. Wright, M. Kaloss, L. King, C. Mech, L. Dinges, W.O. Iverson, A.D. Sherer, J.E. Markovits, R.M. Lyons, M. Kaleko, and S.C. Stevenson. 2003. Receptor interactions involved in adenoviral-mediated gene delivery after systemic administration in non-human primates. *Hum Gene Ther* 14:1595-1604.
192. Waddington, S.N., J.H. McVey, D. Bhella, A.L. Parker, K. Barker, H. Atoda, R. Pink, S.M. Buckley, J.A. Greig, L. Denby, J. Custers, T. Morita, I.M. Francischetti, R.Q. Monteiro, D.H. Barouch, N. van Rooijen, C. Napoli, M.J. Havenga, S.A. Nicklin, and A.H. Baker. 2008. Adenovirus serotype 5 hexon mediates liver gene transfer. *Cell* 132:397-409.
193. Tao, N., G.P. Gao, M. Parr, J. Johnston, T. Baradet, J.M. Wilson, J. Barsoum, and S.E. Fawell. 2001. Sequestration of adenoviral vector by Kupffer cells leads to a nonlinear dose response of transduction in liver. *Mol Ther* 3:28-35.
194. Campos, S.K., and M.A. Barry. 2007. Current advances and future challenges in Adenoviral vector biology and targeting. *Curr Gene Ther* 7:189-204.
195. Eto, Y., Y. Yoshioka, Y. Mukai, N. Okada, and S. Nakagawa. 2008. Development of PEGylated adenovirus vector with targeting ligand. *Int J Pharm* 354:3-8.
196. Kurachi, S., N. Koizumi, F. Sakurai, K. Kawabata, H. Sakurai, S. Nakagawa, T. Hayakawa, and H. Mizuguchi. 2007. Characterization of capsid-modified adenovirus vectors containing heterologous peptides in the fiber knob, protein IX, or hexon. *Gene Ther* 14:266-274.

197. Koizumi, N., T. Yamaguchi, K. Kawabata, F. Sakurai, T. Sasaki, Y. Watanabe, T. Hayakawa, and H. Mizuguchi. 2007. Fiber-modified adenovirus vectors decrease liver toxicity through reduced IL-6 production. *J Immunol* 178:1767-1773.
198. Meulenbroek, R.A., K.L. Sargent, J. Lunde, B.J. Jasmin, and R.J. Parks. 2004. Use of adenovirus protein IX (pIX) to display large polypeptides on the virion--generation of fluorescent virus through the incorporation of pIX-GFP. *Mol Ther* 9:617-624.
199. Parks, R.J. 2005. Adenovirus protein IX: a new look at an old protein. *Mol Ther* 11:19-25.
200. Vellinga, J., J. de Vrij, S. Myhre, T. Uil, P. Martineau, L. Lindholm, and R.C. Hoeben. 2007. Efficient incorporation of a functional hyper-stable single-chain antibody fragment protein-IX fusion in the adenovirus capsid. *Gene Ther* 14:664-670.
201. Marttila, M., D. Persson, D. Gustafsson, M.K. Liszewski, J.P. Atkinson, G. Wadell, and N. Arnberg. 2005. CD46 is a cellular receptor for all species B adenoviruses except types 3 and 7. *J Virol* 79:14429-14436.
202. Huard, J., H. Lochmuller, G. Acsadi, A. Jani, P. Holland, C. Guerin, B. Massie, and G. Karpati. 1995. Differential short-term transduction efficiency of adult versus newborn mouse tissues by adenoviral recombinants. *Exp Mol Pathol* 62:131-143.
203. Nalbantoglu, J., G. Pari, G. Karpati, and P.C. Holland. 1999. Expression of the primary coxsackie and adenovirus receptor is downregulated during skeletal muscle maturation and limits the efficacy of adenovirus-mediated gene delivery to muscle cells. *Hum Gene Ther* 10:1009-1019.
204. Acsadi, G., A. Jani, J. Huard, K. Blaschuk, B. Massie, P. Holland, H. Lochmuller, and G. Karpati. 1994. Cultured human myoblasts and myotubes show markedly different transducibility by replication-defective adenovirus recombinants. *Gene Ther* 1:338-340.
205. Cho, W.K., S. Ebihara, J. Nalbantoglu, R. Gilbert, B. Massie, P. Holland, G. Karpati, and B.J. Petrof. 2000. Modulation of Starling forces and muscle fiber maturity permits adenovirus-mediated gene transfer to adult dystrophic (mdx) mice by the intravascular route. *Hum Gene Ther* 11:701-714.
206. Acsadi, G., A. Jani, B. Massie, M. Simoneau, P. Holland, K. Blaschuk, and G. Karpati. 1994. A differential efficiency of adenovirus-mediated in vivo gene transfer into skeletal muscle cells of different maturity. *Hum Mol Genet* 3:579-584.
207. Guibinga, G.H., S. Ebihara, J. Nalbantoglu, P. Holland, G. Karpati, and B.J. Petrof. 2001. Forced myofiber regeneration promotes dystrophin gene transfer and improved muscle function despite advanced disease in old dystrophic mice. *Mol Ther* 4:499-507.
208. Bramson, J.L., N. Grinshtein, R.A. Meulenbroek, J. Lunde, D. Kottachchi, I.A. Lorimer, B.J. Jasmin, and R.J. Parks. 2004. Helper-dependent adenoviral vectors containing modified fiber for improved transduction of developing and mature muscle cells. *Hum Gene Ther* 15:179-188.
209. van Deutekom, J.C., B. Cao, R. Pruchnic, T.J. Wickham, I. Kovesdi, and J. Huard. 1999. Extended tropism of an adenoviral vector does not circumvent the maturation-dependent transducibility of mouse skeletal muscle. *J Gene Med* 1:393-399.

210. Cao, B., J.R. Mytinger, and J. Huard. 2002. Adenovirus mediated gene transfer to skeletal muscle. *Microsc Res Tech* 58:45-51.
211. van Deutekom, J.C., S.S. Floyd, D.K. Booth, T. Oligino, D. Krisky, P. Marconi, J.C. Glorioso, and J. Huard. 1998. Implications of maturation for viral gene delivery to skeletal muscle. *Neuromuscul Disord* 8:135-148.
212. Yurchenco, P.D. 1990. Assembly of basement membranes. *Ann N Y Acad Sci* 580:195-213.
213. Vracko, R., and E.P. Benditt. 1972. Basal lamina: the scaffold for orderly cell replacement. Observations on regeneration of injured skeletal muscle fibers and capillaries. *J Cell Biol* 55:406-419.
214. Carpenter, S., Karpati, G. 1984. Pathology of Skeletal Muscle. Churchill Livingstone, New York.
215. Huard, J., W.G. Feero, S.C. Watkins, E.P. Hoffman, D.J. Rosenblatt, and J.C. Glorioso. 1996. The basal lamina is a physical barrier to herpes simplex virus-mediated gene delivery to mature muscle fibers. *J Virol* 70:8117-8123.
216. Feero, W.G., J.D. Rosenblatt, J. Huard, S.C. Watkins, M. Epperly, P.R. Clemens, S. Kochanek, J.C. Glorioso, T.A. Partridge, and E.P. Hoffman. 1997. Viral gene delivery to skeletal muscle: insights on maturation-dependent loss of fiber infectivity for adenovirus and herpes simplex type 1 viral vectors. *Hum Gene Ther* 8:371-380.
217. Pruchnic, R., B. Cao, Z.Q. Peterson, X. Xiao, J. Li, R.J. Samulski, M. Epperly, and J. Huard. 2000. The use of adeno-associated virus to circumvent the maturation-dependent viral transduction of muscle fibers. *Hum Gene Ther* 11:521-536.
218. Cao, B., R. Pruchnic, M. Ikezawa, X. Xiao, J. Li, T.J. Wickham, I. Kovesdi, W.A. Rudert, and J. Huard. 2001. The role of receptors in the maturation-dependent adenoviral transduction of myofibers. *Gene Ther* 8:627-637.
219. Burnett, R.M. 1985. The structure of the adenovirus capsid. II. The packing symmetry of hexon and its implications for viral architecture. *J Mol Biol* 185:125-143.
220. Kurachi, S., N. Koizumi, K. Tashiro, H. Sakurai, F. Sakurai, K. Kawabata, S. Nakagawa, and H. Mizuguchi. 2008. Modification of pIX or hexon based on fiberless Ad vectors is not effective for targeted Ad vectors. *J Control Release* 127:88-95.
221. Verma, I.M., and N. Somia. 1997. Gene therapy -- promises, problems and prospects. *Nature* 389:239-242.
222. O'Neal, W.K., E. Rose, H. Zhou, C. Langston, K. Rice, D. Carey, and A.L. Beaudet. 2000. Multiple advantages of alpha-fetoprotein as a marker for in vivo gene transfer. *Mol Ther* 2:640-648.
223. Morral, N., W. O'Neal, H. Zhou, C. Langston, and A. Beaudet. 1997. Immune responses to reporter proteins and high viral dose limit duration of expression with adenoviral vectors: comparison of E2a wild type and E2a deleted vectors. *Hum Gene Ther* 8:1275-1286.
224. Peng, K.W., S. Facteau, T. Wegman, D. O'Kane, and S.J. Russell. 2002. Non-invasive in vivo monitoring of trackable viruses expressing soluble marker peptides. *Nat Med* 8:527-531.

225. Maelandsmo, G.M., P.J. Ross, M. Pavliv, R.A. Meulenbroek, C. Evelegh, D.A. Muruve, F.L. Graham, and R.J. Parks. 2005. Use of a murine secreted alkaline phosphatase as a non-immunogenic reporter gene in mice. *J Gene Med* 7:307-315.
226. Manes, T., K. Glade, C.A. Ziomek, and J.L. Millan. 1990. Genomic structure and comparison of mouse tissue-specific alkaline phosphatase genes. *Genomics* 8:541-554.
227. Gerber, L.D., K. Kodukula, and S. Udenfriend. 1992. Phosphatidylinositol glycan (PI-G) anchored membrane proteins. Amino acid requirements adjacent to the site of cleavage and PI-G attachment in the COOH-terminal signal peptide. *J Biol Chem* 267:12168-12173.
228. Berger, J., J. Hauber, R. Hauber, R. Geiger, and B.R. Cullen. 1988. Secreted placental alkaline phosphatase: a powerful new quantitative indicator of gene expression in eukaryotic cells. *Gene* 66:1-10.
229. Terao, M., and B. Mintz. 1987. Cloning and characterization of a cDNA coding for mouse placental alkaline phosphatase. *Proc Natl Acad Sci U S A* 84:7051-7055.
230. Berger, J., A.D. Howard, L. Brink, L. Gerber, J. Hauber, B.R. Cullen, and S. Udenfriend. 1988. COOH-terminal requirements for the correct processing of a phosphatidylinositol-glycan anchored membrane protein. *J Biol Chem* 263:10016-10021.
231. Watanabe, T., N. Wada, E.E. Kim, H.W. Wyckoff, and J.Y. Chou. 1991. Mutation of a single amino acid converts germ cell alkaline phosphatase to placental alkaline phosphatase. *J Biol Chem* 266:21174-21178.
232. Birnboim, H.C., Doly, J. 1979. A rapid alkaline extraction procedure for screening recombinant plasmid DNA. *Nucleic Acids Research* 1513-1523.
233. Sambrook, J., Fritsch, E.F., Maniatis, T. 1989. Molecular Cloning: A laboratory Manual. Cold Spring Harbor Laboratory Press, Cold Spring Harbor, NY.
234. Shayakhmetov, D.M., and A. Lieber. 2000. Dependence of adenovirus infectivity on length of the fiber shaft domain. *J Virol* 74:10274-10286.
235. Chartier, C., E. Degryse, M. Gantzer, A. Dieterle, A. Pavirani, and M. Mehtali. 1996. Efficient generation of recombinant adenovirus vectors by homologous recombination in Escherichia coli. *J Virol* 70:4805-4810.
236. Addison, C.L., M. Hitt, D. Kunsken, and F.L. Graham. 1997. Comparison of the human versus murine cytomegalovirus immediate early gene promoters for transgene expression by adenoviral vectors. *J Gen Virol* 78 ( Pt 7):1653-1661.
237. Ross, P.J., and R. Parks. 2007. Construction of First-generation Adenoviral Vectors. In Gene Transfer: Delivery and Expression of DNA and RNA. T. Friedmann, and J. Rossi, editors. Cold Spring Harbor Laboratory Press, Cold Spring Harbor. 149-166.
238. Dangain, J., and G. Vrbova. 1984. Muscle development in mdx mutant mice. *Muscle Nerve* 7:700-704.
239. Parks, R.J., J.L. Bramson, Y. Wan, C.L. Addison, and F.L. Graham. 1999. Effects of stuffer DNA on transgene expression from helper-dependent adenovirus vectors. *J Virol* 73:8027-8034.
240. Nalbantoglu, J., N. Larochelle, E. Wolf, G. Karpati, H. Lochmuller, and P.C. Holland. 2001. Muscle-specific overexpression of the adenovirus primary receptor CAR

overcomes low efficiency of gene transfer to mature skeletal muscle. *J Virol* 75:4276-4282.

241. Xiong, F., S. Xiao, F. Peng, H. Zheng, M. Yu, Y. Ruan, W. Li, Y. Shang, C. Zhao, W. Zhou, H. Chen, J.S. Chamberlain, L. Fang, and C. Zhang. 2007. Herpes simplex virus VP22 enhances adenovirus-mediated microdystrophin gene transfer to skeletal muscles in dystrophin-deficient (mdx) mice. *Hum Gene Ther* 18:490-501.
242. Liu, M., Y. Yue, S.Q. Harper, R.W. Grange, J.S. Chamberlain, and D. Duan. 2005. Adeno-associated virus-mediated microdystrophin expression protects young mdx muscle from contraction-induced injury. *Mol Ther* 11:245-256.
243. Abramoff, M.D., Magelhaes, P.J., Ram, S.J. 2004. Image Processing with ImageJ. *Biophotonics International* 11:36-42.
244. Christ, M., M. Lusky, F. Stoeckel, D. Dreyer, A. Dieterle, A.I. Michou, A. Pavirani, and M. Mehtali. 1997. Gene therapy with recombinant adenovirus vectors: evaluation of the host immune response. *Immunol Lett* 57:19-25.
245. Michou, A.I., L. Santoro, M. Christ, V. Julliard, A. Pavirani, and M. Mehtali. 1997. Adenovirus-mediated gene transfer: influence of transgene, mouse strain and type of immune response on persistence of transgene expression. *Gene Ther* 4:473-482.
246. Wadsworth, S.C., H. Zhou, A.E. Smith, and J.M. Kaplan. 1997. Adenovirus vector-infected cells can escape adenovirus antigen-specific cytotoxic T-lymphocyte killing in vivo. *J Virol* 71:5189-5196.
247. Huard, J., H. Lochmuller, G. Acsadi, A. Jani, B. Massie, and G. Karpati. 1995. The route of administration is a major determinant of the transduction efficiency of rat tissues by adenoviral recombinants. *Gene Ther* 2:107-115.
248. Maione, D., C. Della Rocca, P. Giannetti, R. D'Arrigo, L. Liberatoscioli, L.L. Franlin, V. Sandig, G. Ciliberto, N. La Monica, and R. Savino. 2001. An improved helper-dependent adenoviral vector allows persistent gene expression after intramuscular delivery and overcomes preexisting immunity to adenovirus. *Proc Natl Acad Sci U S A* 98:5986-5991.
249. Wang, Y., J.K. Hu, A. Krol, Y.P. Li, C.Y. Li, and F. Yuan. 2003. Systemic dissemination of viral vectors during intratumoral injection. *Mol Cancer Ther* 2:1233-1242.
250. Hartigan-O'Connor, D., C.J. Kirk, R. Crawford, J.J. Mule, and J.S. Chamberlain. 2001. Immune evasion by muscle-specific gene expression in dystrophic muscle. *Mol Ther* 4:525-533.
251. Mei, Y.F., and G. Wadell. 1995. Molecular determinants of adenovirus tropism. *Curr Top Microbiol Immunol* 199 ( Pt 3):213-228.
252. Chroboczek, J., R.W. Ruigrok, and S. Cusack. 1995. Adenovirus fiber. *Curr Top Microbiol Immunol* 199 ( Pt 1):163-200.
253. Kirby, I., R. Lord, E. Davison, T.J. Wickham, P.W. Roelvink, I. Kovesdi, B.J. Sutton, and G. Santis. 2001. Adenovirus type 9 fiber knob binds to the coxsackie B virus-adenovirus receptor (CAR) with lower affinity than fiber knobs of other CAR-binding adenovirus serotypes. *J Virol* 75:7210-7214.
254. Larochelle, N., J.R. Deol, V. Srivastava, C. Allen, H. Mizuguchi, G. Karpati, P.C. Holland, and J. Nalbantoglu. 2008. Downregulation of CD46 during muscle

differentiation: implications for gene transfer to human skeletal muscle using group B adenoviruses. *Hum Gene Ther* 19:133-142.

255. Sinnreich, M., C.A. Shaw, G. Pari, J. Nalbantoglu, P.C. Holland, and G. Karpati. 2005. Localization of coxsackie virus and adenovirus receptor (CAR) in normal and regenerating human muscle. *Neuromuscul Disord* 15:541-548.
256. Roelvink, P.W., I. Kovesdi, and T.J. Wickham. 1996. Comparative analysis of adenovirus fiber-cell interaction: adenovirus type 2 (Ad2) and Ad9 utilize the same cellular fiber receptor but use different binding strategies for attachment. *J Virol* 70:7614-7621.
257. Hidaka, C., E. Milano, P.L. Leopold, J.M. Bergelson, N.R. Hackett, R.W. Finberg, T.J. Wickham, I. Kovesdi, P. Roelvink, and R.G. Crystal. 1999. CAR-dependent and CAR-independent pathways of adenovirus vector-mediated gene transfer and expression in human fibroblasts. *J Clin Invest* 103:579-587.
258. Rezcallah, M.S., K. Hodges, D.B. Gill, J.P. Atkinson, B. Wang, and P.P. Cleary. 2005. Engagement of CD46 and alpha5beta1 integrin by group A streptococci is required for efficient invasion of epithelial cells. *Cell Microbiol* 7:645-653.
259. Yao, C.C., B.L. Ziober, A.E. Sutherland, D.L. Mendrick, and R.H. Kramer. 1996. Laminins promote the locomotion of skeletal myoblasts via the alpha 7 integrin receptor. *J Cell Sci* 109 ( Pt 13):3139-3150.
260. Blaschuk, K.L., and P.C. Holland. 1994. The regulation of alpha 5 beta 1 integrin expression in human muscle cells. *Dev Biol* 164:475-483.
261. Olwin, B.B., and Z.W. Hall. 1985. Developmental regulation of laminin accumulation in the extracellular matrix of a mouse muscle cell line. *Dev Biol* 112:359-367.
262. Watanabe, Y., Y. Sawaishi, H. Tada, E. Sato, T. Suzuki, and G. Takada. 2000. Immunoliposome-mediated gene transfer into cultured myotubes. *Tohoku J Exp Med* 192:173-180.
263. Kitzmann, M., G. Carnac, M. Vandromme, M. Primig, N.J. Lamb, and A. Fernandez. 1998. The muscle regulatory factors MyoD and myf-5 undergo distinct cell cycle-specific expression in muscle cells. *J Cell Biol* 142:1447-1459.
264. Russell, W.C., R.C. Valentine, and H.G. Pereira. 1967. The effect of heat on the anatomy of the adenovirus. *J Gen Virol* 1:509-522.
265. Maheshwari, G., R. Jannat, L. McCormick, and D. Hsu. 2004. Thermal inactivation of adenovirus type 5. *J Virol Methods* 118:141-146.
266. Rexroad, J., C.M. Wiethoff, A.P. Green, T.D. Kierstead, M.O. Scott, and C.R. Middaugh. 2003. Structural stability of adenovirus type 5. *J Pharm Sci* 92:665-678.
267. Croyle, M.A., B.J. Roessler, B.L. Davidson, J.M. Hilfinger, and G.L. Amidon. 1998. Factors that influence stability of recombinant adenoviral preparations for human gene therapy. *Pharm Dev Technol* 3:373-383.
268. Nyberg-Hoffman, C., and E. Aguilar-Cordova. 1999. Instability of adenoviral vectors during transport and its implication for clinical studies. *Nat Med* 5:955-957.
269. Murase, N., and F. Franks. 1989. Salt precipitation during the freeze-concentration of phosphate buffer solutions. *Biophys Chem* 34:293-300.
270. Schoggins, J.W., and E. Falck-Pedersen. 2006. Fiber and penton base capsid modifications yield diminished adenovirus type 5 transduction and proinflammatory

gene expression with retention of antigen-specific humoral immunity. *J Virol* 80:10634-10644.

271. Schoggins, J.W., M. Nociari, N. Philpott, and E. Falck-Pedersen. 2005. Influence of fiber detargeting on adenovirus-mediated innate and adaptive immune activation. *J Virol* 79:11627-11637.
272. Niwa, M., S.D. Rose, and S.M. Berget. 1990. In vitro polyadenylation is stimulated by the presence of an upstream intron. *Genes Dev* 4:1552-1559.
273. Cheng, C., J.G. Gall, W.P. Kong, R.L. Sheets, P.L. Gomez, C.R. King, and G.J. Nabel. 2007. Mechanism of ad5 vaccine immunity and toxicity: fiber shaft targeting of dendritic cells. *PLoS Pathog* 3:e25.
274. Ontell, M. 1981. Muscle fiber necrosis in murine dystrophy. *Muscle Nerve* 4:204-213.
275. Yoshimura, K., and K. Harii. 1999. A regenerative change during muscle adaptation to denervation in rats. *J Surg Res* 81:139-146.
276. Yoshimura, K., W.M. Kuzon, and K. Harii. 1998. Myosin heavy chain expression in skeletal muscle autografts under neural or aneural conditions. *J Surg Res* 75:135-147.
277. Le Du, M.H., and J.L. Millan. 2002. Structural evidence of functional divergence in human alkaline phosphatases. *J Biol Chem* 277:49808-49814.
278. Cross, G.A. 1987. Eukaryotic protein modification and membrane attachment via phosphatidylinositol. *Cell* 48:179-181.
279. Berger, J., A.D. Howard, L. Gerber, B.R. Cullen, and S. Udenfriend. 1987. Expression of active, membrane-bound human placental alkaline phosphatase by transfected simian cells. *Proc Natl Acad Sci U S A* 84:4885-4889.
280. Micanovic, R., L.D. Gerber, J. Berger, K. Kodukula, and S. Udenfriend. 1990. Selectivity of the cleavage/attachment site of phosphatidylinositol-glycan-anchored membrane proteins determined by site-specific mutagenesis at Asp-484 of placental alkaline phosphatase. *Proc Natl Acad Sci U S A* 87:157-161.
281. Hoylaerts, M.F., T. Manes, and J.L. Millan. 1992. Allelic amino acid substitutions affect the conformation and immunoreactivity of germ-cell alkaline phosphatase phenotypes. *Clin Chem* 38:2493-2500.
282. Hoylaerts, M.F., T. Manes, and J.L. Millan. 1992. Molecular mechanism of uncompetitive inhibition of human placental and germ-cell alkaline phosphatase. *Biochem J* 286 ( Pt 1):23-30.
283. Sarkioja, M., S. Pesonen, M. Raki, T. Hakkarainen, J. Salo, M.T. Ahonen, A. Kanerva, and A. Hemminki. 2008. Changing the adenovirus fiber for retaining gene delivery efficacy in the presence of neutralizing antibodies. *Gene Ther* 15:921-929.
284. Sumida, S.M., D.M. Truitt, M.G. Kishko, J.C. Arthur, S.S. Jackson, D.A. Gorgone, M.A. Lifton, W. Koudstaal, M.G. Pau, S. Kostense, M.J. Havenga, J. Goudsmit, N.L. Letvin, and D.H. Barouch. 2004. Neutralizing antibodies and CD8+ T lymphocytes both contribute to immunity to adenovirus serotype 5 vaccine vectors. *J Virol* 78:2666-2673.
285. Chen, Y., D.C. Yu, D. Charlton, and D.R. Henderson. 2000. Pre-existent adenovirus antibody inhibits systemic toxicity and antitumor activity of CN706 in the nude

mouse LNCaP xenograft model: implications and proposals for human therapy. *Hum Gene Ther* 11:1553-1567.

286. Sumida, S.M., D.M. Truitt, A.A. Lemckert, R. Vogels, J.H. Custers, M.M. Addo, S. Lockman, T. Peter, F.W. Peyerl, M.G. Kishko, S.S. Jackson, D.A. Gorgone, M.A. Lifton, M. Essex, B.D. Walker, J. Goudsmit, M.J. Havenga, and D.H. Barouch. 2005. Neutralizing antibodies to adenovirus serotype 5 vaccine vectors are directed primarily against the adenovirus hexon protein. *J Immunol* 174:7179-7185.

287. Parks, R., C. Evelegh, and F. Graham. 1999. Use of helper-dependent adenoviral vectors of alternative serotypes permits repeat vector administration. *Gene Ther* 6:1565-1573.

288. Shayakhmetov, D.M., Z.Y. Li, S. Ni, and A. Lieber. 2004. Analysis of adenovirus sequestration in the liver, transduction of hepatic cells, and innate toxicity after injection of fiber-modified vectors. *J Virol* 78:5368-5381.

# *Appendix I: Reagents*

## *General solutions and reagents*

1M Tris-HCl pH 8.0
121.14g Tris
Up to 1L $H_2O$
Adjust to pH 8.0 with HCl

0.5M EDTA
146.13g EDTA (ethylenediaminetetraacetic acid)
Up to 1L $H_2O$
Adjust to pH 8.0 with HCl

Tris-EDTA (TE)
146.13g EDTA
Up to 1L $H_2O$
Adjust to pH 8.0 with HCl

10M NaOH
39.978g NaOH
Up to 100ml $H_2O$

5M NaCl
146.11g NaCl
Up to 500ml $H_2O$

20% SDS
100g SDS (sodium dodecyl sulfate)
Up to 500ml $H_2O$

## *Cloning*

| | |
|---|---|
| Restriction enzymes: | |
| PacI, XbaI, MfeI, AgeI, EheI, BstBI, BamHI, XhoI, SgraI | (NEB) |
| Bsu15I | (MBI Fermentas) |
| T4 DNA ligase | (NEB) |
| T4 DNA polymerase | (NEB) |
| Calf Intestinal phosphatase | (NEB) |

LB Broth

20g LB broth up to 1L $H_2O$ (Fisher)
Autoclave 45min at 121°C

LB Broth with AMP
500ml LB broth
500µl 50mg/ml Ampicillin (50µg/ml)

30% Glycerol
30ml glycerol (Fisher)
Up to 100ml $H_2O$

PCR Reaction
30ml glycerol
Up to 100ml $H_2O$

***Plasmid Preparation***

Solution I
4.5g dextrose (50mM)
12.5mL 1M Tris-HCl pH 7.5 (250mM)
10ml 0.5M EDTA pH 8.0 (10mM)
Up to 500ml $H_2O$
Adjust pH to 8.0, filter sterilize

Solution II
200µl 10M NaOH (200mM)
500µl 20% SDS (1%)
Up to 10ml $H_2O$

Solution III
147.21g potassium acetate
57.5ml glacial acetic acid (11.5%)
Up to 500ml $H_2O$

10X SSC (standard saline citrate)
87.66g NaCl
13.23g sodium citrate
Up to 1L $H_2O$

0.1X SSC (standard saline citrate)
5ml 10X SSC
Up to 500ml $H_2O$

## *Agarose Gel Electrophoresis*

50X TAE (Tris-acetic acid –EDTA)
- 242g Tris
- 57ml acetic acid (5.7%)
- 100ml 0.5M EDTA
- Up to 1L $H_2O$

1X TAE (Tris-acetic acid –EDTA)
- 80ml 50X TAE
- Up to 4L $H_2O$

1.2% Agarose gel
- 1.2 g agarose (1.2%)
- Up to 100ml 1X TAE
- 1µl ethidium bromide

6X Loading Buffer
- 40g sucrose (40%)
- 0.125g bromophenol blue (0.125%)
- 20ml 0.5M EDTA pH 8.0 (0.1M)
- Up to 100ml $H_2O$

Loading Buffer + RNAse
- 1.5ml 6X loading buffer
- 10µl 50mg/ml RNAse

## *Tissue Culture*

| | |
|---|---|
| Modified Eagle Medium | (Sigma) |
| Dulbecco's Modofied Eagle Medium | (Sigma) |
| Dublecco's Phosphate Buffered Saline | (HyClone) |
| Superfect | (Qiagen) |
| Lipofectamine 2000 | (Invitrogen) |

MEM/DMEM with 10% FBS

| | |
|---|---|
| 500ml MEM/DMEM | |
| 50ml FBS (10%) | (HyClone) |
| 5ml antibiotic/antimycotic (1%) | (Invitrogen) |
| 5ml Glutamax (1%) | (Invitrogen) |

DMEM with 0.5% FBS
500ml MEM/DMEM
2.5ml FBS (0.5%)
5ml antibiotic/antimycotic (1%)
5ml Glutamax (1%)

10X Citric Saline
100.66g KCl (1.35M)
44.11g sodium citrate (150mM)
Up to 1L $H_2O$
Autoclave 45 min at 121°C

1X Citric Saline
50ml 10X Citric Saline
Up to 500ml $H_2O$

1X Trypsin
10ml 10X Trypsin (Invitrogen)
Up to 500ml D-PBS

***Dissection***

OTC mounting medium (Tissue-tek)
Isopentane (Sigma)

***Histology***

Permount mounting medium (Fisher)

10X PBS
80g NaCl
2g KCl
22g $Na_2HPO_4$ X $7H_2O$
2g $KH_2PO_4$
To 1L $H_2O$
Autoclave

1X PBS
50ml 10X PBS
Up to 500ml $H_2O$

β-gal Fixative
6g of paraformaldehyde dissolved in 300ml heated PBS (2%)
0.12g $MgCl_2$(2mM)

1.2ml of 50% w/w gluteraldehyde (0.2%)
Filter sterilize

β-gal Stain

2.11g of $K_4Fe(CN)_6$
1.65g of $K_3Fe(CN)_6$
0.41g of $MgCl_2$
To 1L in PBS
Filter sterilize

## *Immunoflourescence*

2.5% paraformaldehyde

1.5 ml of 10% PFA in 4.5ml PBS

10% paraformaldehyde

1.5 ml of 10% PFA in 4.5ml PBS

Blocking solution (1% Bovine serum albumin (BSA), 0.5% TritionX)

| | |
|---|---|
| 0.1 g of BSA | (Sigma) |
| 5ul of Triton X | (Fisher) |
| Up to 10ml PBS | |

Primary antibodies

| | |
|---|---|
| Mouse anti- embryonic MHC, (F1.652): sc-53091 | (Santa Cruz Biotechnology) |
| Rabbit anti-B-gal, (A-11132) | (Molecular probes) |

Secondary antibodies

| | |
|---|---|
| TRITC conjugated Goat Anti-mouse, 115-025-044 | (Jackson ImmunoResearch) |
| Alexa fluor 448 conjugated Donkey Anti-rabbit (A21206) | (Invitrogen) |

| | |
|---|---|
| Hoechst | (Fisher) |
| DAKO fluorescent mounting media | (DAKO) |
| Glass coverslips | (Fisher) |
| Superfrost Plus Microscope Slides | (Fisher) |

# *Curriculum Vitae*

## KRISTIN REGINA WILLEMSEN

### EDUCATION

**Masters of Science** Expected September 2008

***University of Ottawa, Ottawa, Ontario***

- Specialization: Microbiology and Immunology.
- Related course work: Advanced Topics in Virology (A+), Advanced topics in Cell Death (A+).
- Independent research project: Improving Adenoviral vectors for muscle-directed gene therapy.

**Technical Skills Developed**

- Construction and purification of replication defective adenoviral vectors.
- Cloning and microbiology techniques (ligation, recombination, gel purification, PCR).
- Viral infections and titers (plaque assays, particle counts).
- NIAUT trained and certified for mouse husbandry, restraint, IP IM and IV injections, blood collection, and tissue removal.
- Tissue sectioning, histology, Immunohistochemistry
- Tissue culture, sterile technique

**Publications**

- **Willemsen KR** and Parks RJ, Optimization of the murine secreted embryonic alkaline phosphatase (mSEAP) reporter gene. (Manuscript in preparation).

**Honors Bachelor of Science** 2002- 2006

***University of Toronto, Mississauga, Ontario***

- Specialization: Molecular Biology
- Related Course work: Independent Biology Research project (A+), Functional Genomics and Bioinformatics (A), Modern Approaches to Biotechnology (A-), Trends in Biotechnology and Biochemistry (A-), Techniques in biological chemistry (A-), Organizational behavior (A-).
- Independent Research Project: On the role of satellite cells in testosterone-mediated rescue of reproductive neuromuscular systems of neonatal rats.

**Technical Skills Developed**

- Rat husbandry and surgical technique.
- Tissue sectioning.
- Histology and Immunohistochemistry

**Publications**

- Niel L, **Willemsen KR,** Volante SN, Monks DA, Sexual Dimorphism and androgen regulation of satellite cell population in differentiated rat levator ani muscle. Developmental Neurobiology 68(1): 115-122 (2008).

## RESEARCH EXPERIENCE

**Process Managerial Research Assistant** 2000 to 2001

***Nortel Networks, Ottawa, Ontario***

- Investigated and revised quality control inspection criteria for High-Speed Microelectronics fabrication process.

**Technical Skills Developed**

- Atomic Force Microscopy
- Scanning Electron Microscopy

**Radiation Biology Research Student** Summer 1999

***Atomic Energy of Canada, Ltd., Chalk River, Ont.***

- Independent Research project: Investigating the role of heat and ionizing radiation on Indian Muntjac Fibroblasts.

**Technical Skills Developed**

- Irradiation of biological samples
- Fluorescence *in situ* hybridization
- Tissue culture, sterile technique.

## LEADERSHIP

**Charity Leader, MINGA Living and Learning Community**

***University of Toronto***

- Founded a charity service project to rebuild and renovate an elementary school in Guatemala.
- Managed, motivated, and engaged a team of 30 University of Toronto students to raise the necessary $ 30,000 to complete the planned outreach projects in Guatemala (2004-2006).

**Member, Youth Transition Committee**

***Ottawa, Ontario***

- Advised municipal government how to include the youth voice in the amalgamated City of Ottawa by proposing and implementing the Ottawa Youth Cabinet.
- Received the United Way Ottawa Youth Community Builder of the Year Award (2001).

**Volunteer Coach, Canadian Figure Skating Association**

***Ottawa, Ontario***

- Instructed youth Canskate, Canfigureskate and Special Olympic program (1994-2002)
- Received Junior Citizen of the Year Award for my volunteer work in the Ottawa community (1998).